Distribution Agreement

In presenting this thesis or dissertation as a partial fulfillment of the requirements for an advanced degree from Emory University, I hereby grant to Emory University and its agents the non-exclusive license to archive, make accessible, and display my thesis or dissertation in whole or in part in all forms of media, now or hereafter known, including display on the world wide web. I understand that I may select some access restrictions as part of the online submission of this thesis or dissertation. I retain all ownership rights to the copyright of the thesis or dissertation. I also retain the right to use in future works (such as articles or books) all or part of this thesis or dissertation.

_____ _____

Kelly M. Lohr Date

Neurochemical, neuroprotective, and behavioral effects of enhanced vesicular storage of dopamine

By

Kelly M. Lohr

Doctor of Philosophy

Graduate Division of Biological and Biomedical Sciences

Neuroscience Program

_____

Gary W. Miller, Ph.D.

Advisor

_____ _____

W. Michael Caudle, Ph.D. Ellen Hess, Ph.D.

Committee Member Committee Member

_____ _____

Yoland Smith, Ph.D. Malu Tansey, Ph.D.

Committee Member Committee Member

Accepted:

_____

Lisa A. Tedesco, Ph.D.

Dean of the James T. Laney School of Graduate Studies

_____

Date

Neurochemical, neuroprotective, and behavioral effects of enhanced vesicular storage of dopamine

By

Kelly M. Lohr

B.S., Dickinson College 2010

Advisor: Gary W. Miller, Ph.D.

An abstract of

a dissertation submitted to the Faculty of the

James T. Laney School of Graduate Studies

of Emory University in partial fulfillment

of the requirements for the degree of

Doctor of Philosophy

Neuroscience Program

Graduate Division of Biological and Biomedical Sciences

2015

Abstract

Neurochemical, neuroprotective, and behavioral effects of enhanced vesicular storage of dopamine

By

Kelly M. Lohr

The vesicular monoamine transporter 2 (VMAT2; SLC18A2) is responsible for both packaging monoamine neurotransmitters and for sequestering neurotoxic species in the cytosol, thereby protecting neurons. Recently, reduced vesicular filling via decreased VMAT2 function has been demonstrated in Parkinson's disease brains. These findings, along with work from mouse models of reduced VMAT2 levels, suggest that increasing vesicular filling may be beneficial to the health of the dopamine system. To assess this, we generated a mouse model of increased vesicular function via bacterial artificial chromosome-mediated overexpression of VMAT2. VMAT2-overexpressing mice show an enhanced vesicular capacity for dopamine storage (56% increase), dopamine vesicle volume (33%), and total striatal dopamine content (21%). This elevated vesicular capacity also leads to increased stimulated dopamine release (84%) and extracellular dopamine levels (44%) in the striatum. Additionally, the VMAT2-HI mice exhibit altered dopamine handling following treatment with L-DOPA, the neurochemical precursor to dopamine. These findings suggest that elevated vesicular storage may allow more efficient use of L-DOPA, a common Parkinson's disease therapeutic. Perhaps most importantly, it also appears that VMAT2 overexpression does not cause negative behavioral side effects. VMAT2-overexpressing mice show improved outcomes on anxiety and depressive-like behaviors and only a mild increase in locomotor activity during their active period (41%). Finally, we examined whether elevated VMAT2 levels altered the vulnerability of the nigrostriatal pathway to toxicant exposure. The VMAT2-HI mice show significant protection from the dopaminergic toxicants 1-methyl-4-phenyl-1,2,3,6-tetrahydropyridine (MPTP) and methamphetamine in the nigrostriatal pathway. Together, the VMAT2-overexpressing mice show that enhanced vesicular capacity is indeed possible and that these changes are capable of augmenting dopamine output without compensation in the rest of the dopamine system. The increased dopamine release, improved L-DOPA efficacy, and neuroprotection in the VMAT2-overexpressing mice suggest that interventions aimed at enhancing vesicular capacity may be of therapeutic benefit in disorders of reduced dopamine like Parkinson's disease.

Neurochemical, neuroprotective, and behavioral effects of enhanced vesicular storage of dopamine

By

Kelly M. Lohr

B.S., Dickinson College 2010

Advisor: Gary W. Miller, Ph.D.

A dissertation submitted to the Faculty of the

James T. Laney School of Graduate Studies

of Emory University in partial fulfillment

of the requirements for the degree of

Doctor of Philosophy

Neuroscience Program

Graduate Division of Biological and Biomedical Sciences

2015

Table of Contents

CHAPTER I: INTRODUCTION

Dopamine neuromodulation

Dopamine was first synthesized in 1910, but the compound was thought to be merely an intermediary chemical in the synthesis of norepinephrine for decades (Hornykiewicz, 2002). In 1958, dopamine was identified in the brain (Carlsson et al., 1958), and the massive depletion of dopamine was linked to Parkinson's disease in the 1960s (Ehringer and Hornykievicz, 1960; Hornykiewicz, 1966). Despite this disease link and other work showing the release of dopamine from neuronal populations (Portig and Vogt, 1969), it was not until the identification of the dopamine receptors and the activation of their downstream signaling cascades that the field was confident in dopamine as a neurotransmitter (Kebabian et al., 1972; Seeman et al., 1976).

Dopamine neuron populations and pathways were soon identified as responsible for reward, cognition, psychosis, and motor function (Swerdlow and Koob, 1987a; Haber, 2014). The mesolimbic dopamine circuit projects from the ventral tegmental area (VTA) to the limbic areas (nucleus accumbens, ventral striatum, and the amygdala), and there is overwhelming evidence to support the importance of mesolimbic dopamine release in reward (Fibiger and Phillips, 1988; Koob, 1992). The mesocortical dopamine pathway sends projections from the VTA to the prefrontal, cingulate, and entorhinal cortices and mediates cognition (Bannon and Roth, 1983). The tuberoinfundibular pathway connects the arcuate and periventricular nuclei of the hypothalamus to the intermediate lobe of the pituitary gland, which controls the release of prolactin (Moore and Wuerthele, 1979; Porter et al., 1990). Finally, dopamine is released from the nigrostriatal pathway which sends projections from the substantia nigra pars compacta (SNpc) to the dorsal striatum (Obeso et al., 1997). In the striatum, dopamine modulates function of the direct and indirect

pathways, which takes input from motor cortex, relays it through the thalamus and back to the cortex, controlling movement (Crittenden and Graybiel, 2011; Calabresi et al., 2014).

Dopamine is called a social neurotransmitter or a neuromodulator because it exerts its effects beyond the synaptic cleft. This term is reinforced by the localization of both the plasma membrane dopamine transporter (DAT), which is responsible for dopamine uptake back into the neuron, and the localization of dopamine receptors, most of which are located outside of the synapse itself (Cragg and Rice, 2004; Sotnikova et al., 2006). Dopamine receptors are not saturated upon typical neurotransmission, suggesting that the dopamine system is capable of a large range of signaling intensities, the uppermost of which are not tapped in a baseline state. Thus, the dopamine system is not acting at its maximum function (Rice and Cragg, 2008). The best examples of this functional range are the responses to psychostimulants (e.g. dopamine-releasing compounds like cocaine or amphetamine), where large extracellular floods of dopamine induce massive receptor activation and behavioral effects (Koob, 1992; Howell and Kimmel, 2008). This large range in signaling leaves room for novel manipulations that could augment dopaminergic neurotransmission. Here we describe a transgenic mouse model of enhanced dopamine output via increased vesicular capacity. These mice provide a novel insight into the neurochemical, behavioral, and neuroprotective effects of modified dopamine dynamics at the synapse.

Synaptic vesicle function

Neurotransmission relies on the proper storage and release of neurotransmitters from synaptic vesicles. Without precise control of the quantal release of these molecules, the fundamental processes of effective signaling would be disrupted. Synaptic vesicles are small spherical lipid bilayers formed in the Golgi apparatus and transported to the synaptic

terminal (Zimmermann et al., 1993; Südhof, 2004). In the terminal, vesicles are responsible for packaging and concentrating neurotransmitters (including glutamate, GABA, glycine, dopamine, serotonin, norepinephrine, and histamine) for signaling events. The majority of neurotransmitters are sequestered into synaptic vesicles at any given moment, making vesicular storage the primary determinant of the transmitter capacity of the brain.

Vesicular neurotransmitter filling

Through active transport mechanisms, synaptic vesicles package high concentrations of neurotransmitters inside the vesicular lumen. The vesicular monoamine transporter 2 (VMAT2, SLC18A2) is responsible for the packaging of cytosolic monoamines (dopamine, serotonin, norepinephrine, histamine) into small synaptic and dense core vesicles in monoaminergic neurons throughout the brain (Erickson et al., 1992; Liu et al., 1992a; Erickson and Eiden, 1993; Eiden and Weihe, 2011). VMAT2 is a member of the SLC18 family of transporter proteins, which also comprises both VMAT1 and the vesicular acetylcholine transporter (VAChT) (Lawal and Krantz, 2013). VMAT1 is preferentially expressed in large dense core vesicles of neuroendocrine cells, including chromaffin and enterochromaffin cells, while VMAT2 is primarily expressed in monoaminergic neurons in the CNS, sympathetic nervous system, mast cells, and histamine-containing cells in the gut (Peter et al., 1995; Schuldiner et al., 1995). Though its crystal structure is unknown, VMAT2 is characterized by 12 transmembrane helices (**Fig. 1.1**) (Peter et al., 1994). Both the N- and C-termini of VMAT2 are localized in the cytosol, and there is a large glycosylated intralumenal loop between the first and second transmembrane domains of the transporter (Wimalasena, 2011). VMAT2 is an H^+-ATPase antiporter, which uses the vesicular electrochemical gradient to drive transport (Parsons et

al., 1993; Reimer et al., 1998). The pH gradient across the vesicular membrane is established by the vacuolar H^+-ATPase, which uses ATP hydrolysis to generate the energy required to move H^+ ions into the vesicle (Kanner and Schuldiner, 1987; Moriyama and Futai, 1990). It is this movement of H^+ ions that creates the vesicular proton gradient and establishes an acidic environment inside the vesicle (pH of ~5.5). This electrochemical gradient drives VMAT2-mediated transport (Rudnick et al., 1990). For every single monoamine molecule transported into the vesicular lumen via VMAT2, two protons are extruded into the cytosol. By driving the sequestration of neurotransmitter into the vesicle, VMAT2 is a critical mediator of dopamine dynamics in the neuronal terminal.

Neurotoxic mechanisms of cytosolic dopamine

Dopamine is synthesized via the conversion of the amino acid tyrosine into L-dihydroxyphenylalanine (L-DOPA) by the rate-limiting enzyme tyrosine hydroxylase (TH) (Axelrod and Weinshilboum, 1972). L-DOPA is then converted into dopamine by amino acid decarboxylase (AADC) in the neuronal cytosol (Kuhar et al., 1999). Cytosolic dopamine causes toxicity via dopamine breakdown by two mechanisms: deamination by cytosolic enzymes or autooxidation. Dopamine can be deaminated by monoamine oxidase (MAO) produced in the mitochondria, which converts cytosolic dopamine to DOPAL, an aldehyde intermediate, and hydrogen peroxide (Eisenhofer et al., 2004a; Rees et al., 2009; Goldstein et al., 2013). Luckily, DOPAL is most often converted to DOPAC, a relatively benign metabolite, via aldehyde dehydrogenase. However, the understanding of the role of DOPAL toxicity in disease pathology, like that seen in Parkinson's disease, is growing. DOPAL itself can be oxidized, creating reactive oxygen species (Eisenhofer et al., 2004a). DOPAL has been shown to induce neurotoxicity in numerous culture systems and in mice

model lacking cytosolic and mitochondrial aldehyde dehydrogenases (Mattammal et al., 1995; Kristal et al., 2001; Rees et al., 2009; Wey et al., 2012). Additionally, DOPAL is increased in the post mortem brains of individuals with Parkinson's disease, suggesting a dysfunctional compartmentalization or breakdown of dopamine in those affected by the disease (Goldstein et al., 2011).

Cytosolic dopamine can be also autooxidized to form reactive oxygen species including hydroxyl radicals, superoxide, and hydrogen peroxide (Graham, 1978; Jenner, 2003). Oxidized dopamine can then be converted to dopamine-quinones and protein function-altering cysteinyl adducts (LaVoie and Hastings, 1999; Rabinovic et al., 2000; Lotharius and O'Malley, 2001). Additionally, dopamine synthesis proteins have been reported to interact with VMAT, helping to accumulate dopamine in synaptic vesicles. For example, TH and AADC have been immunoprecipitated with VMAT, and vesicular filling is reduced following the disruption of these interactions (Cartier et al., 2010). Based on the detrimental effects of cytosolic dopamine, it has been speculated that the relative distribution of dopamine within the neuronal terminal, perhaps mediated by vesicular storage, may be responsible for a neuron's vulnerability to injury (Uhl, 1998; Miller et al., 1999b; Guillot and Miller, 2009).

VMAT2 as a neuroprotective mechanism

The correlation between vesicular function and neuronal vulnerability is well established (**Fig. 1.2**). VMAT2 is phylogenetically related to a family of toxin extruding antiporters (TEXANs) in prokaryotes and eukaryotes and is also a member of the major facilitator superfamily (MFS) which remove toxins from the cytosol and sequester them into other intracellular compartments (Schuldiner et al., 1995; Vardy et al., 2004; Guillot

and Miller, 2009). In fact, the cloning of VMAT and its initial characterization was based on the protein's ability to confer protection from MPP+ toxicity in Chinese hamster ovary fibroblasts (CHO cells) (Liu et al., 1992a). In addition to its ability to protect from exogenous toxic insult, VMAT2 has also been shown to protect against native threats to neuronal health, including cytosolic dopamine (Guillot and Miller, 2009). While dopamine is protected when sequestered in the vesicle, it can accumulate in the cytosol following its synthesis, uptake from the extracellular space via the DAT, or even after nonspecific leak out of the synaptic vesicle (Eisenhofer et al., 2004b). As mentioned above, this unpackaged dopamine in the cytosol can be neurotoxic.

Pharmacological manipulations of vesicular filling

VMAT2 has two well-characterized inhibitors, reserpine and tetrabenazine. Reserpine, a compound isolated from Indian snakeroot *Rauwolfia serpentine,* was originally used in the treatment of hypertension (Freis, 1954). However, in addition to reserpine's ability to inhibit dopamine uptake (Kirshner, 1962; Kirshner et al., 1963), it was also noted that reserpine treatment causes a variety of side effects including gastrointestinal dysfunction, movement deficits, and negative mood (Carlsson, 1972, 1976). These mood-altering effects of reserpine gave rise to the idea that monoamine neurotransmitters may be key in affective behaviors. While the pharmacological target of reserpine was not identified for many years (Erickson et al., 1992; Liu et al., 1992b), reserpine treatment in rats recapitulated many of the behavioral effects seen in parkinsonian humans, including profound akinesia (Colpaert, 1987). In this way, reserpine provided a Parkinson's disease-like set of behavioral characteristics. VMAT2 inhibition via reserpine is also reversible by the application of a dopamine replacement therapy like L-DOPA

(Carlsson, 1972). However, because reserpine is not specific for VMAT1 or VMAT2 (Peter et al., 1994), combined with the differing central and peripheral distributions of VMAT1 and VMAT2 in the body, the reserpine-mediated CNS-specific effects of VMAT2 inhibition are often difficult to assess. Tetrabenazine (TBZ), is considered as a VMAT2-selective inhibitor, because its affinity for VMAT1 (IC_{50} = 3 μM) is much lower than for VMAT2 (IC_{50} = 0.3 μM) (Pothos, 2002; Chaudhry et al., 2008; Wimalasena, 2011; Lawal and Krantz, 2013). Unlike reserpine, TBZ acts at a binding site on VMAT2 distinct from the substrate binding site, which allows for reversible VMAT2-specific inhibition of vesicular filling (Peter et al., 1994). TBZ and other derivate compounds are currently used clinically in the treatment of hyperkinetic disorders such as chorea associated with Huntington's disease in Canada, Australia, the United Kingdom, and, more recently, in the United States (Yero and Rey, 2008; Wimalasena, 2011). In disorders of increased movement, VMAT2 inhibition dampens dopaminergic tone and release, reducing movement.

Based on the importance of vesicular storage in neurotransmission and neuroprotection, an increase in VMAT2 function could be a novel therapeutic target for diseases characterized by loss of neurons and, subsequently, decreased dopamine release. Despite an extensive history of studying the effects of pharmacological VMAT2 inhibition, there are no known positive modulators of VMAT2 function (Osherovich, 2014).

Presynaptic machinery and Parkinson's disease

Parkinson's disease is the most common neurodegenerative movement disorder. Parkinson's disease pathology is characterized by the loss of the neurotransmitter dopamine, due to the death of dopaminergic neurons in the SNpc and the accumulation of

α-synuclein inclusions known as Lewy bodies (Olanow and Tatton, 1999). Dr. James Parkinson made the first descriptions of the motor hallmarks of Parkinson's disease in 1817. In his essay titled the *Shaking Palsy*, Parkinson described the rigidity, slowed movement, and tremors that are now known as hallmarks of the disease. The dopamine deficit in the Parkinson's disease brain was first described in 1960 (Ehringer and Hornykievicz, 1960), and the subsequent replacement of the lost dopamine with L-DOPA, the neurochemical precursor in the dopamine synthesis pathway, was described the following year (Birkmayer and Hornykiewicz, 1961). As mentioned above, motor output occurs by dopamine's activation of D1 dopamine receptors in the basal ganglia's direct pathway, which disinhibits the thalamic inputs to the cortex. Dopamine release in the striatum also activates D2 dopamine receptors in the indirect pathway, which leads to thalamocortical inhibition and reduced movement. Following the loss of dopamine release from the SNpc in Parkinson's disease, an imbalance between the direct and indirect pathway emerges, and the result is a loss of motor output (Obeso et al., 1997; Calabresi et al., 2014).

Genetic mutations linked to Parkinson's disease often affect synaptic vesicle machinery, leading to deficits in trafficking, transmitter storage, and release. α-Synuclein, the first PARK locus identified, has long been known to bind to phospholipids on the vesicle membrane (Lotharius et al., 2002; Volles and Lansbury, 2002; Nemani et al., 2010). Protofibrillar α-synuclein can permeabilize the vesicular membrane, spilling dopamine into the cytosol (Volles and Lansbury, 2002); this oxidized dopamine stabilizes protofibrillar α-synuclein, creating a potentially vicious cycle of pathology (Mosharov et al., 2009; Ulusoy et al., 2012). While the normal functions of α-synuclein are poorly understood,

genetic ablation of the synuclein genes (α, β, γ) increases dopamine release, suggesting that the protein may act as a brake on transmitter release (Anwar et al., 2011).

Though perhaps the best characterized Parkinson's disease-related protein, α-synuclein is not the only link between Parkinson's disease and vesicular function. Leucine rich repeat kinase 2 (LRRK2) mutations, responsible for the majority of familial Parkinson's disease cases, alter vesicle trafficking, localization of vesicular proteins, and the release of dopamine (Piccoli et al., 2011; Belluzzi et al., 2012; Cirnaru et al., 2014). Reduced PINK1 function also decreases synaptic efficiency by immobilizing synaptic vesicles of the reserve pool (Morais et al., 2009). DJ-1 interacts with synaptic vesicle proteins such as synaptophysin and Rab3A and modifies the expression of VMAT2 (Usami et al., 2011; Osherovich, 2014). DJ-1, PINK1 and parkin knock-out mouse models all show substantial presynaptic deficits in dopamine release (Goldberg, 2005; Kitada et al., 2007; Cookson, 2012). Most recently, synaptojanin, a vesicular protein integral for endocytotic traffic at synapses was identified as a disease-causing gene of parkinsonism (Krebs et al., 2013). These results lend further support to the convergence of disrupted synaptic vesicle function and the pathogenesis in Parkinson's disease.

VMAT2 function as a disease modifier in Parkinson's disease

Although a handful of familial and spontaneous mutations have been linked to the disease, it is estimated that nearly 90-95% of Parkinson's disease cases are of unknown causes (Dauer and Przedborski, 2003; Hatcher et al., 2008). Parkinson's disease incidence rates between monozygotic and dizygotic twins are similar and the concordance rate between twins sets is extremely low (Tanner et al., 1999; Wirdefeldt et al., 2011a, 2011b). These findings in human populations suggest that additional factors contribute largely to

the development of Parkinson's disease. There has been growing evidence that environmental toxicants, including organochlorine pesticides and polychlorinated biphenyl compounds, are capable of inhibiting VMAT2 function and altering aspects of the nigrostriatal pathway (Bemis and Seegal, 2004; Richardson and Miller, 2004; Guillot and Miller, 2009). Additionally, it has been shown that chronic exposure of these toxicants and structurally-related compounds (polybrominated diphenyl ethers, PBDEs) modify transporter levels, such as DAT and VMAT2, and other dopamine-related proteins (Caudle et al., 2012; Bradner et al., 2013; Wilson et al., 2014). This may be particularly relevant in the pathophysiology of Parkinson's disease because these compounds have been identified in post-mortem Parkinson's disease brains (Hatcher-Martin et al., 2012) and correlated with the incidence of the disease (Hatcher et al., 2008; Cannon and Greenamyre, 2011).

There is growing evidence that vesicular function, perhaps in the form of VMAT2 function or expression, is a modifier of Parkinson's disease risk in human populations. Post-mortem Parkinson's disease brains show dramatically reduced VMAT2-mediated vesicular filling, and this loss is greater than what could be explained by terminal loss alone (Pifl et al., 2014). These results demonstrate that impaired dopamine storage in vesicles influences the disease process. Parkinson's disease brain has also been shown to have higher dopamine turnover, suggesting a higher level of cytosolic dopamine (Goldstein et al., 2011, 2013). These findings could be due to an impaired storage of dopamine or to non-specific dopamine leak described above. Single nucleotide polymorphisms (SNPs) or mutations within the coding regions of the VMAT2 gene (SLC18A2) are rare, likely due to the fundamental requirement of the protein for neurotransmission. The first report of a mutation within the VMAT2 gene described a Saudi Arabian family that had multiple

family members with an infantile-onset parkinsonian condition with profound motor and cognitive impairments in those affected (Rilstone et al., 2013). When the mutation was introduced in vitro, it was shown to cause drastic reductions in vesicular filling.

Increased VMAT2 level or function protects against the development of Parkinson's disease in human populations. Gain-of-function VMAT2 promoter haplotypes protect against the development of Parkinson's disease in women (Glatt et al., 2006). Two other SNPs in the promoter region of the VMAT2 gene have also been linked with a reduced Parkinson's disease risk, suggesting that increases in VMAT2 level protect against the disease (Brighina et al., 2013). Based on this growing evidence in humans, we aimed to assess the neurochemical and toxicological effects of elevated vesicular function in a mammalian system.

Phenotypes of VMAT2-deficient mice

Previous data clearly show that disruption of VMAT2 function produces adverse effects (Caudle et al., 2008a; Taylor et al., 2011). Pharmacological VMAT2 inhibition by reserpine or tetrabenazine results in monoamine depletion and negative behavioral consequences, including akinesia and depressive behaviors (Kirshner, 1962; Kirshner et al., 1963; Pettibone et al., 1984). Genetic knockout of VMAT2 gene is lethal, with animals dying a few days after birth (Wang et al., 1997a; Mooslehner et al., 2001). Through serendipitous recombination events, mice with only 5% of VMAT2 levels were also created (Mooslehner et al., 2001; Caudle et al., 2007). These mice survive into adulthood, allowing for assessments of long-term vesicular deficits. The large reduction in VMAT2 levels in the VMAT2-deficient mice dramatically reduces vesicular filling (approximately 80% reduction) and also causes depletion of dopamine, norepinephrine, and serotonin

levels throughout the brain (Caudle et al., 2007; Taylor et al., 2014). VMAT2-deficient mice also show progressive neurodegeneration in multiple monoaminergic regions, including the SNpc and the locus coeruleus (Fon et al., 1997; Caudle et al., 2007; Taylor et al., 2014). Additionally, these animals show accumulation of α-synuclein, the signature protein component in Lewy body pathology (Caudle et al., 2007).

VMAT2-deficient mice and VMAT2 heterozygote mice also show exacerbated responses in their dopaminergic pathways to toxicant exposure, including treatment with both MPTP and methamphetamine (Takahashi et al., 1997; Guillot et al., 2008b). Reduced VMAT2 also modifies a variety of monoamine-mediated behaviors, including reduced locomotor activity (Caudle et al., 2007); VMAT2-deficient mice also present non-motor behaviors reminiscent of pre-clinical Parkinson's disease, including increased depressive-like and anxiety-like behaviors, olfactory deficits, alterations to sleep latency, and gastrointestinal disturbances (Taylor et al., 2009). Taken together, evidence from the VMAT2-deficient mice has pointed out the numerous deficits arising from reduced vesicular function, while also highlighting the potential benefits of upregulating vesicular storage.

Research Overview: VMAT2-overexpressing mice

Although the detrimental effects of reduced VMAT2 function are recognized as discussed above, our understanding of the potential benefits of increased VMAT2 function in vivo has been limited to a *Drosophila* model (Chang et al., 2006a; Sang et al., 2007; Lawal et al., 2010). Increasing VMAT2 function holds great potential to both increase neurochemical output and neuroprotection in vulnerable nigrostriatal cell populations (**Fig. 1.3**). Thus, we generated VMAT2-overexpressing mice using a bacterial artificial

chromosome (BAC) to determine whether increased vesicular packaging could provide an elevation of monoamine output in a mammalian system.

Through BAC-mediated VMAT2 overexpression, the studies that follow examine the effects of permanently elevated vesicular storage on neurochemical, behavioral, and toxicological outcomes in a mouse. In brief, we show that elevated VMAT2 expression enhances the capacity of the vesicle to store dopamine. Due to this enhanced storage, VMAT2-overexpressing mice have increased total dopamine content and synaptic vesicle size. The elevated vesicular filling translates to elevated dopamine release and changes to monoamine-related behaviors. Additionally, VMAT2-overexpressing mice are resistant to neurotoxic insults, including MPTP and methamphetamine intoxication, based on VMAT2's neuroprotective abilities. Finally, VMAT2 has been shown to modify the neuron's response to a large increase in exogenous dopamine, via elevated extracellular clearance of dopamine following L-DOPA treatment. These data are complemented by new results from backcrossed VMAT2-deficient mice, providing a tool to assess the genotypic continuum of vesicular function in multiple mouse lines. Together, these findings suggest that elevated VMAT2 would be beneficial to enhance neuronal monoamine output, protect vulnerable dopamine neuronal populations, and improve monoamine handling at the synapse.

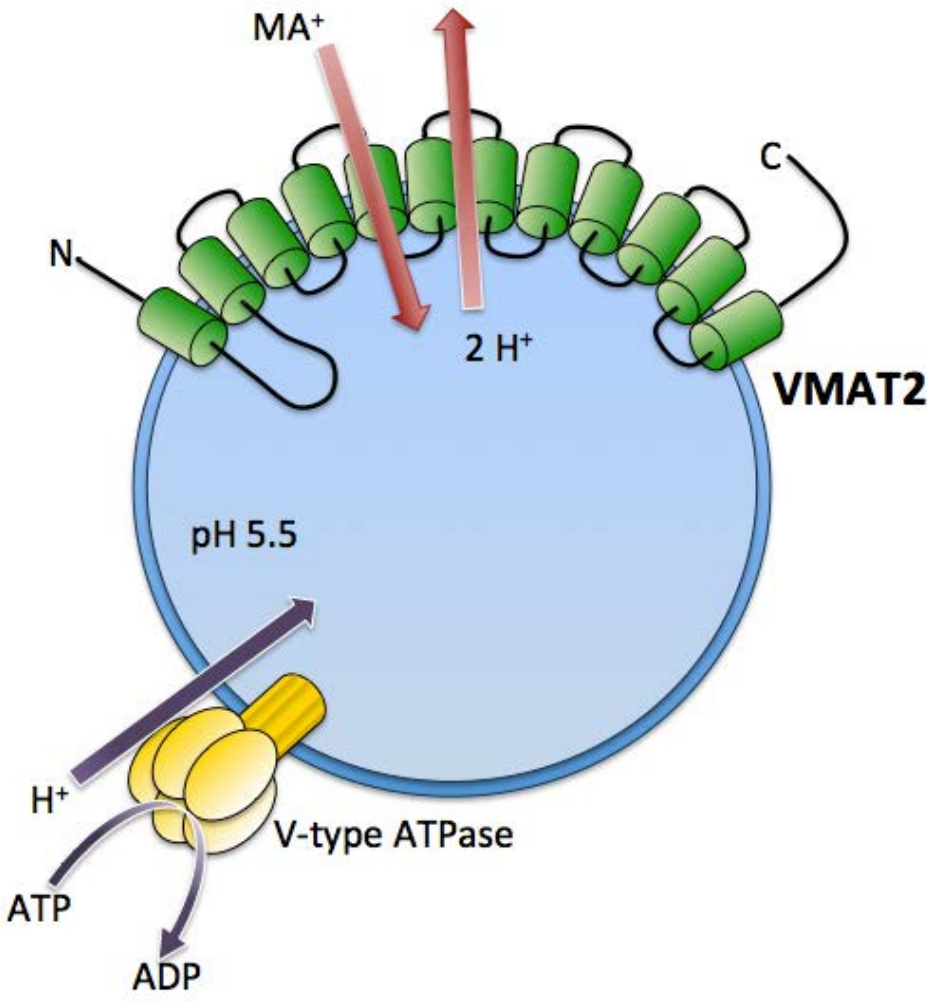
MA+
C
N
2 H+
VMAT2
pH 5.5
H+
V-type ATPase
ATP
ADP

Figure 1.1. The vesicular monoamine transporter 2 (VMAT2; Slc18a2).

VMAT2 packages monoamine (MA) neurotransmitters (dopamine, norepinephrine, serotonin, and histamine) into vesicles so that they may be released from the neuron upon an action potential. The V-type ATPase establishes the acidic intravesicular compartment, which provides the driving force for VMAT2 to transport neurotransmitter. VMAT2 has 12 transmembrane domains and a large intralumenal loop that has multiple glycosylation sites within the vesicles.

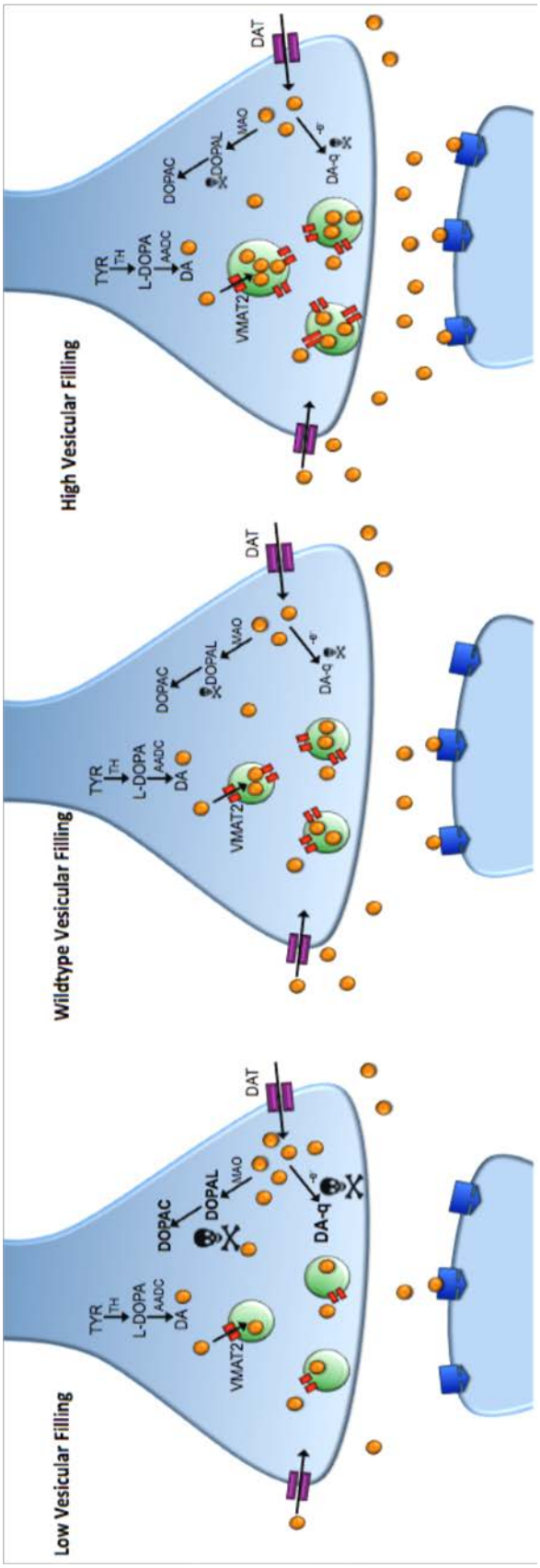
High Vesicular Filling
Wildtype Vesicular Filling
Low Vesicular Filling
TYR
TH
L-DOPA
AADC
DA
VMAT2
DOPAC
DOPAL
MAO
DA-q
DAT

Figure 1.2. Model of altered vesicular function.

(Left) Animals with low expression of VMAT2 (VMAT2-LO) have massively reduced vesicular filling. Thus, these VMAT2-LO mice also have high levels of potentially harmful cytosolic dopamine, which likely contributes to their progressive neurodegeneration in catecholaminergic regions. Additionally, VMAT2-LO mice have low levels of stored transmitter, resulting in less released neurotransmitter and behavioral changes. (Right) Conversely, animals with higher VMAT2 expression (VMAT2-HI) have increased vesicular filling. These VMAT2-HI mice would presumably have less cytosolic dopamine accumulation, increased synaptic neurotransmitter output, and altered behavioral outcomes. Until the work described here, it was unclear if such permanent augmentation of vesicular capacity was possible in a mammalian system. (Center) Wildtype animals would fall in between these two genotypes with intermediate levels of transmitter release and behavioral outputs.

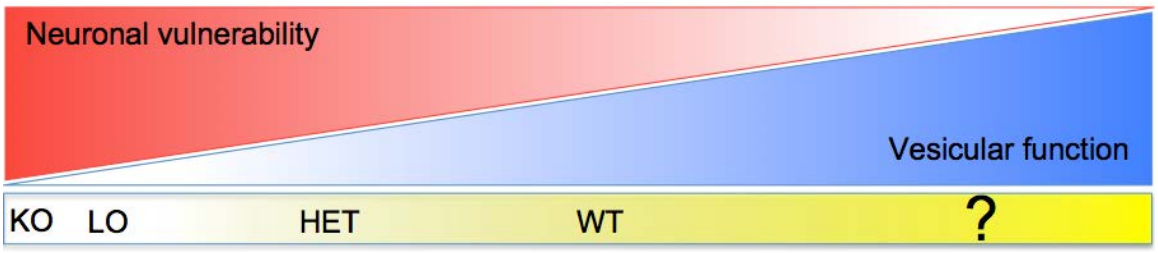
Neuronal vulnerability
Vesicular function
KO
LO
HET
WT
?

Figure 1.3. The vesicular function continuum.

In the predicted model of vesicular function, vesicular storage lies on a continuum (low to high), and neuronal vulnerability to an insult is inversely correlated with this vesicular filling. Thus, mice with low vesicular function (VMAT2-LO) will have higher vulnerability to insult than their wildtype littermates. However, an animal model to assess the effects of increased vesicular function beyond a wildtype level did not exist until the work described here. Thus, it was our hypothesis that animals with very high levels of vesicular filling (VMAT2-HI) would be resistant to insult.

CHAPTER II: BAC-MEDIATED VMAT2 OVEREXPRESSION INCREASES VMAT2 PROTEIN CONTENT AND DOPAMINE OUTPUT IN THE VMAT2-HI MICE

These findings have been previously reported as written in:

Lohr KM et al. (2014) Increased vesicular monoamine transporter enhances dopamine release and opposes Parkinson disease-related neurodegeneration in vivo. *Proc Natl Acad Sci* 111:9977–82.

Introduction

Limitations to vesicular filling

It had been previously postulated that a variety of factors that may limit the packaging of neurotransmitter into monoaminergic vesicles (Edwards, 2007). These models include the set point, equilibrium, leak, and swelling models of vesicular storage. The set point model suggests that vesicles have a set maximum independent of the number of vesicular transporters on the membrane. This could be dictated by equilibrium across the membrane or even physical limitations of the biomechanics of the vesicular membrane. In the equilibrium model, the vesicular ATPase creates the electrochemical H^+ gradient that is the driving force for filling via VMAT2. Once the H^+ gradient is eliminated and equilibrium is reached between the cytosol and the vesicular lumen, monoamine packaging would stop. Finally, it is possible that the biomechanics of the vesicular membrane may act as the limiting factors of filling. In vitro evidence has shown that L-DOPA application and VMAT2 inhibition has the potential to alter vesicle size (Bruns et al., 2000; Colliver et al., 2000; Pothos, 2002; Gong et al., 2003). This suggests that the inner concentration of transmitter inside of a vesicle does not increase; rather it is merely the volume of the vesicle increasing. These previous results also showed that the limitations to the elasticity of membranes may be less stringent than previously thought. Finally, it was assumed that an increase in vesicular filling would result in compensatory changes to the rest of the dopamine system (e.g. increased DAT function, decreased TH activity, altered receptor sensitivity) that would downregulate dopamine output. Based on the assumptions the dopamine system was limited by these factors, manipulations to enhance vesicular storage have not been explored in an in vivo model of permanently increased vesicular packaging.

Faulty monoamine neurotransmission is characteristic of many disorders, including Parkinson disease, depression, dystonia, attention deficit hyperactivity disorder, schizophrenia, addiction, and Huntington disease (Freis, 1954; Carlsson, 1972; Klawans et al., 1972; Creese et al., 1976; Eisenberg et al., 1988; Ritz et al., 1988; Song et al., 2012). Several strategies have been used to enhance monoamine signaling: administration of precursors to increase synthesis, inhibition of enzymes to prevent metabolism/degradation, inhibition of plasma membrane transporters to increase synaptic lifespan, and administration of receptor agonists to directly activate postsynaptic targets. However, these therapies fail to preserve many, if not all, of the critical aspects of chemical neurotransmission: normal transmitter synthesis, activity-dependent transmitter release and receptor activation, and receptor recovery following signal termination both by transmitter uptake and metabolism. Thus, these approaches often produce deleterious side effects or lose efficacy over time.

As mentioned in the Introduction, increasing the neurotransmitter content in the synaptic vesicle may represent a therapeutic approach capable of increasing the release of monoamines without the aforementioned adverse effects. VMAT2is responsible for the packaging of neurotransmitter into vesicles for subsequent release from monoaminergic neurons(Erickson et al., 1992; Liu et al., 1992b; Erickson and Eiden, 1993). VMAT2 is also essential for survival of dopamine neurons as cytosolic dopamine is neurotoxic (Sulzer and Zecca, 1999; Goldstein et al., 2013). By sequestering intracellular dopamine into vesicles, VMAT2 prevents cytosolic dopamine accumulation and its subsequent conversion to neurotoxic species (Ben-Shachar et al., 1995; Caudle et al., 2008b; Mosharov et al., 2009; Ulusoy et al., 2012; Alter et al., 2013). Thus, VMAT2 serves two primary

functions: to mediate monoamine neurotransmission and to counteract intracellular toxicity.

Previous data clearly show that disruption of VMAT2 function produces adverse effects. Pharmacological VMAT2 inhibition by reserpine or tetrabenazine results in monoamine depletion and negative behavioral consequences, including akinesia and depressive behaviors (Kirshner, 1962; Kirshner et al., 1963; Pettibone et al., 1984). Genetic reduction of VMAT2 in mice also causes depletion of dopamine, norepinephrine, and serotonin and progressive neurodegeneration in multiple monoaminergic regions (Fon et al., 1997; Takahashi et al., 1997; Wang et al., 1997b; Caudle et al., 2007; Taylor et al., 2014). Similarly, a VMAT2 mutation in humans that dramatically reduces vesicular function was recently linked to an infantile parkinsonism-like condition with symptoms caused by deficits in all of the monoamines (Rilstone et al., 2013). SNPs in the VMAT2 gene have also been associated with neurocognitive function in relatives of patients with schizophrenia and even in posttraumatic stress disorder (Simons and van Winkel, 2013; Solovieff et al., 2014). Interestingly, haplotypes within the VMAT2 promoter region that increase VMAT2 expression have been associated with a decreased risk of Parkinson's disease (Glatt et al., 2006; Brighina et al., 2013). Although the detrimental effects of reduced VMAT2 function are recognized, our understanding of the potential benefits of increased VMAT2 function in vivo has been limited to a Drosophila model (Chang et al., 2006b; Sang et al., 2007; Lawal et al., 2010).

BAC transgenic overexpression of VMAT2

We generated VMAT2-overexpressing mice using a bacterial artificial chromosome (BAC) to determine whether increased vesicular packaging could provide an

elevation of monoamine output in a mammalian system. We report here that VMAT2-overexpressing mice (VMAT2-HI) have increased vesicle capacity and increased synaptic dopamine release. These data demonstrate that the manipulation of vesicular capacity is capable of providing a sustained enhancement of the dopamine system and suggest that the vesicle is a viable therapeutic target for numerous monoamine-deficient disorders.

Methods

Generation of Transgenic Mice

BAC RP23-292H20 contains the entire vesicular monoamine transporter 2 (VMAT2) (Slc18a2) locus (35 kb), 100 kb upstream and 60 kb downstream. The choice of the BAC was important so that the endogenous promoter sequence of the VMAT2 gene would remain intact and allow for proper transcriptional control of the gene. BAC DNA was introduced into C57BL/6 and FVB embryos using pronuclear injection. A total of 12 lines were generated (8 FVB and 4 C57BL/6), 5 of which showed functional elevated VMAT2 as confirmed by Western blot and [^{3}H]-dopamine vesicular uptake assays. Positive founders were identified by PCR genotyping using primers against BAC sequences and confirmed by Southern blotting. Line 1 was chosen based on its robust VMAT2 expression and increased vesicular uptake and was designated VMAT2-HI.

Animals

VMAT2-HI founders were bred to Charles River C57BL/6 breeders for characterization. Four- to 6-month-old male and female mice were used for all studies except where noted; 6- to 8-month-old mice were used for voltammetry. Mice received food and water ad libitum on a 12:12 light cycle unless otherwise noted. All procedures were conducted in accordance with the National Institutes of Health Guide for Care and Use of Laboratory Animals and approved by the Institutional Animal Care and Use Committee at Emory University.

Western blotting

Western blots were performed as previously described (Caudle et al., 2007). Primary antibodies used were: polyclonal rabbit anti-VMAT2 serum (1:20,000), rat anti-DAT (1:5,000), rabbit anti-TH (1:1,000), mouse anti-GFAP (1:5,000) and mouse anti-β-

actin (1:5,000). The appropriate HRP-linked secondary antibodies (1:5,000) were used. Analysis was calibrated to coblotted dilutional standards of pooled sample from all VMAT2-HI samples.

Immunohistochemistry

Immunohistochemistry was performed as previously described (Caudle et al., 2007). Primary antibodies used were: polyclonal rabbit anti-VMAT2 serum (1:50,000), rat anti-DAT (1:1,000), mouse anti-GFAP (1:1,000) or rabbit anti-TH (1:1,000). The appropriate biotinylated secondary antibodies (1:200) were used. Nissl stain was performed for stereological analysis by a 3 min Cresyl Violet dip of mounted sections prior to dehydration, xylene clearing and coverslipping. All images were acquired with NeuroLucida (MicroBrightField).

Stereological Analysis

Stereological sampling was performed using the Stereo Investigator software, and the number of neurons in the SNpc was estimated using the optical fractionator method (MicroBrightField). Parameters, cell-type definition, and counting intervals were also the same as previously described (Taylor et al., 2014).

HPLC determination of catecholamines and metabolites

Mice were decapitated and their brains were immediately dissected for dorsal striata. Tissues were frozen in liquid nitrogen, and catechol levels were measured by liquid chromatography with electrochemical detection after batch alumina extraction at the Clinical Neurochemistry Laboratory of the Clinical Neurocardiology Section in intramural NINDS (Goldstein et al., 2011). Catechols of interest included dopamine and dihydroxyphenylacetic acid (DOPAC, the main neuronal metabolite of DA).

Fast-scan cyclic voltammetry in striatal slice

Slice FSCV was performed as previously described (Kile et al., 2012). A 5-recording survey of 4 different dorsal striatal release sites was taken for each animal with a 5-minute rest interval between each synaptic stimulation (2.31 V). Application of waveform, stimulus, and current monitoring was controlled by TarHeel CV [University of North Carolina (UNC)] using a custom potentiostat (UEI, UNC Electronics Shop). The waveform for dopamine detection consisted of a −0.4 V holding potential versus an Ag/AgCl (In Vivo Metric) reference electrode. The applied voltage ramp goes from −0.4 V to 1.0 V and back to -0.4 V at a rate of 600 V/s at 60 Hz. Maximal release at striatal sites in a slice was averaged. Carbon-fiber microelectrodes were calibrated with dopamine standards using a flow-cell injection system. Kinetic constants were extracted using nonlinear regression analysis of release and uptake of dopamine.

Statistical analysis

All data were analyzed in GraphPad Prism. Differences between genotypes were compared by two-tailed *t* tests, except where indicated. One-tailed *t* tests, assuming increases in the VMAT2-HI mice, were used in analyses where lower VMAT2 function has previously been shown to result in reduced outcomes (e.g., HPLC) (Caudle et al., 2007, 2008b). Outliers were defined by the Grubbs' test for outliers ($\alpha = 0.05$). All errors shown are SEM.

Results

VMAT2 overexpression in VMAT2-HI mice

BAC transgenic mice were generated by pronuclear injection of linearized BAC clone RP23-292H20, which contains the full-length *Slc18a2* sequence and presumably all of the promoter and regulatory sequences for proper spatial and temporal VMAT2

expression. Founders were identified by PCR and confirmed by Southern blot with probes against the BAC sequence. We observed increased VMAT2 expression and vesicular uptake in multiple C57BL/6 and FVB BAC-positive mouse lines, suggesting that the results presented here are not due to a founder or insertion effect. We focused on one line that exhibited significant VMAT2 overexpression, designated VMAT2-HI. Copy-number estimation by genomic quantitative PCR (qPCR) for *Slc18a2* confirmed that BAC-positive VMAT2-HI mice carry three copies of the BAC, bringing their total number of VMAT2 gene copies to five ($p < 0.0001$) (**Fig. 2.2**, Southern blot *Inset*). These three BAC copies have likely integrated in tandem at a single locus because we observe Mendelian inheritance patterns of the BAC in the VMAT2-HI colony. VMAT2 overexpression was confirmed in midbrain dopamine pathways (**Fig. 2.2**) and in serotonergic and noradrenergic cell bodies (**Fig. 2.3**) by immunohistochemistry. We observed no changes in expression of other presynaptic dopamine markers, including tyrosine hydroxylase (TH) and the dopamine transporter (DAT) as measured by immunoblotting and immunohistochemistry (**Fig. 2.4**). We also saw no overt health concerns, reproductive or fecundity issues, or premature deaths.

Increased vesicular capacity for dopamine increases striatal dopamine content in VMAT2-HI mice

VMAT2-HI mice showed a 21% increase in striatal dopamine content as measured by HPLC ($p < 0.05$, one-tailed t test) (**Fig. 2.5**). Stereological counts of both nigral tyrosine hydroxylase-positive (TH+) neurons (WT v. HI, 4,884 ± 399 v. 5,121 ± 396, $p = 0.68$, $n = 6$) and Nissl-positive neurons (WT v. HI, 3,206 ± 503 v. 3,293 ± 591, $p = 0.91$) showed no difference between genotypes, confirming that this enhanced dopamine content is not due

to an increase in the number of midbrain neurons in the VMAT2-HI mice and have shown that they have normal body weight (data not shown).

Increased synaptic dopamine release in VMAT2-HI mice

To determine whether the increased vesicular dopamine capacity in the VMAT2-HI mice leads to enhanced neurotransmitter release, we assessed dopamine terminal function using fast-scan cyclic voltammetry (FSCV) in striatal slices. VMAT2-HI mice had an 84% increase in stimulated dopamine release in the dorsal striatum ($p < 0.05$) (**Fig. 2.6**), demonstrating that enhanced vesicular capacity translates to increased synaptic release of dopamine. There was no change in the DAT-mediated uptake of extracellular dopamine as measured by the rate constant tau ($p > 0.05$).

Discussion

VMAT2-HI mice reveal an unexpected enhancement of vesicular storage capacity

We have shown that the overexpression of VMAT2 enhances vesicular uptake and capacity in vivo and that the vesicles from wildtype mice never reach the same level of vesicular filling as those from VMAT2-HI mice, no matter the length of time allowed for this uptake in a time-course experiment (data not shown). These results are in contrast to some common perceptions about in vivo vesicle capacity, which had assumed that baseline vesicular storage might be at its maximum once equilibrium is reached across the membrane. In this scenario, the amount of VMAT2 would have no effect on vesicle content. However, in vitro work has shown in both chromaffin cells and dopamine neurons that VMAT2 overexpression alters quantal size independent of activity (i.e., regardless of the speed of vesicle recycling) (Pothos et al., 2000). Recent evidence, including the in vivo results presented here with the VMAT2-HI mice, suggests that membrane equilibrium is not a limiting factor to monoamine vesicle filling(Colliver et al., 2000; Pothos et al., 2000; Pothos, 2002; Gong et al., 2003).

VMAT2 overexpression increases dopamine release and neurotransmission without compensatory changes to other presynaptic functions

Overexpression of VMAT2 has been shown to increase dopamine release by increasing quantal size in both chromaffin cells and primary midbrain culture (Pothos et al., 2000; Pothos, 2002). Similarly, VMAT2-HI mice show an 84% increase in stimulated striatal dopamine release (**Fig. 2.6**) and a corresponding 44% increase in basal extracellular dopamine levels (data not shown). This enhanced transmitter release suggests elevated dopamine neurotransmission in these mice, a finding reflected in previous work on the overexpression of the Drosophila vesicular monoamine transporter (DVMAT-A) (Chang

et al., 2006a; Sang et al., 2007; Lawal et al., 2010). Together with previous findings demonstrating reduced dopamine release and locomotion in VMAT2-deficient animals, the results from the VMAT2-HI mice suggest that there is a gene dosage-dependent regulation of vesicular capacity and dopamine output (Fon et al., 1997; Travis et al., 2000; Patel et al., 2003).

Evidence suggests that enhanced dopamine release via molecules like amphetamine or cocaine can change DAT expression and localization (Kahlig and Galli, 2003). Because VMAT2-HI mice show both increased dopamine release and increased extracellular dopamine levels, we anticipated that there would be compensatory changes to DAT or other dopamine mediators. However, VMAT2-HI mice show no differences in levels of DAT or TH (**Fig. 2.4**), or in indirect estimates of transmitter clearance by voltammetry (rate constant, tau) and microdialysis (data not shown). These data suggest that the enhancement of the dopamine system is sustained without major compensatory changes to other mediators of presynaptic dopamine dynamics in the VMAT2-HI mice. In addition, VMAT2-HI mice display and maintain monoamine-mediated behavioral phenotypes, suggesting that receptor levels or function have not overcome these presynaptic alterations.

VMAT2-HI phenotypes contrast with vesicular transporter overexpression in nonmonoamine transmitter systems

We present many positive effects of VMAT2 overexpression; however, overexpression of other vesicular transporters has produced mixed results. Vesicular acetylcholine transporter (VAChT) overexpression increases EPSCs in Xenopus (Song et al., 1997) and increases acetylcholine release in mouse hippocampal slice (Nagy and Aubert, 2012). ChAT–ChR2–EYFP mice, which also carry several copies of the VAChT

gene, show severe cognitive deficits in attention and memory (Kolisnyk et al., 2013). Evidence from the glutamate system had suggested that compensatory changes would override any increased monoamine output in the VMAT2-HI mice. Overexpression of the vesicular glutamate transporter (VGLUT1) increases excitatory synaptic transmission in hippocampal culture (Wilson et al., 2005). Additionally, DVGLUT overexpression in Drosophila increases both quantal size and synaptic vesicle volume (Daniels et al., 2004). However, these changes are accompanied by compensatory decreases in the number of synaptic vesicles released, resulting in no net change in neurotransmission. Thus, the enhanced dopamine release in the VMAT2-HI mice, an intact mammalian model also subject to compensation, indeed provide an unexpected contrast to the acetylcholine and glutamate systems.

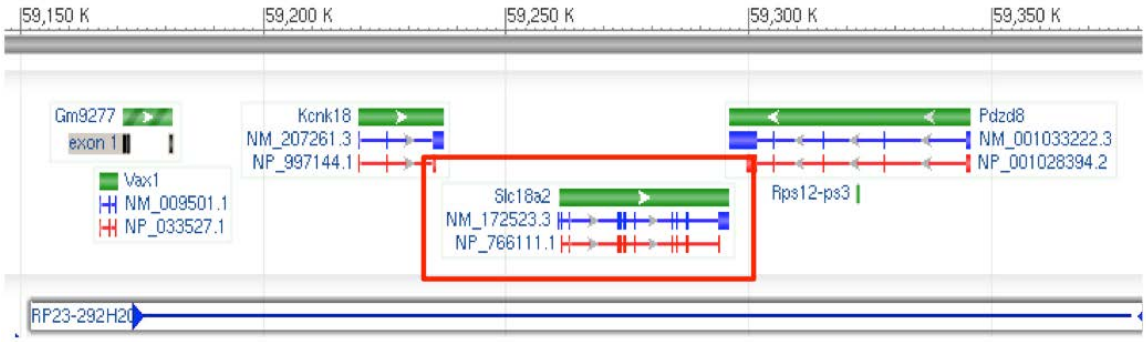
59,150 K
59,200 K
59,250 K
59,300 K
59,350 K
Gm9277
exon 1
Vax1
NM_009501.1
NP_033527.1
Kcnk18
NM_207261.3
NP_997144.1
Slc18a2
NM_172523.3
NP_766111.1
Rps12-ps3
Pdzd8
NM_001033222.3
NP_001028394.2
RP23-292H20

Figure 2.1. The bacterial artificial chromosome.

BAC RP23-292H20 contains the entire vesicular monoamine transporter 2 (VMAT2) (Slc18a2) locus (35 kb), 100 kb upstream and 60 kb downstream.

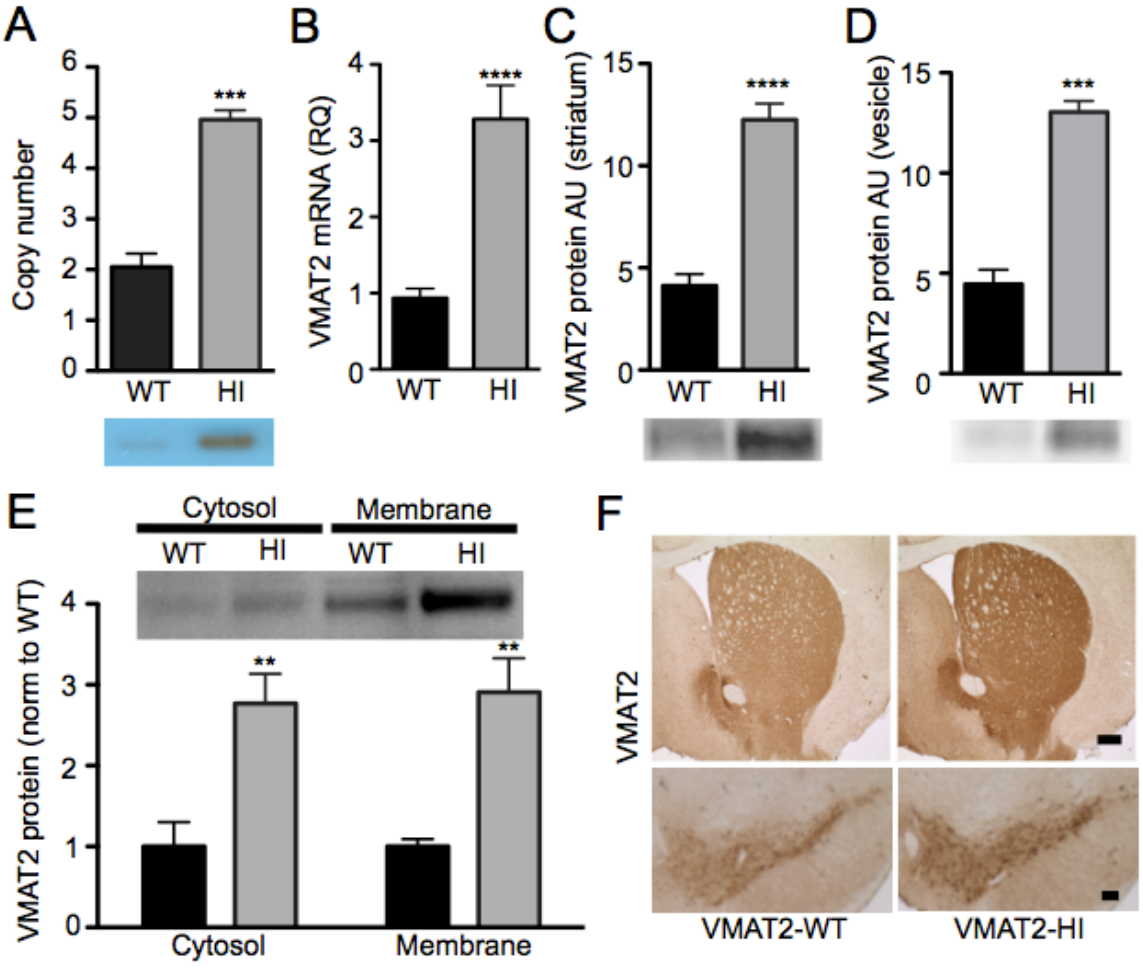
A
Copy number
6
5
4
3
2
1
0
***
WT
HI
B
VMAT2 mRNA (RQ)
4
3
2
1
0
****
WT
HI
C
VMAT2 protein AU (striatum)
15
10
5
0
****
WT
HI
D
VMAT2 protein AU (vesicle)
15
10
5
0
***
WT
HI
E
Cytosol
Membrane
WT
HI
WT
HI
VMAT2 protein (norm to WT)
4
3
2
1
0
**
**
Cytosol
Membrane
F
VMAT2
VMAT2-WT
VMAT2-HI

Figure 2.2. Increased VMAT2 expression in the VMAT2-HI mice.

(A) The VMAT2- HI genome contain three insertions of the BAC by genomic qPCR (n = 4). Southern blot against Slc18a2 (Inset). (B) VMAT2-HI mice have 3.5-fold more VMAT2 mRNA than wildtype by qPCR (n = 12–13). (C and D) VMAT2-HI mice show a threefold increase in VMAT2 expression by immunoblot of striatal tissue (n = 6) and whole brain vesicular fraction (n = 6). (E) VMAT2-HI mice show a threefold increase in VMAT2 expression in both cytosolic and membrane fractions. (F) VMAT2 immunohistochemistry of striatal and midbrain sections. Scale bar = 200 μm.

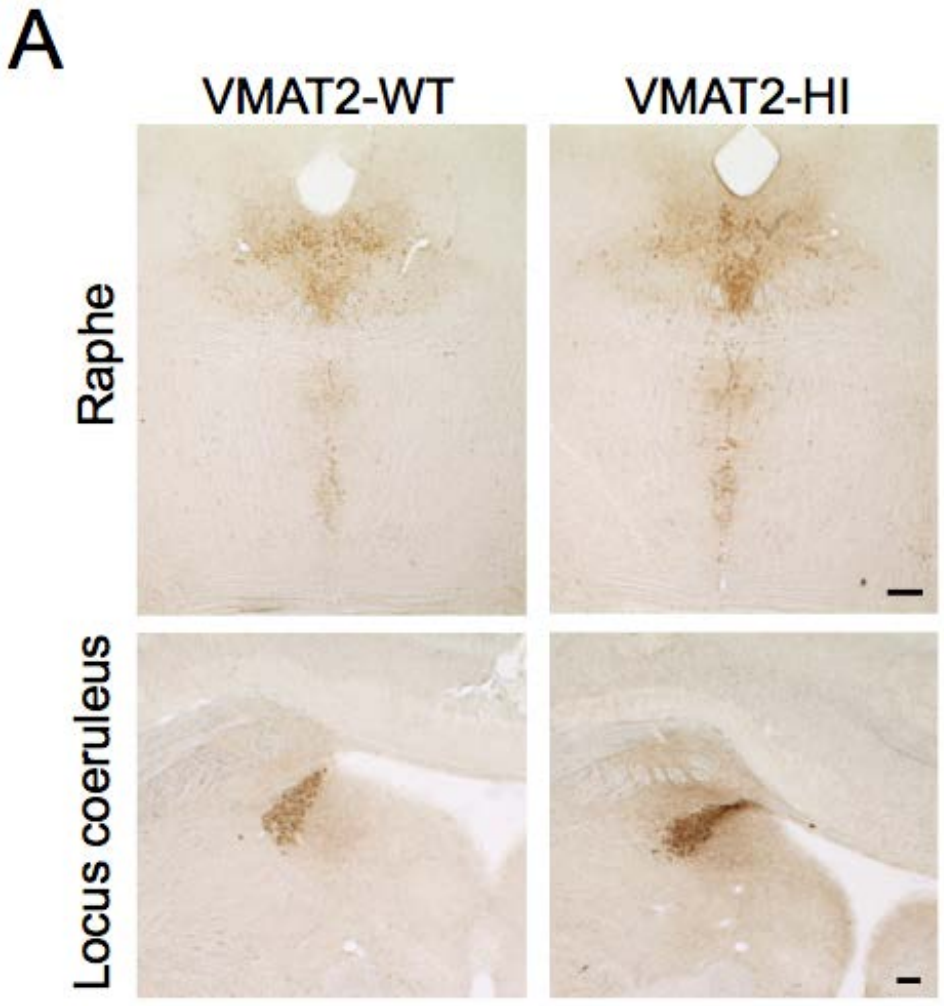
A
VMAT2-WT
VMAT2-HI
Raphe
Locus coeruleus

Figure 2.3. VMAT2 overexpression occurs in all monoaminergic brain regions in the VMAT2-HI mice.

VMAT2 overexpression is seen in both the serotonin-producing regions of the raphe nucleus and the norepinephrine-producing regions of the locus coeruleus. Scale bar = 200 μm

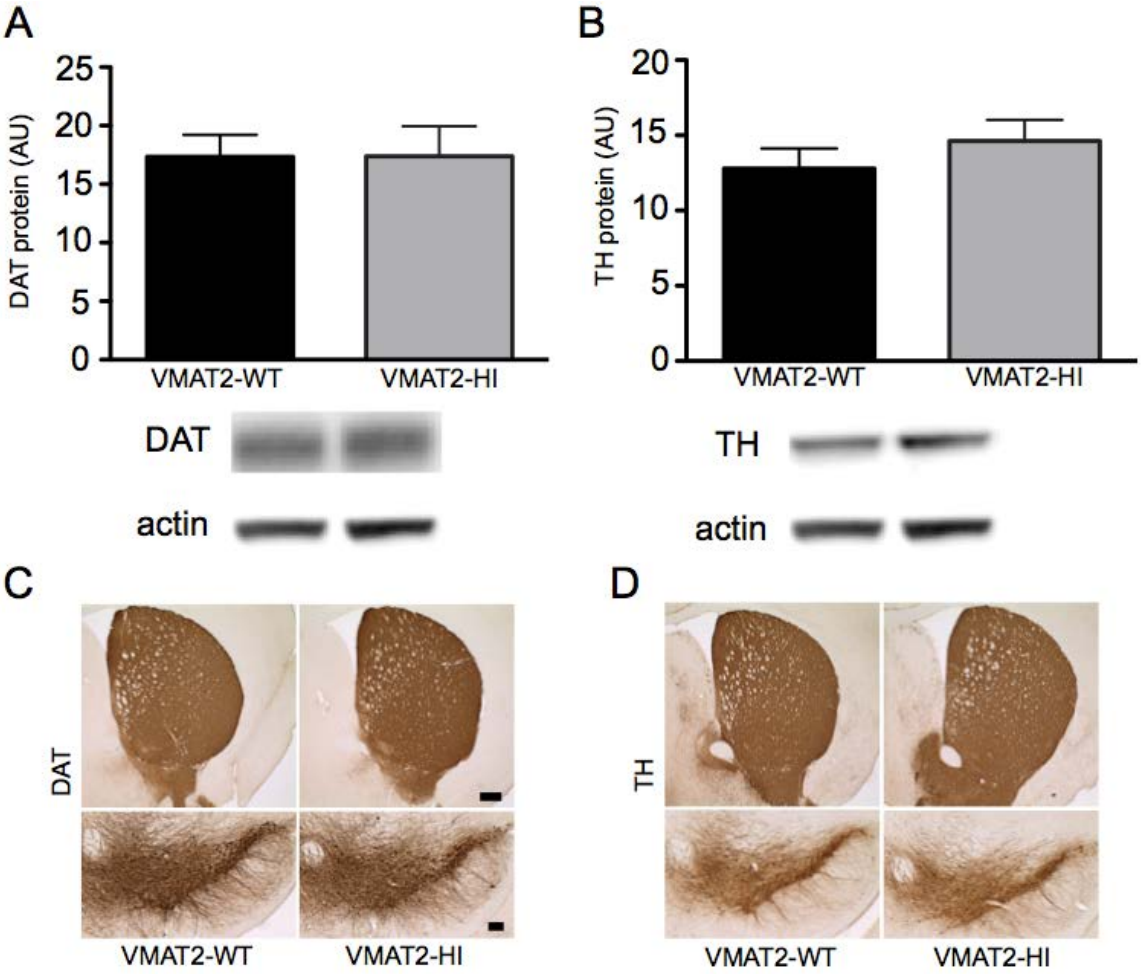
A
DAT protein (AU)
25
20
15
10
5
0
VMAT2-WT
VMAT2-HI
DAT
actin
B
TH protein (AU)
20
15
10
5
0
VMAT2-WT
VMAT2-HI
TH
actin
C
DAT
VMAT2-WT
VMAT2-HI
D
TH
VMAT2-WT
VMAT2-HI

Figure 2.4. DAT and TH levels are unchanged in the VMAT2-HI mice.

Both by immunoblotting and immunohistochemistry, VMAT2-HI mice show no changes in expression levels of either DAT (A,C) or TH (B,D) in dopaminergic brain regions. Scale bar = 200 μm

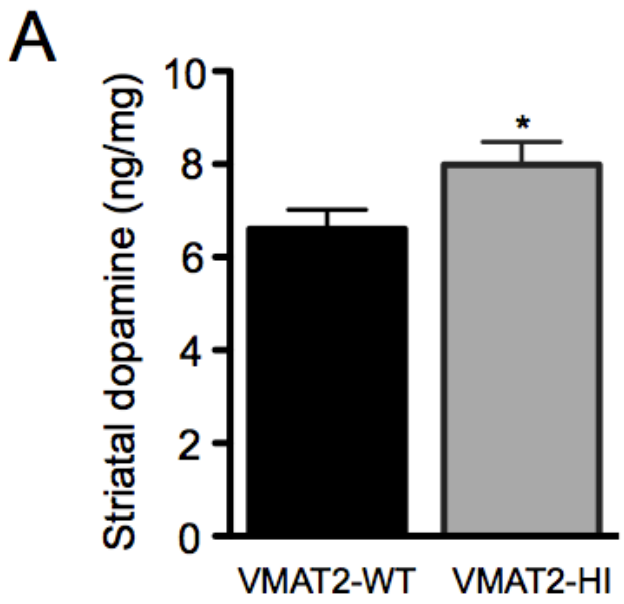
A
Striatal dopamine (ng/mg)
10
8
6
4
2
0
*
VMAT2-WT
VMAT2-HI

Figure 2.5. Increased dopamine levels in the striatum of VMAT2-HI mice.

HPLC measurements of total dopamine levels from striatal brain dissections shows a ~20% increase in dopamine content in the VMAT2-HI mice (one-tailed, $p < 0.05$; $n = 20$).

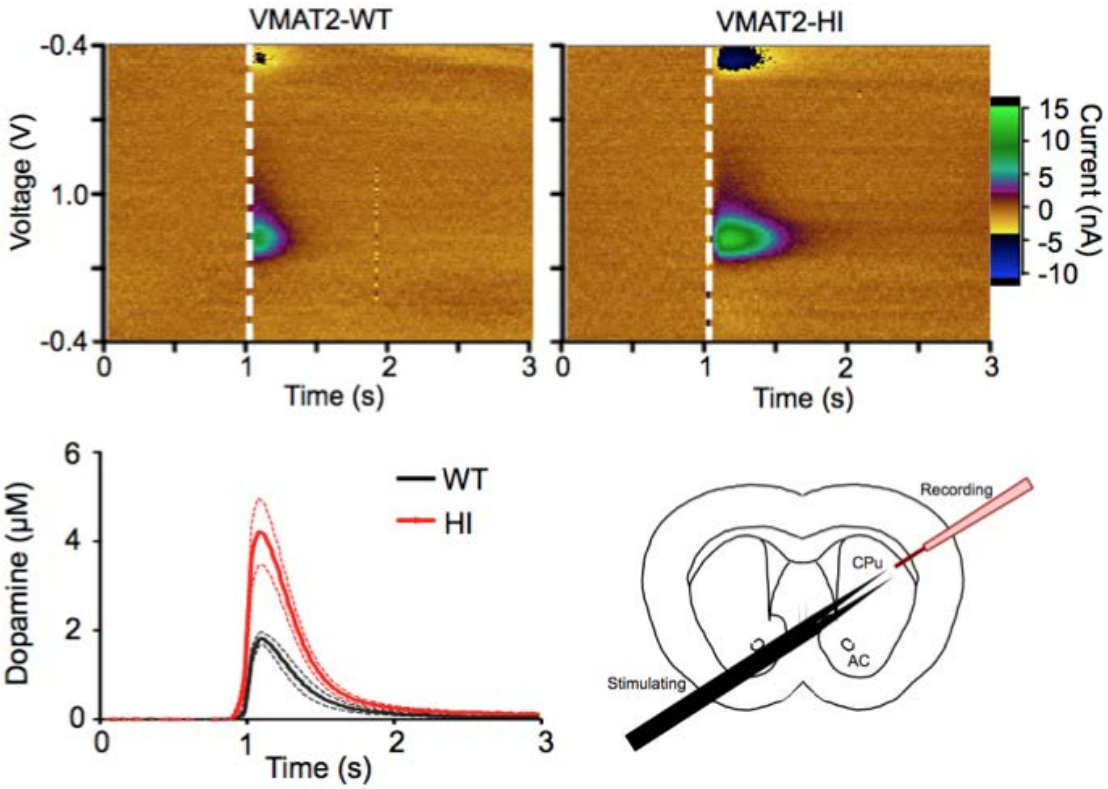
VMAT2-WT
VMAT2-HI
-0.4
1.0
-0.4
Voltage (V)
0
1
2
3
Time (s)
15
10
5
0
-5
-10
Current (nA)
6
4
2
0
Dopamine (μM)
WT
HI
Time (s)
Recording
CPu
AC
Stimulating

Figure 2.6. Increased stimulated dopamine release in VMAT2-HI mice.

Increased striatal dopamine release and extracellular dopamine in the VMAT2-HI mice. VMAT2-HI mice show an 84% increase in stimulated dopamine release as measured by fast-scan cyclic voltammetry in striatal slice (n = 5–6). (top) Representative colorplots (uncalibrated to electrode sensitivity). (bottom) Average stimulated dopamine-release traces and experimental schematic

(Acknowledgment for FSCV drawing, A. Dunn)

CHAPTER III: VMAT2-OVEREXPRESSING (VMAT2-HI) MICE SHOW ALTERED OUTCOMES IN MONOAMINE-MEDIATED BEHAVIORS

These findings have been previously reported as written in:

Lohr KM et al. (2014) Increased vesicular monoamine transporter enhances dopamine release and opposes Parkinson disease-related neurodegeneration in vivo. *Proc Natl Acad Sci* 111:9977–82.

Introduction

Monoamine neurotransmitters (dopamine, serotonin, and norepinephrine) are integral to many mammalian behaviors. Based on the increased neurochemical output measured in the VMAT2-HI mice (Chapter II), it was expected that they would display alterations in monoamine-mediated behaviors. It should be noted that all of the behaviors discussed here are thought to be mediated by, but not solely dependent upon, single monoamine neurotransmitters. Since the VMAT2-HI mice are not characterized in all of the monoamine systems, we must assume that they exhibit augmented release in the serotonin and norepinephrine-producing regions of the brain as well.

Dopamine is most often linked to movement and reward-seeking behaviors (Beninger, 1983; Koob, 1992; Haber, 2014). Dopamine cell bodies are located in the midbrain with projections in the dorsal and ventral striatum (Swerdlow and Koob, 1987b). Dopamine release in the dorsal striatum mediates movement, whereas dopamine release in the ventral striatum or the nucleus accumbens mediates reward signaling (Fibiger and Phillips, 1988). To assess changes in motor output, VMAT2-HI and wildtype mice were assessed on circadian activity. VMAT2-deficient mice (95% reduction in VMAT2 level) develop progressive locomotor deficits with aging (Caudle et al., 2007) and pharmacological VMAT2 inhibition by reserpine and tetrabenazine have also been shown to reduce movement (Quinn et al., 1959; Pettibone et al., 1984; Zarrindast and Eliassi, 1991). Based on these results, we predicted that the VMAT2-HI mice would exhibit elevated locomotor activity levels. We also examined sleep latency measures in the VMAT2-HI mice based on the importance of monoamine modulation of alertness. Abnormal sleep latencies following perturbation were shown in the VMAT2-deficient

mice (Taylor et al., 2009), so it was important to eliminate this as a potential confound of circadian changes in the VMAT2-HI mice.

To examine reward-associated behaviors, we performed sucrose consumption, a measure of anhedonia (Papp et al., 1991), and preliminary assessments of response to psychostimulants in the VMAT2-HI mice. VMAT2-heterozygous mice (50% reduction in VMAT2 level) show a reduced preference for various concentrations of sucrose solution compared to wildtype littermates, suggesting an anhedonic phenotype when VMAT2 expression is decreased (Fukui et al., 2007). Thus, we predicted that the VMAT2-HI mice would show increases in sucrose consumption. We also assessed psychostimulant response in the VMAT2-HI mice using a low dose of amphetamine (1 mg/kg). Because amphetamine induces an efflux of dopamine stores and the VMAT2-HI mice show a significant increase in basal dopamine content and stimulated dopamine release (Chapter II), we expected the VMAT2-HI mice to have an increased response to amphetamine.

Serotonin is a mediator of many behaviors including affective behaviors, feeding, and arousal (Frazer and Hensler, 1999). Serotonin is produced in cells originating in the dorsal raphe of the midbrain, with projections throughout the forebrain and cortex (Aghajanian et al., 1967; Moore et al., 1978). Depression is an extremely difficult behavior to assess in an animal model. The forced swim test, for example, is actually a measure of antidepressant efficacy (Porsolt, 1979). Immobility measures on this behavior may also reflect variations in stress-induced behavioral depression or locomotor activity and should be interpreted cautiously. VMAT2-deficient mice show an age-dependent depressive-like phenotype demonstrated by an increased immobility time on the forced swim test (Taylor et al., 2009). This deficit in the VMAT2-deficient mice also can be rescued to wildtype

levels with antidepressants (Taylor et al., 2009). Based on these data, the VMAT2-HI mice were assessed on various measures, including depressive-like and anxiety-like behaviors. It was predicted that the VMAT2-HI mice would show improved outcomes on anxiety and depressive-like behavioral assays.

In conjunction with the behavioral tasks above, we also performed a series of control experiments to eliminate any potential behavioral confounds such as altered taste, smell, or tactile perception in the VMAT2-HI mice. We performed the quinine taste aversion paradigms to assess changes in taste, the dot removal test to assess tactile stimulation, and the social odor discrimination task to assess olfactory discrimination. Olfactory discrimination is modulated by dopamine release (Hildebrand and Shepherd, 1997; Escanilla et al., 2009), and deficits in olfactory discrimination can serve as an early indicator in a variety of neurodegenerative diseases (Doty, 2012; Lerche et al., 2014). Decreased olfactory discrimination also has been described previously in VMAT2-deficient mice (Taylor et al., 2009). Thus, it was possible that elevated VMAT2 levels might alter olfaction in the VMAT2-HI mice.

Methods

Animals

Four- to 6-month-old male and female VMAT2-HI and wildtype mice were used for all behavioral studies. Mice received food and water ad libitum on a 12:12 light cycle unless otherwise noted. All procedures were conducted in accordance with the National Institutes of Health Guide for Care and Use of Laboratory Animals and approved by the Institutional Animal Care and Use Committee at Emory University.

Circadian locomotor activity

Locomotor activity was assessed using an automated system (San Diego Instruments) with infrared photobeams that recorded ambulations (consecutive beam breaks). Mice were placed into individual chambers and recorded for 24 hours to encompass both the dark and light periods. Data are presented in 1 hour bins.

Amphetamine-stimulated locomotor activity

Amphetamine-stimulated locomotor activity was assessed using the system described above. Briefly, mice were placed into the individual chamber, allowed to acclimate and injected with 1 mg/kg (freebase) d-amphetamine (Sigma). Ambulations (consecutive beam breaks) were summed in the 60 minutes following the injection. Data are presented in 5 minute bins.

Forced-Swim Test

After 7 days of individual housing, mice were placed in glass cylinders (24 × 16 cm) with 15 cm of water maintained at 25 °C for 6 minutes. After the first 2 minutes, the total duration of time spent immobile was recorded during a 4 minute test. The mouse was

deemed immobile when it was floating passively. All trials were recorded using a video camera and scored by blinded observers.

Marble-Burying Assay

Mice were individually housed for 7 days before behavioral battery. The protocol was modified based on work from the literature (Saadat et al., 2006; Egashira et al., 2012). Mice were placed into their home cage that contained 6 inches of lightly pressed cobb bedding. Within each home cage, 20 black marbles were evenly arranged in a 5 x 4 grid. The mouse was placed into the cage for 30 minutes, after which the number of marbles at least 2/3 covered with bedding was counted and verified by photo by a blinded observer.

Tail suspension test

The tail suspension test (TST) was performed according to a previous publication (Taylor et al., 2009). Briefly, mice were suspended 50 cm above the floor by adhesive tape placed approximately 1 cm from the tip of the tail. The test was videotaped, and immobility time was measured for 6 minutes. Immobility was defined as the absence of any limb or body movements, with the exception of those caused by respiration, when the mice hung passively and completely motionless. During the test, the mice were separated from each other to prevent visual and acoustic associations. The number of seconds spent immobile was recorded. Observers were blind to the group treatment of the mice.

Sleep latency

Four hours before the circadian nadir, mice were placed into new behavioral cages for acclimation without food or water (Taylor et al., 2009). Before starting test, mice were injected with 100 μL 0.9% saline and placed back in cage. Observers then monitored the

time to sleep in the mice. Sleep was classified by 2 minutes of uninterrupted sleep with 75% of the next 10 minutes asleep (Taylor et al., 2009).

Sucrose preference

An 8-day sucrose preference protocol was used in which mice remained individually housed 3 days before the start day (day 1) and during the course of the remaining 8 days. On day 1, their normal water bottles were replaced with two 50-ml tubes (bottle "A" and bottle "B") fitted with bottle stoppers containing two-balled sipper tubes. The position of bottles A and B were switched daily to avoid a side bias, and the fluid consumed from each bottle was measured daily. During days 1 and 2, bottles A and B were filled with normal drinking water (wt/wt). During days 3 and 4, both bottles were filled with a solution of 1% sucrose dissolved in drinking water (s/s). On days 5–8, bottle A contained 1% sucrose, and bottle B contained drinking water (s/w). Preference on each day for each mouse was calculated as 100·(VolA/[VolA+VolB]) and averaged across the days for a given condition (wt/wt, s/s, or s/w). Total fluid consumed was calculated as [VolA + VolB] and averaged similarly.

Olfactory discrimination (social odor)

Single wooden blocks were placed in 50 mL conical tubes containing 1 g of animal bedding from the test animals' cages (or strangers' cages) for at least 12 hours prior to testing. The test animal was presented with two blocks at a time, one scented with its own bedding and one block scented with a stranger's bedding of the same sex. The two blocks were placed onto the bedding on opposite ends of the test cage. It is critical to note the placement of the blocks for each trial and to switch placements to eliminate side bias. The

time spent in contact with each block was recorded for a 2 minute trial. All trials were videotaped and scored by a blind observer.

Dot test (tactile stimulation)

An adhesive dot (Staples) was placed between the ears of a single mouse in a behavioral test cage. The mouse was then placed back in home cage, and the latency to remove the dot was recorded. Each trial was 60 seconds.

Quinine taste aversion

The tip of a cotton swab was placed into an aliquot of 2 mg/ml quinine. Mice were removed from the home cage and the tip of the swab was placed in their mouth. The test mouse was then immediately placed back into the home cage. The latency to groom or drag face on the cage floor was measured. Each trial was 60 seconds.

Elevated plus maze

The elevated plus maze (EPM) was adapted and performed as previously published (Schank et al., 2008; Taylor et al., 2009). The apparatus had two open arms and two enclosed arms arranged in a plus-sign orientation. Rodents prefer dark compartments, so exploration in the open arms indicates decreased anxiety (Pellow et al., 1985). Mice were placed into the center compartment of the elevated plus maze for a 6 minute trial. Time spent in open vs. closed arms and crossovers between the compartments were recorded. Videos were later scored by an observer who was blind to mouse genotypes.

Statistical analysis

All data were analyzed in GraphPad Prism. Differences between genotypes were compared by two-tailed *t* tests, except where indicated. Outliers were defined by the Grubbs' test for outliers ($\alpha = 0.05$). All errors shown are SEM.

Results

Increased locomotor activity in VMAT2-HI mice.

We evaluated whether the VMAT2-HI mice display increased locomotor activity, a dopamine-mediated behavior (Beninger, 1983). The VMAT2-HI mice showed a 41% increase in total ambulations in the active period (dark cycle) compared with wildtype littermates ($p < 0.01$) (**Fig. 3.1**). No difference in locomotor activity was observed in the inactive period.

Enhanced amphetamine-stimulated locomotor activity in VMAT2-HI mice.

Following a single 1 mg/kg injection of d-amphetamine (i.p.), VMAT2-HI mice show a significant increase in ambulations in the 60 min following the injection ($p < 0.05$) (**Fig. 3.2**).

Reduced anxiety-like and depressive-like behaviors in VMAT2-HI mice.

VMAT2-HI mice showed reduced immobility time on the forced-swim test ($p < 0.05$) (**Fig. 3.3**) and reduced marble burying in the marble-burying assay ($p < 0.01$) (**Fig. 3.3**), suggesting that VMAT2-HI mice actually show improved outcomes on other anxiety and depressive-like measures. No significant difference was found between genotypes on the elevated plus maze (**Fig. 3.4)** suggesting that VMAT2-HI mice do not have increased anxiety-like behavior by this measure. We performed a behavioral battery to assess overall behavioral health (including taste, olfaction, social approach, anxiety, and sleep disturbances) and found no differences in these other measures (**Fig. 3.4**)

Discussion

VMAT2 overexpression increases locomotor activity

We have previously shown that overexpression of VMAT2 in the VMAT2-HI mice increases stimulated dopamine release and extracellular dopamine content. Knowing that locomotor activity is largely a dopamine-mediated behavior (Beninger, 1983), it is not surprising that augmented dopamine release results in slightly elevated locomotor activity in these animals (**Fig. 3.1**). However, the behavioral phenotype is relatively mild and should not be considered a hyperactive phenotype. For example, treatment with a psychostimulant like amphetamine can increase locomotor activity scores by about 10-fold (Salahpour et al., 2008). Based on those approximations, the increase in movement shown in the VMAT2-HI mice is minimal. Despite this, these behavioral results suggest that increased vesicular capacity enhance neurotransmitter signaling and that there is minimal receptor compensation.

Interestingly, we also show a small increase in amphetamine-stimulated locomotor activity in the VMAT2-HI mice following a 1 mg/kg injection of amphetamine (**Fig. 3.2**). This is likely due to the increase in basal dopamine content in the brains of the VMAT2-HI mice (Chapter II). However, it has also been shown that the VMAT2-HI mice do not show an increase in the rewarding effects of dopamine releasers like methamphetamine, suggesting that enhanced vesicular storage may not exacerbate addiction-related behavior (Lohr et al., 2015). Future experiments should further examine the mechanistic effects of altered vesicular function on amphetamine and methamphetamine-induced output.

VMAT2 overexpression improves outcomes in measures of depressive-like and anxiety-like behaviors

Monoamine neurotransmission has been strongly associated with affective disorders. The monoamine hypothesis of depression was largely based on the dramatic mood changes observed in patients taking the VMAT2 inhibitor reserpine (Krishnan and Nestler, 2008). Increased monoamines also have been implicated in a variety of psychiatric conditions, including bipolar disorder, mania, schizophrenia, and psychosis, all of which include symptoms of mood disturbances (Swerdlow and Koob, 1987b). Due to these examples, we hypothesized that the increased dopamine signaling in the VMAT2-HI mice would result in anxiety or mania-like behaviors (Nestler and Hyman, 2010).

We have shown that the VMAT2-HI mice display no increase in anxiety-like behaviors (**Fig. 3.3** and **3.4**). Instead, the VMAT2-HI mice display decreased anxiety-like behavior in the marble-burying assay and decreased depressive-like behavior on the forced-swim test. Both of these results suggest that the VMAT2-HI mice actually have improved outcomes in these measures. Although elevated locomotor activity may confound the results from the VMAT2-HI mice on the forced-swim test, the output from the marble-burying assay is not dependent on activity. While the behavioral paradigms described here undoubtedly involve additional monoamine neurotransmitters beyond dopamine (e.g., serotonin and norepinephrine), these findings suggest that elevated VMAT2 function in vivo may have benefits in altering mood and affective behaviors. Future studies should also examine the effects of antidepressants on these mice, since they already show a resilient behavioral phenotype. Furthermore, these results also suggest that the

neurochemical outputs of the other monoamine systems of the VMAT2-HI mice are worth characterizing more thoroughly.

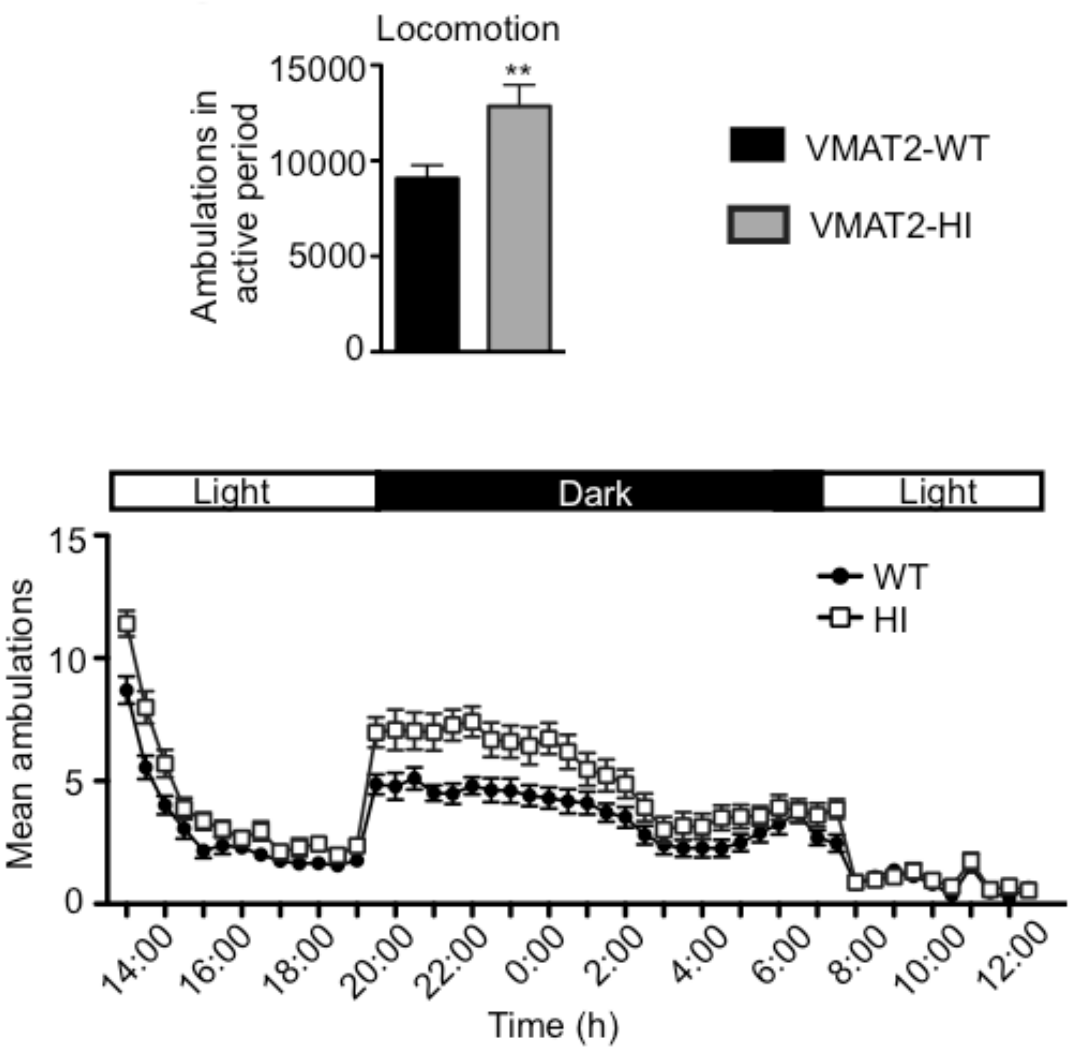
Locomotion
Ambulations in active period
15000
10000
5000
0
**
VMAT2-WT
VMAT2-HI
Light
Dark
Light
Mean ambulations
15
10
5
0
WT
HI
14:00
16:00
18:00
20:00
22:00
0:00
2:00
4:00
6:00
8:00
10:00
12:00
Time (h)

Figure 3.1. Increased locomotor activity in the VMAT2-HI mice.

VMAT2-HI mice show elevated total ambulations in the active (dark) period. Average 24 hour circadian locomotor activity trace (1 hour bins; n = 27).

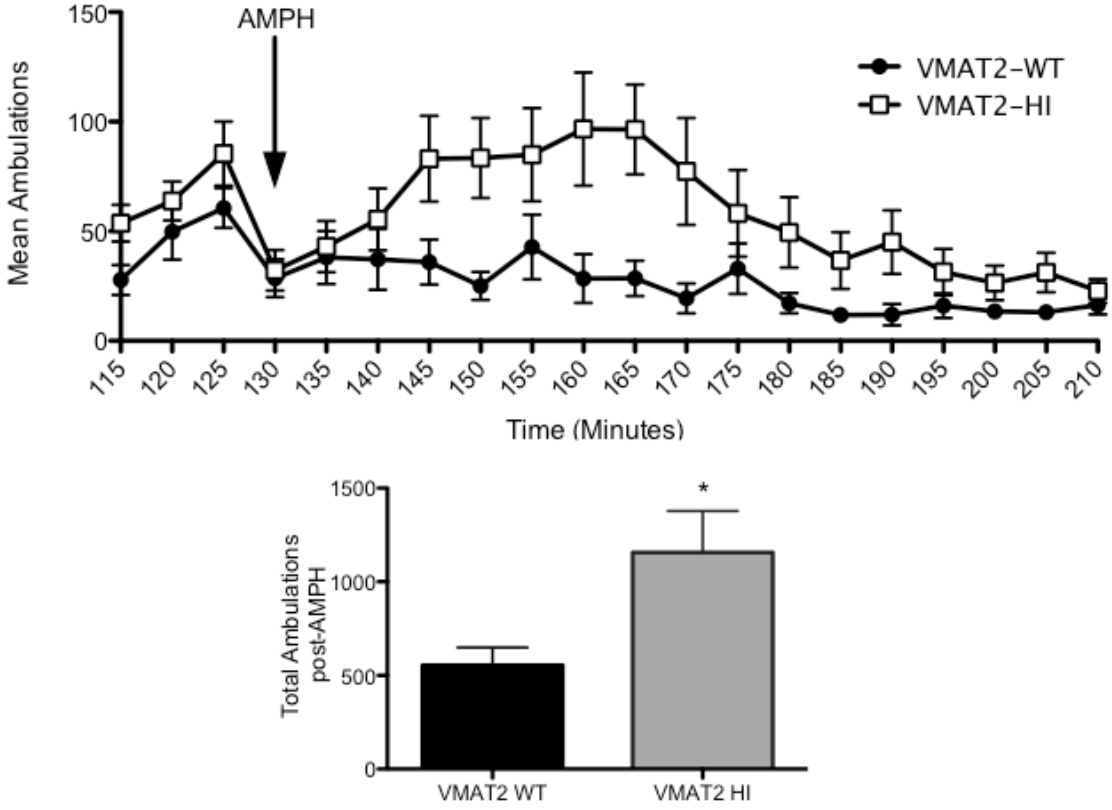
AMPH
VMAT2-WT
VMAT2-HI
Mean Ambulations
150
100
50
0
115
120
125
130
135
140
145
150
155
160
165
170
175
180
185
190
195
200
205
210
Time (Minutes)
Total Ambulations post-AMPH
1500
1000
500
0
*
VMAT2 WT
VMAT2 HI

Figure 3.2. VMAT2-HI mice show a small increase in amphetamine-stimulated locomotor activity.

Following a single 1 mg/kg injection of amphetamine (i.p.), VMAT2-HI mice show a significant increase in ambulations in the 60 minutes following the injection (n=12). (A) Locomotor traces of both genotypes following amphetamine injection (arrow). (B) Total ambulations in the 60 minutes following injection between both genotypes.

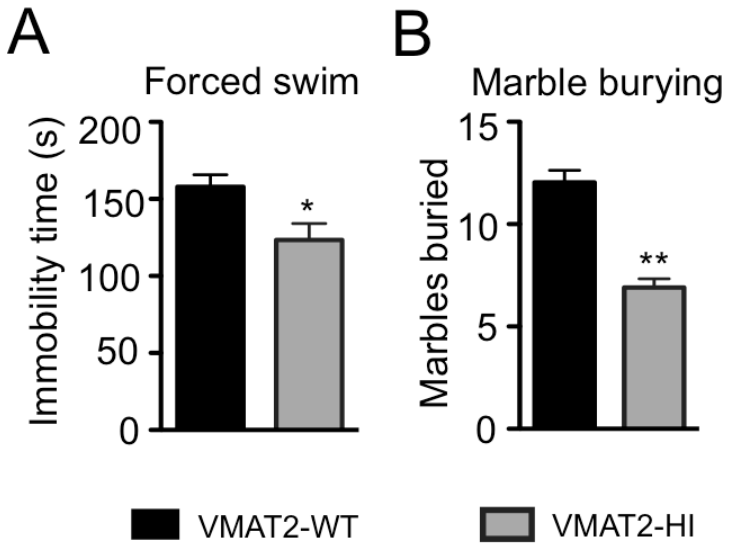
A
Forced swim
Immobility time (s)
200
150
100
50
0
*
B
Marble burying
Marbles buried
15
10
5
0
**
VMAT2-WT
VMAT2-HI

Figure 3.3. Improved outcomes on measures of depressive- and anxiety-like behaviors.

Improved depressive-like and anxiety-like behaviors in the VMAT2-HI mice. (A) VMAT2-HI mice show decreased immobility time on the forced-swim test (n = 21). (B) VMAT2-HI mice show decreased marble burying on the marble-burying assay (n = 11).

Behavior	Output	VMAT2-WT (Average ± SEM)	VMAT2-HI (Average ± SEM)	P-value
Elevated plus maze (n=10)	Open arm entries	6.5 ± 0.7	7.7 ± 2.4	> 0.05
Social odor discrimination (n=9)	Time spent sniffing stranger (% of total investigation time)	68.3 ± 4.6	67.5 ± 4.1	> 0.05
Sleep latency (n=9)	Latency to sleep (min)	23.5 ± 3.0	19.8 ± 3.8	> 0.05
Quinine taste aversion (n=9)	Latency to groom (s)	12.4 ± 2.9	13.0 ± 2.7	> 0.05
Sucrose preference (n=8-10)	Sucrose consumed (mL)	10.81 ± 1.43	13.62 ± 1.51	> 0.05

Table 3.4. Non-significant behavioral differences between the VMAT2-HI mice and wildtype littermates.

Based on the importance of monoaminergic signaling in behavioral responses, it was critical to assess behavioral changes in a variety of tasks in the VMAT2-HI compared to wildtype littermates.

CHAPTER IV: VMAT2-OVEREXPRESSING (VMAT2-HI) MICE ARE PROTECTED FROM MPTP TOXICANT EXPOSURE

These findings have been previously reported as written in:

Lohr KM et al. (2014) Increased vesicular monoamine transporter enhances dopamine release and opposes Parkinson disease-related neurodegeneration in vivo. *Proc Natl Acad Sci* 111:9977–82.

Introduction

MPTP (1-methyl-4-phenyl-1,2,3,6 tetrahydropyridine) is perhaps the first chemical target that linked the etiology of Parkinson's disease to a direct environmental cause. This theory of Parkinson's disease originated from the discovery of a group of intravenous drug users in California who had inadvertently injected themselves with a meperidine (Demerol) analog that was contaminated with MPTP (Langston et al., 1983). In these individuals, MPTP induced a severe and acute parkinsonism that was reversible by L-DOPA administration. MPTP soon became the most commonly used toxicant-induced model of Parkinson's disease.

After peripheral administration, MPTP crosses the blood brain barrier and is metabolized by monoamine oxidase-B (MAO-B) in astroglia to 1-methyl-4-phenyl-2,3-dihydropyridinium (Ransom et al., 1987; Brooks et al., 1989). Through oxidation, this metabolite is converted to the active toxin 1-methyl-4-phenylpyridinium (MPP+). MPP+ exits astroglia and accumulates in dopaminergic neurons via uptake through the dopamine transporter (DAT) (Javitch et al., 1985; Bezard et al., 1999).

Once MPP+ passes through DAT and enters the cytosol, it enters mitochondria (**Fig. 4.1**). The negative membrane potential in mitochondria allows for MPP+ uptake where it binds and inhibits complex I of the electron transport chain. Inhibition of complex I causes ATP depletion and increases in reactive oxygen species (Rossetti et al., 1988; Schapira, 1994). These factors are major contributors to the toxicity of MPTP (Richardson et al., 2007). Once MPP+ enters the vesicle, it also causes a redistribution of vesicular dopamine into the cytosol (Choi et al., 2015). Cytosolic dopamine accumulation induced by MPP+ can cause neurotoxicity, while also inducing an efflux of dopamine via the DAT

into the extracellular space and reductions in DAT-mediated plasmalemmal uptake (Lotharius and O'Malley, 2000). MPTP administration also inhibits dopamine breakdown, leading to elevation of cytosolic dopamine and neurotoxic cascades (Blesa and Przedborski, 2014). VMAT2 is capable of both sequestering MPP+ into the vesicle away from its mitochondrial site of action (Liu et al., 1992a; Guillot and Miller, 2009) and repackaging displaced dopamine. Thus VMAT2 opposes multiple mechanisms of MPTP toxicity in dopamine neurons.

Previous studies have assessed the detrimental effects of reduced vesicle function, both through pharmacological inhibition of VMAT2 with reserpine or tetrabenazine or genetic reduction of VMAT2 function (Freis, 1954; Quinn et al., 1959; Kirshner et al., 1963; Pettibone et al., 1984; Caudle et al., 2007). We have recently shown that overexpression of the VMAT2 in mice (VMAT2-HI) increases the capacity of synaptic vesicles to store and release dopamine and enhances dopaminergic output (Chapter II). Due to the close connection between VMAT2 and intracellular toxicity discussed above, we assessed whether enhanced vesicular filling in the VMAT2-HI mice modulates sensitivity to MPTP-induced degeneration of dopamine neurons in nigrostriatal pathway, a neurotoxic model of Parkinson's disease. Here we show that VMAT2-HI mice are less vulnerable to two different MPTP doses targeting both dopamine neuron terminals and cell bodies. These results suggest that enhanced vesicular capacity, via overexpression of VMAT2, is indeed capable of lessening the toxic burden of midbrain dopamine neurons.

Methods

Animals

Six- to 8-month-old male VMAT2-HI and wildtype mice were used for voltammetry. Mice received food and water ad libitum on a 12:12 light cycle unless otherwise noted. All procedures were conducted in accordance with the National Institutes of Health Guide for Care and Use of Laboratory Animals and approved by the Institutional Animal Care and Use Committee at Emory University.

MPTP injection schedules

Male mice were injected (s.c.) with either MPTP-HCl (M0896, Sigma,) or saline (0.9%). The “terminal” lesion consisted of two injections of 15 mg/kg MPTP (freebase) with an interinjection interval of 12 hours. Mice were killed 7 days after the final dose. The “cell body” lesion consisted of five injections of 20 mg/kg MPTP (freebase) with an interinjection interval of 24 hours. Mice were killed 21 days after the final injection.

Western blotting

Western blots were performed as previously described (Caudle et al., 2007). Primary antibodies used were: polyclonal rabbit anti-VMAT2 serum (1:20,000), rat anti-DAT (1:5,000), rabbit anti-TH (1:1,000), mouse anti-GFAP (1:5,000) and mouse anti-β-actin (1:5,000). The appropriate HRP-linked secondary antibodies (1:5,000) were used. Analysis was calibrated to coblotted dilutional standards of pooled sample from all VMAT2-HI samples.

Immunohistochemistry

Immunohistochemistry was performed as previously described (Caudle et al., 2007). Primary antibodies used were: polyclonal rabbit anti-VMAT2 serum (1:50,000), rat

anti-DAT (1:1,000), mouse anti-GFAP (1:1,000) or rabbit anti-TH (1:1,000). The appropriate biotinylated secondary antibodies (1:200) were used. Nissl stain was performed for stereological analysis by a 3 min Cresyl Violet dip of mounted sections prior to dehydration, xylene clearing and coverslipping. All images were acquired with NeuroLucida (MicroBrightField).

Stereological Analysis

Stereological sampling was performed using the Stereo Investigator software as previously described, and the number of neurons in the SNpc was estimated using the optical fractionator method (MicroBrightField). Parameters, cell-type definition, and counting intervals were also the same as previously described (Taylor et al., 2014).

Statistical analysis

All data were analyzed in GraphPad Prism. Stereological counts and densitometric analysis were analyzed using two-way ANOVA (with treatment and genotype as factors) with Bonferroni post hoc tests. Outliers were defined by the Grubbs' test for outliers ($\alpha = 0.05$). All errors shown are SEM.

Results

Reduced MPTP neurotoxicity in VMAT2-HI mice following a terminal-targeting MPTP lesion.

We examined whether VMAT2-HI mice are protected from the dopaminergic toxicant MPTP. Following a low dose of MPTP (2 × 15 mg/kg s.c., 12 hours apart), VMAT2-HI mice showed protection from both striatal TH and DAT loss, indicative of sparing of striatal dopamine terminals ($p < 0.05$) (**Fig. 4.2**).

Reduced MPTP neurotoxicity in VMAT2-HI mice following a cell body-targeting MPTP lesion.

Following a multiday MPTP regimen known to cause □50% cell body loss in the SNpc (5 × 20 mg/kg s.c., 24 hours apart) (Kaur et al., 2003), VMAT2-HI mice were also protected from striatal TH loss following this high MPTP dosing regimen ($p < 0.05$) (**Fig. 4.3**). Though not significant, there was a trend toward protection of striatal DAT levels as well. VMAT2-HI mice also showed significant protection from TH+ cell loss as measured by unbiased stereology ($p < 0.05$) (**Fig. 4.4**).

Discussion

VMAT2 overexpression protects against MPTP-induced terminal and cell loss in the substantia nigra.

The current study shows that VMAT2 overexpression is protective against both terminal and cell body loss induced by two different MPTP dosing paradigms. VMAT itself was first identified due to its protective effects against MPP+ toxicity in culture (Liu et al., 1992a, 1992b). VMAT2 protects against the parkinsonian neurotoxicant, MPTP, by sequestering this active metabolite, MPP+, into the vesicular lumen away from its site of action at complex I of the mitochondrial electron transport chain (Liu et al., 1992a; Gainetdinov et al., 1998; Mooslehner et al., 2001). Complex I inhibition by MPP+ results in a cellular energy crisis and produces oxygen radicals. Thus, the findings presented here suggest that increased vesicular transport in the VMAT2-HI mice acts to sequester cytosolic toxicants, like MPP+, in addition to increasing the vesicle's capacity for dopamine. This protective role for VMAT2 in vivo was first described in VMAT2 heterozygote mice (50% of wildtype VMAT2 levels), which show greater dopaminergic terminal damage by MPTP as indicated by dopamine content, DAT levels, and nigral cell loss (Takahashi et al., 1997; Gainetdinov et al., 1998). These results also complement previous findings showing that transient increases in VMAT2 expression in PC12 cells (Vergo et al., 2007) and in mouse brain through treatment with the pituitary adenylyl cyclase activating polypeptide (PACAP38) is neuroprotective (Guillot et al., 2008a).

DAT to VMAT2 expression ratio as a determinant of vulnerability to MPTP in midbrain dopamine pathways.

MPTP is metabolized into MPP+ by MAO extracellularly (Ransom et al., 1987). After MPP+ enters dopaminergic neurons via the DAT, it then can be sequestered into the vesicle via VMAT2. Based on the critical actions of both of these transporter mechanisms, the ratio of DAT to VMAT2 function has previously been suspected as a mediator of MPTP vulnerability (Miller et al., 1999b; Masoud et al., 2015). Further, it has been speculated that differences in the ratio between DAT and VMAT2 midbrain dopamine pathways may explain the preferential loss of nigrostriatal projections in both Parkinson's disease models. As seen in the immunohistochemical staining of DAT and VMAT2, dorsal striatum expresses greater levels of the DAT relative to VMAT2 compared to the ventral striatum (nucleus accumbens), which sees considerable sparing following MPTP administration and in Parkinson's disease (Miller et al., 1997, 1999a, 1999b; Uhl, 1998). It has also been speculated that vesicular uptake of MPP+ in rats is approximately twice that of a mouse, presumably due to VMAT2 expression differences (Staal et al., 2000). Inhibition of VMAT2 in these same rats increased the toxicity of MPTP.

VMAT2 overexpression as a mediator of cytosolic toxic burden in dopaminergic neurons.

The mechanism that induces dopaminergic nigrostriatal neuronal death in Parkinson's disease remains unknown. Using a variety of toxicant models to destroy dopaminergic neurons, previous studies have illuminated a variety of leads as to the molecular basis of the dopaminergic cell loss in Parkinson's disease (Blesa and Przedborski, 2014). Though these models replicate many of the clinical and pathological hallmarks, no single model encompasses all of the Parkinson's disease features. MPTP,

however, is the most commonly used toxicant Parkinson's disease model (Przedborski et al., 2001). Thus, researchers operate under the assumption that dopaminergic neurons may have a stereotyped death cascade that can be activated by a range of insults, including neurotoxicants like MPTP. Taken together, the results presented in this study suggest that modifying vesicular function may alter some of the effects of the toxicological cascade inside of a dopamine neuron.

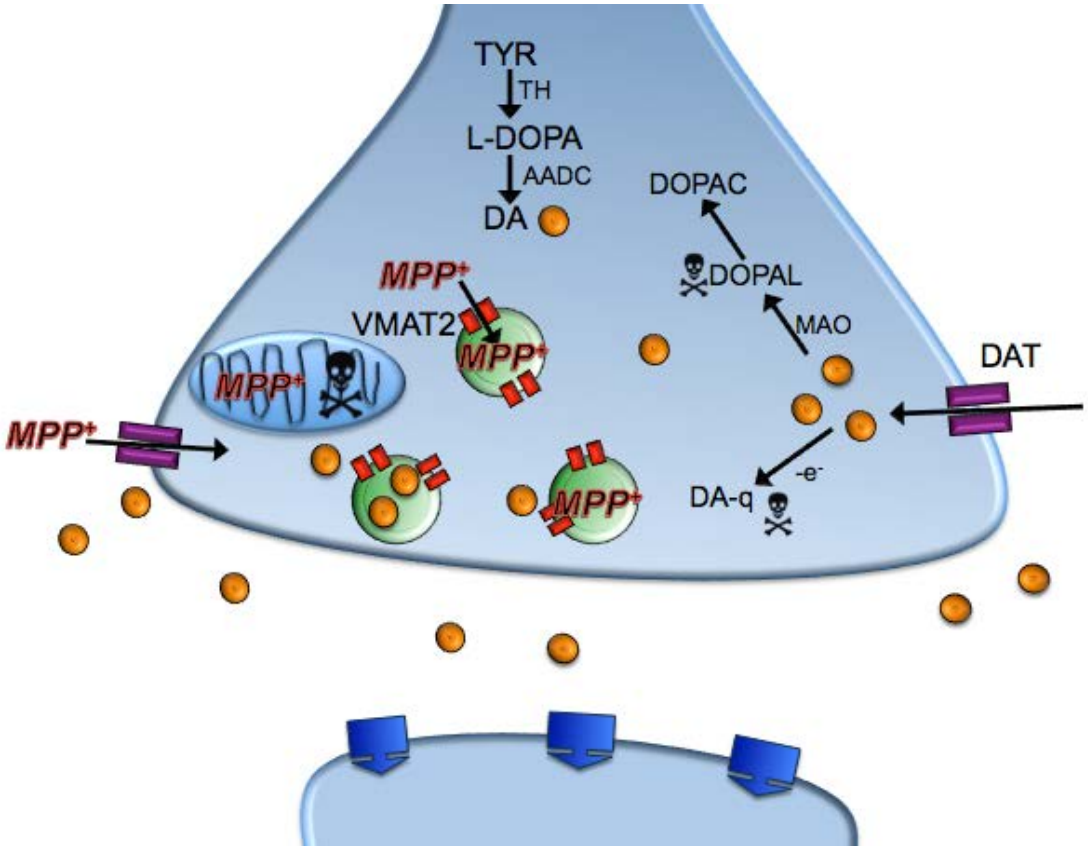
TYR
TH
L-DOPA
AADC
DA
DOPAC
DOPAL
MAO
MPP+
VMAT2
MPP+
MPP+
MPP+
DAT
MPP+
-e-
DA-q

Figure 4.1. Schematic of MPTP toxicity in a dopaminergic neuron terminal.

The parkinsonian neurotoxicant, MPTP, is converted into MPP+ extracellularly by MAO. VMAT2 protects against MPP+ by sequestering this active metaboliteinto the vesicular lumen away from its site of action at complex I of the mitochondrial electron transport chain. Complex I inhibition by MPP+ results in a cellular energy crisis and produces oxygen radicals. Additionally, MPP+ that is sequestered by VMAT2 displaces vesicular dopamine stores. Increased vesicular filling sequesters such cytosolic toxicants and protects dopaminergic neurons.

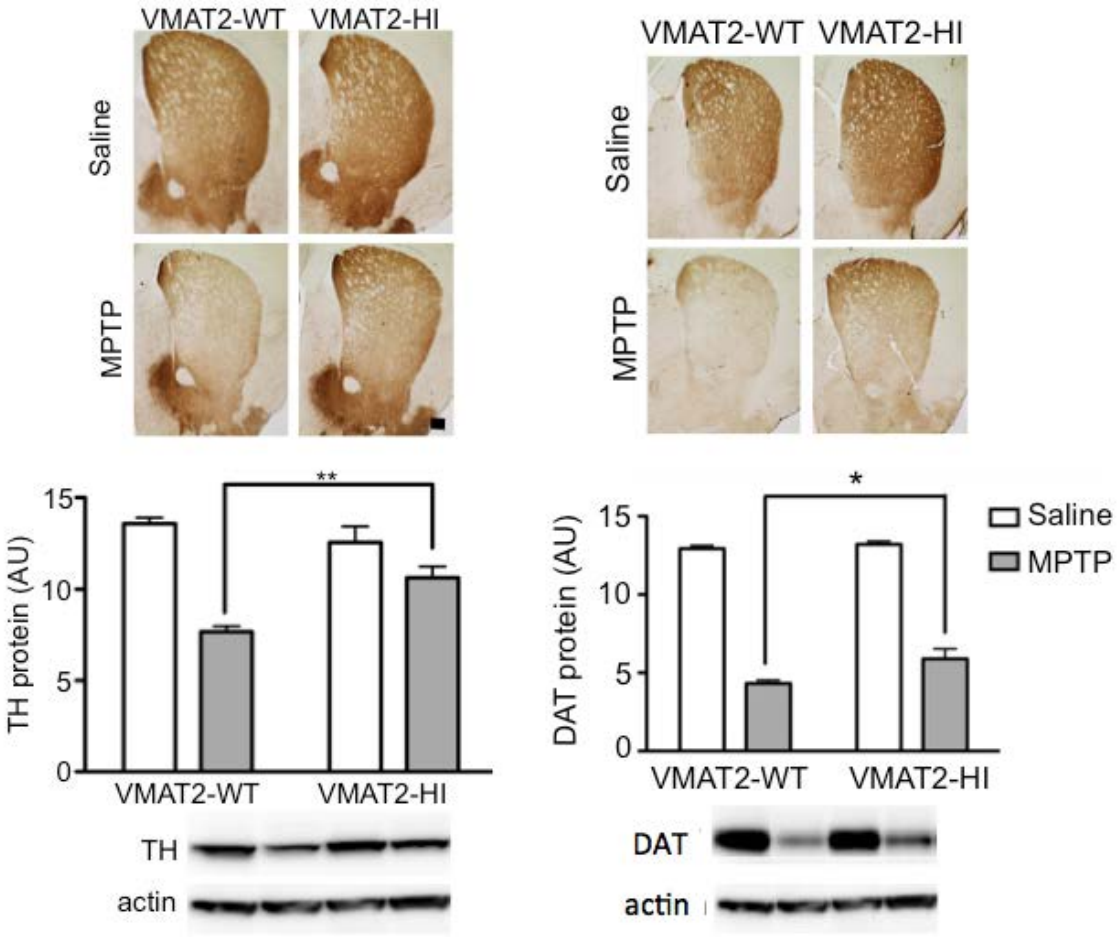
VMAT2-WT
VMAT2-HI
Saline
MPTP
VMAT2-WT
VMAT2-HI
Saline
MPTP
TH protein (AU)
15
10
5
0
**
VMAT2-WT
VMAT2-HI
TH
actin
DAT protein (AU)
15
10
5
0
*
Saline
MPTP
VMAT2-WT
VMAT2-HI
DAT
actin

Figure 4.2. VMAT2-HI mice are protected from terminal toxicity following 2 x 15 mg/kg MPTP.

A) Following a 2 × 15 mg/kg MPTP dose, VMAT2-HI mice show protection from striatal TH loss by immunoblotting and immunohistochemistry (n = 4). (B) VMAT2-HI mice also show protection from striatal DAT loss by immunoblotting and immunohistochemistry (n = 4).

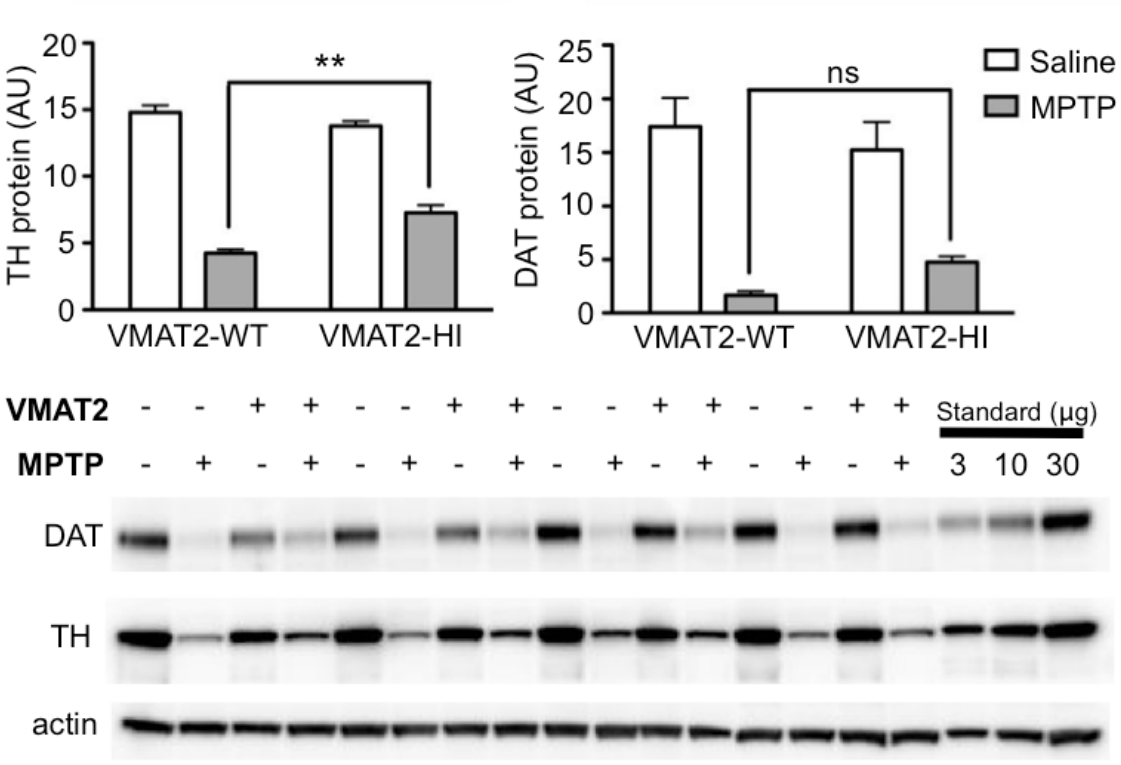
TH protein (AU)
20
15
10
5
0
**
VMAT2-WT
VMAT2-HI
DAT protein (AU)
25
20
15
10
5
0
ns
VMAT2-WT
VMAT2-HI
Saline
MPTP
VMAT2 - - + + - - + + - - + + - - + +
MPTP - + - + - + - + - + - + - + - +
Standard (µg)
3 10 30
DAT
TH
actin

Figure 4.3. Reduced toxicity in VMAT2-HI mice following 5 x 20 mg/kg MPTP.

VMAT2-HI mice show significant protection from striatal TH loss and a trend toward protection from striatal DAT loss following a 5 × 20 mg/kg MPTP dose (n = 4). Western blot of both genotypes (− indicates the absence of the BAC aka wildtype; + indicates the presence of the BAC aka VMAT2-HI) following MPTP treatment with codilutional standard of pooled control tissue used for quantification (3 μg, 10 μg, and 30 μg of protein).

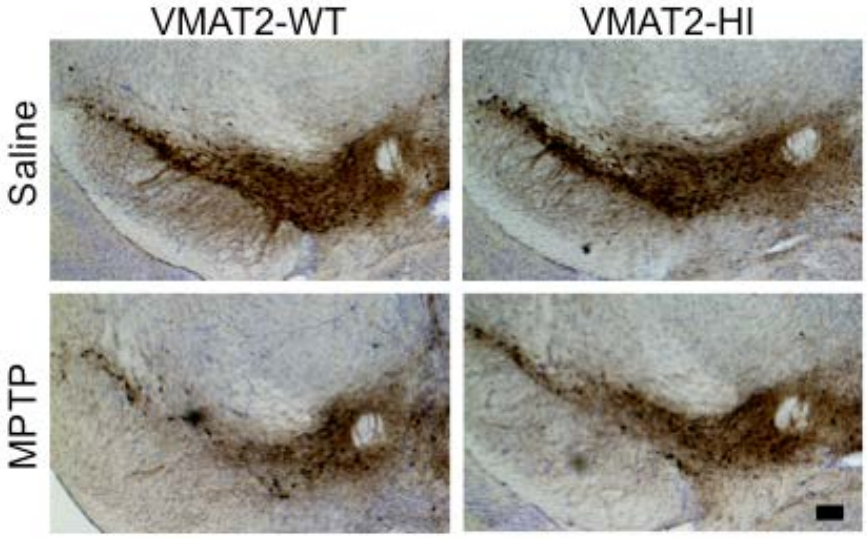
VMAT2-WT
VMAT2-HI
Saline
MPTP

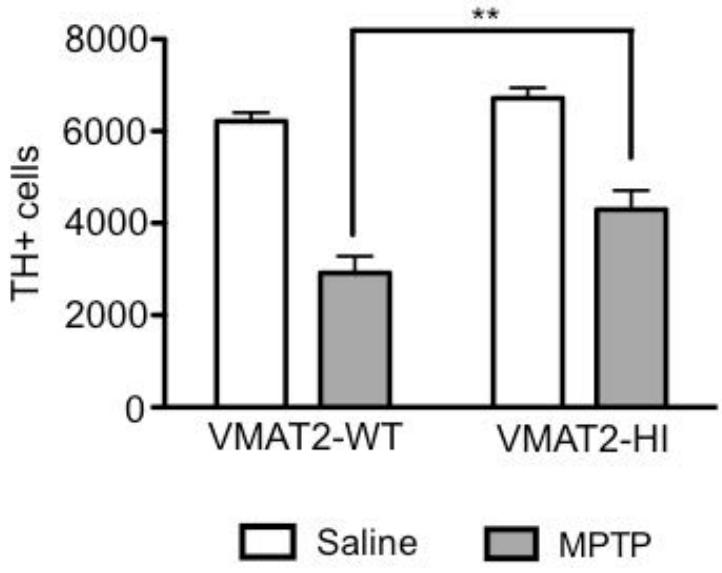
**
8000
6000
4000
2000
0
TH+ cells
VMAT2-WT
VMAT2-HI
Saline
MPTP

Figure 4.4. VMAT2-HI mice are significantly protected from nigral cell loss following 5 x 20 mg/kg MPTP.

Following a 5 × 20 mg/kg MPTP dose, VMAT2-HI mice show a significantly higher number of remaining TH^+ neurons in the substantia nigra pars compacta (n = 6). No difference was seen in $Nissl^+$ cells between genotypes ($P > 0.05$). (Scale bar: 200 μm)

CHAPTER V: VMAT2-OVEREXPRESSING (VMAT2-HI) MICE ARE PROTECTED FROM METHAMPHETAMINE TOXICANT EXPOSURE

These findings have been previously reported as written in:

Lohr KM et al. (2015) Increased Vesicular Monoamine Transporter 2 (VMAT2; Slc18a2) Protects against Methamphetamine Toxicity. *ACS Chem Neurosci* 6:790–9.

Introduction

The addictive psychostimulant methamphetamine (METH) is severely neurotoxic to the dopamine system, selectively targeting dopaminergic projections, depleting striatal dopamine levels, and initiating a large neuroinflammatory cascade (Ricaurte et al., 1982, 1984; Cubells et al., 1994; LaVoie et al., 2004; Kuhn et al., 2006). METH induces a massive efflux of intracellular dopamine into the extracellular space by reducing the pH gradient across the vesicular membrane, emptying vesicular dopamine stores, and reversing plasmalemmal dopamine transporter (DAT) function (Sulzer et al., 1995). In this way, METH causes a disruption of dopamine compartmentalization at the synaptic terminal. The accumulation of cytosolic dopamine following METH treatment is thought to be central to the neurotoxicity of the compound (**Fig. 5.1**) (Cubells et al., 1994; LaVoie and Hastings, 1999; Lotharius and O'Malley, 2001). Cytosolic dopamine, when not sequestered into the vesicular compartment, is vulnerable to oxidation and conversion to neurotoxic species, including the formation of dopamine-quinones and cysteinyl adducts (Sulzer and Zecca, 1999). Additionally, METH promotes dopamine synthesis via upregulation of tyrosine hydroxylase (TH) function (Larsen et al., 2002) and opposes dopamine degradation via reductions in monoamine oxidase (MAO) activity (Osamu Suzuki et al., 1980). These mechanisms elevate cytosolic dopamine levels and potentially exacerbate METH toxicity. METH toxicity is indicated by losses of the dopamine terminal markers DAT and TH in the striatum (Ricaurte et al., 1982, 1984). This damage to dopamine terminals also induces extensive neuroinflammation through the activation of both astrocytes and microglia, which also contribute to neurodegeneration over prolonged

periods of inflammation (Hess et al., 1990; O'Callaghan and Miller, 1994; Guilarte et al., 2003; LaVoie et al., 2004; Thomas et al., 2004).

The vesicular monoamine transporter 2 (VMAT2, SLC18A2) is a critical mediator of dopamine dynamics in the neuronal terminal. VMAT2 is an H+-ATPase antiporter, which uses the vesicular electrochemical gradient to drive the packaging of cytosolic monoamines (dopamine, serotonin, norepinephrine, histamine) into small synaptic and dense core vesicles (Erickson et al., 1992; Liu et al., 1992a; Erickson and Eiden, 1993; Eiden and Weihe, 2011). By preventing the accumulation of dopamine in the neuronal cytosol, VMAT2 also counters intracellular dopamine toxicity (Lotharius and O'Malley, 2001; Alter et al., 2013; Goldstein et al., 2013). While genetic knockout of VMAT2 in mice is lethal (Fon et al., 1997; Takahashi et al., 1997; Wang et al., 1997b), mice with a 95% reduction in VMAT2 survive and display both lower monoamine levels and progressive neurodegeneration with aging (Caudle et al., 2007; Taylor et al., 2014). These VMAT2-deficient mice show increased dopamine turnover and increased cysteinyl-DOPA and DOPAC adducts, suggesting that improper dopamine storage leads to an accumulation of potentially neurotoxic byproducts. Most recently, reduced vesicular storage has been linked to dysfunction in the dopamine system in humans (Rilstone et al., 2013) and in post mortem Parkinson's disease brains beyond what could be explained by terminal loss alone (Pifl et al., 2014). These data suggest that manipulation of synaptic terminal dopamine handling promotes nigrostriatal neurodegeneration in human populations.

While the detrimental effects of reduced VMAT2 function have been examined in the studies above, an in vivo model of permanently increased vesicular storage has only recently become available using BAC-transgenic VMAT2-overexpressing (VMAT2-HI)

mice (Lohr et al., 2014). As a result of their elevated VMAT2 expression, VMAT2-HI mice display increased vesicular capacity, increased striatal dopamine content and release, and increased locomotor activity. VMAT2-HI mice are also protected from the neurotoxic effects of 1-methyl-4-phenyl-1,2,3,6-tetrahydropyridine (MPTP) since its metabolite, MPP+, is sequestered by VMAT2. VMAT2 is also a known target of METH, and METH treatment reduces VMAT2-mediated vesicular uptake (Ugarte et al., 2003; Torres and Ruoho, 2014). Mice with reductions in VMAT2 are more vulnerable to METH toxicity, as measured by exacerbated dopamine terminal degeneration, dopamine depletion, and neuroinflammatory responses (Fumagalli et al., 1998; Guillot et al., 2008b). Based on this work, it was predicted that elevated vesicular function would oppose the neurotoxic and neuroinflammatory consequences of METH. To explore the additional benefits of permanently elevated VMAT2, this study examined the effects of increased vesicular capacity on in vivo METH toxicity in the VMAT2-HI mice.

Methods

Animals

Six to 8 month old VMAT2-HI and wildtype male mice were used for METH studies. Mice received food and water ad libitum on a 12:12 light cycle unless otherwise noted. All procedures were conducted in accordance with the National Institutes of Health Guide for Care and Use of Laboratory Animals and approved by the Institutional Animal Care and Use Committee at Emory University.

Methamphetamine injection schedule

(+)-Methamphetamine HCl (Sigma, St Louis, MO, USA) was dissolved in 0.9% saline and administered subcutaneously. Mice were given a neurotoxic regimen of four doses of either 5 or 10 mg/kg (free base) METH, 2 hours apart and killed by rapid decapitation 48 hours after the last dose. Tissue for immunoblotting was flash frozen in liquid nitrogen. Tissue for immunohistochemical analysis was drop-fixed in 4% paraformaldehyde.

Core body temperature

Core body temperature was taken 30 minutes before the first injection and 1 hour after the three subsequent injections of saline or METH. Temperature was taken rectally by a digital thermometer (VWR International, Westchester, PA, USA) lubricated with 100% petroleum jelly.

Western blotting

Western blots were performed as previously described (Caudle 2007). Primary antibodies used were: polyclonal rabbit anti-VMAT2 serum (1:20,000), rat anti-DAT (1:5,000), rabbit anti-TH (1:1,000), mouse anti-GFAP (1:5,000) and mouse anti-β-actin

(1:5,000). The appropriate HRP-linked secondary antibodies (1:5,000) were used. Analysis was calibrated to coblotted dilutional standards of pooled sample from all VMAT2-HI samples.

Immunohistochemistry

Immunohistochemistry was performed as previously described (Caudle 2007). Primary antibodies used were: polyclonal rabbit anti-VMAT2 serum (1:50,000), rat anti-DAT (1:1,000), mouse anti-GFAP (1:1,000) or rabbit anti-TH (1:1,000). The appropriate biotinylated secondary antibodies (1:200) were used. Nissl stain was performed for stereological analysis by a 3 minute Cresyl Violet dip of mounted sections prior to dehydration, xylene clearing and coverslipping. All images were acquired with NeuroLucida (MicroBrightField).

Isolectin B4

For microglial visualization, sections were incubated with biotinylated isolectin B4 (1:250; Invitrogen) overnight at room temperature and then incubated 1 hour in avidin–biotin-HRP conjugate solution (Vectastain ABC kit, Vector Laboratories) as previously reported (Guillot et al., 2008b)(Guillot 2008). Visualization was performed using DAB as above for 25 minutes at room temperature.

Statistical analysis

All data were analyzed in GraphPad Prism. Densitometric analysis was analyzed using two-way ANOVA (with treatment and genotype as factors) with Bonferroni post hoc tests. Outliers were defined by the Grubbs' test for outliers ($\alpha = 0.05$). All errors shown are SEM.

Results

Increased VMAT2 protects against METH-induced loss of dopamine neuron terminal markers in the striatum.

Male wildtype and VMAT2-HI mice were treated with 4 injections (s.c.) of either saline (0.9%) or methamphetamine (free base, 10 mg/kg w/v) every 2 hours and sacrificed 48 hours after the final injection. Due to the accumulation of cytosolic dopamine after METH treatment, METH toxicity preferentially targets striatal dopamine terminals. Following this 4 x 10 mg/kg METH dosing regimen, wildtype mice show dramatic losses in the striatal dopamine terminal markers, DAT and TH, as measured by immunoblotting and immunohistochemistry (**Fig. 5.2**). VMAT2-HI mice show significant protection from this DAT and TH loss following METH treatment. Elevated VMAT2 levels were confirmed in the VMAT2-HI mice and also protected from loss after METH (**Fig. 5.2**). At higher magnifications, the preservation of striatal TH innervation in METH-treated VMAT2-HI mice is dramatic (**Fig. 5.3**). In keeping with the typical terminal-targeting of METH toxicity, this 4 x 10 mg/kg METH dose did not induce any cell body loss in the substantia nigra pars compacta (SNpc) as measured by stereological counts of TH-positive neurons (data not shown).

Increased VMAT2 protects against gliosis in the striatum.

METH is known to induce a large inflammatory response, which can be assessed by glial markers in the striatum. Wildtype mice show a significant increase in glial fibrillary acidic protein (GFAP) expression both by immunoblotting and immunohistochemistry (**Fig. 5.4**). VMAT2-HI mice are protected from this astrocyte response as indicated by a significantly smaller increase in GFAP levels. Similarly, wildtype mice show substantial

activation of microglia in response to METH as measured by isolectin B4 (IB4) staining (**Fig. 5.4**). VMAT2-HI mice show less amoeboid microglia morphology, indicating reduced activation of striatal microglia following METH treatment when compared to wildtype animals.

Preferential targeting of the striosomes following METH treatment.

METH treatment causes preferential loss of dopaminergic markers like DAT and TH in the striosomes of the striatum, rather than the surrounding matrix (Granado et al., 2010). Immunohistochemical analysis also shows a preferential loss of dopaminergic terminals in the striosomes following the 4 x 10 mg/kg METH dose in both genotypes as shown by striatal patches with reduced DAT immunoreactivity (**Fig. 5.5**). At a lower 4 x 5 mg/kg METH dose, wildtype animals still show a striosomal loss of DAT (**Fig. 5.5)**. However, the VMAT2-HI animals are completely spared from this preferential striosome loss at this lower dose**.**

Increased VMAT2 level does not alter the hyperthermic response following METH treatment.

Binge METH treatment induces a significant increase in core body temperature that is critical to the neurotoxic effects of the drug (Miller and O'Callaghan, 1994). Core temperatures were taken at baseline and 1 hour after each METH injection in both genotypes. Both wildtype and VMAT2-HI mice show significant increases in core body temperatures following METH treatment (**Fig. 5.6**). However, the elevated core temperature following METH treatment was the same between the genotypes.

Elevated VMAT2 is also neuroprotective at a lower METH dose.

To determine if VMAT2-mediated protection from METH toxicity occurred at a lower dose, wildtype and VMAT2-HI animals were also treated with a 4 x 5 mg/kg METH dose that induced no hyperthermia. At this dose, wildtype mice show small reductions in DAT and TH in the striatum (**Fig. 5.7**). The VMAT2-HI mice are protected from this loss. Similarly, wildtype mice show a large increase in GFAP expression following the 4 x 5 mg/kg METH dose (**Fig. 5.7**). Again, the VMAT2-HI mice are protected from this METH-induced astrogliosis.

Discussion

Elevated VMAT2 protects against METH toxicity.

Due to its ability to sequester both endogenous (e.g. cytosolic dopamine) and even exogenous toxicants (e.g. MPTP metabolites) into vesicles, VMAT2 acts as a neuroprotective mechanism in dopamine neurons (Guillot and Miller, 2009). Reduced VMAT2 levels increase cytosolic dopamine metabolism and cause both progressive dopaminergic loss and an exaggerated response to a toxic insult (Takahashi et al., 1997; Wang et al., 1997a; Fumagalli et al., 1999; Caudle et al., 2007; Guillot et al., 2008b). Due to the increased vesicular capacity in the VMAT2-HI mice, it was predicted that these mice would have a reduced cytosolic dopamine burden when challenged with METH, thus protecting the midbrain dopamine pathway. This study shows that the VMAT2-HI mice are protected from dopaminergic terminal loss by immunochemical techniques at two different METH doses (**Fig. 5.2 and Fig. 5.7**). Furthermore, there is a preferential targeting of the degeneration in the striosomes, as compared to the surrounding striatal matrix. While the specificity of this loss is unknown, the striosomes are characterized by lower levels of superoxide dismutase 2 (SOD2) to reduce reactive oxygen species (Medina et al., 1996) and also increased vascularization that may increase exposure to the drug (Breuer et al., 2005), both of which may contribute to elevated METH toxicity in these regions. It appears that elevated VMAT2 levels do not alter this striosome-targeting aspect of METH toxicity since the VMAT2-HI mice still see a preferential loss of striosomal markers, just at a higher METH dose (**Fig. 5.5**). These results suggest that the neuroprotection seen in the VMAT2-HI mice represents a shifting of the severity of METH toxicity.

Increased VMAT2 reduces the neuroinflammatory response to METH.

The VMAT2-HI mice show reduced neuroinflammatory responses following METH treatment compared to wildtype animals, including protection from astrogliosis as indicated by significantly reduced GFAP expression (**Fig. 5.4**). Additionally, both genotypes show increased microglial expression in METH-treated mice using isolectin B4 staining. However, it appears that METH-treated wildtype mice show amoeboid morphological changes indicating activated microglia, whereas VMAT2-HI mice show less of this dysmorphic microglial staining. Though it is unclear as to what mechanisms induce the neuroinflammatory cascade following METH treatment, work with mice lacking the DAT has implicated extracellular dopamine in this response. METH treatment in DAT-knockout mice does not induce dopamine efflux (Fumagalli et al., 1998). Interestingly, these DAT-knockout mice also have no METH-induced glial activation, suggesting that the inflammatory cascade is dependent on the efflux of dopamine. Since VMAT2-HI mice have increased vesicular dopamine storage, it is possible that the redistribution of synaptic dopamine may alter the dopamine efflux following METH and reduce the inflammatory response. Admittedly, it is also possible that the reduced neuroinflammatory response in the VMAT2-HI mice is due to an unknown protective mechanism that occurs after injury following the metabolism of METH. Further studies on the time-course of this neuroprotective effect would be needed to address such questions.

Elevated VMAT2 does not change the hyperthermic response to METH.

METH administration raises core body temperature, a mechanism integral to its toxicity (Miller and O'Callaghan, 1994). Pharmacologically lowered core temperature is neuroprotective against METH (Albers and Sonsalla, 1995). Based on decades of work on the hypothermic effects of the VMAT2 inhibitor reserpine (Lessin and Parkes, 1957), it

was necessary to show that the VMAT2-HI mice have no alterations to either their core temperatures at baseline or following METH. Wildtype and VMAT2-HI mice show identical hyperthermic responses following METH treatment (**Fig. 5.6**). These results demonstrate that the neuroprotection seen in the VMAT2-HI mice is not due to an altered response in core temperature.

Elevated VMAT2 does not increase the rewarding potential for METH.

The data presented here show that elevated VMAT2 level or function would be beneficial in protecting against a dopaminergic toxicant. However, the elevated dopamine tissue content and stimulated dopamine release in the VMAT2-HI mice could also cause negative behavioral effects in the presence of a psychostimulant like METH. Surprisingly, the VMAT2-HI mice show no increase in conditioned place preference for 1 mg/kg METH (data not shown), a dose shown to induce conditioned place preference and locomotor sensitization in mice (Shimosato and Ohkuma, 2000; Thiriet et al., 2011). Additionally, the VMAT2-HI mice show the same level of enhanced locomotor activity following this METH dose, even though they have enhanced activity at baseline. These results suggest that vesicle-based approaches aimed at reducing intracellular toxicity may not negatively impact other dopamine-mediated behaviors.

VMAT2-HI mice suggest that dopamine compartmentalization is integral to METH neurotoxicity.

Dopamine molecules left unpackaged in the neuronal cytosol can create neurotoxic byproducts through both oxidative and metabolic processes. Cytosolic dopamine can be converted to form both reactive oxygen species including hydroxyl radicals, superoxide, and hydrogen peroxide (Sulzer and Zecca, 1999). Oxidized dopamine results in the

formation of dopamine-quinones that can be conjugated with cysteine to form 5-cysteinyl-dopamine. This cysteinyl adduct can alter the function of other intracellular proteins and contribute to dopaminergic neurodegeneration (LaVoie and Hastings, 1999). Additionally, there has been evidence linking dopamine-quinones to microglial activation (Kuhn et al., 2006) and inhibition of DAT (Whitehead et al., 2001; Park et al., 2002) and TH (Kuhn et al., 2001). Intracellular dopamine metabolism begins with monoamine oxidase-A conversion of dopamine to the catecholaldehyde, 3,4-dihydroxyphenylacetaldehyde (DOPAL) (Eisenhofer et al., 2004a). If DOPAL is not detoxified through conversion to DOPAC by aldehyde dehydrogenase, DOPAL exerts toxic effects via a variety of mechanisms in the neuron, including quinone and hydroxyl radical formation, protein cross-linking, and oligomerization of α-synuclein (Burke et al., 2003, 2008; Anderson et al., 2011; Goldstein et al., 2013).

These toxic mechanisms are particularly important to midbrain dopamine neurons, which are uniquely vulnerable to degeneration and toxic insults as seen in a variety of genetic and toxicant animal models of dopamine dysfunction (Sulzer, 2007). While some may assume that the elevated striatal dopamine levels in the VMAT2-HI mice would actually be detrimental in a METH model, these data suggest that the majority of this dopamine is distributed into the vesicles, thus preserving terminal integrity. The findings presented here also complement previous work done via VMAT2 overexpression in PC12 cells (Vergo et al., 2007) and on the effects of the pituitary adenylyl cyclase activating polypeptide (PACAP38) in mice (Guillot et al., 2008a), both of which suggested that manipulation of VMAT2 level can ameliorate aspects of METH toxicity.

Potential mechanisms for METH neuroprotection in VMAT2-HI mice.

The results from the current study bring together a large body of work on the interaction of the synaptic vesicle and METH at dopaminergic synapses (**Fig. 5.9**). The reduced METH toxicity in the VMAT2-HI mice complements the "weak base" mechanism of METH action, which suggests that amphetamines act as a weak base once inside the synaptic vesicle, reducing the vesicular pH gradient, and causing a depletion of the vesicular contents (Sulzer and Rayport, 1990; Sulzer et al., 1992). Indeed, the 4 x 10 mg/kg METH dose used in the present study has previously been shown to rapidly decrease vesicular [^{3}H]-dopamine uptake both 1 and 24 hours after treatment in purified synaptic vesicles from rats (Ugarte et al., 2003). This change in vesicular uptake correlates with a redistribution of VMAT2 protein from the vesicular fraction to the plasma membrane of the synaptosome. Besides their higher vesicular function at baseline, it is also likely that the VMAT2-HI mice maintain a higher level of VMAT2 in the vesicular fraction following METH treatment.

One can imagine three ways that the increased vesicular function in the VMAT2-HI mice may protect a dopamine neuron from METH. First, increased VMAT2 levels may maintain vesicular filling in the presence of METH and counteract the METH-induced vesicular depletion of dopamine. This would keep more dopamine sequestered into vesicles and less potentially toxic dopamine byproducts in the cytosol. Alternatively, increased VMAT2 levels could cause a faster recovery of the pH gradient following the disappearance of METH. This would allow for a more efficient restoration of vesicular dopamine contents in the VMAT2-HI mice. Finally, it is possible that the neuroprotection via increased VMAT2 is not directly dependent upon dopamine handling at all. With the

elaborate arborization and large number of synapses made by striatal dopamine neurons, it has been suggested that these cells carry a substantial bioenergetic burden (Bolam and Pissadaki, 2012). If increased VMAT2 more efficiently allows for the packaging of transmitter and toxic molecules, it is possible that the oxidative stress and energy consumption of these synapses may also be reduced.

VMAT2 inhibitors as a treatment for addiction.

Recent work has suggested that the inhibition of VMAT2 may be a therapeutic treatment to reduce psychostimulant abuse (Dwoskin and Crooks, 2002; Nickell et al., 2010). Lobeline, an inhibitor of VMAT2 at the tetrabenazine binding site, decreases amphetamine-evoked dopamine output, but not electrically-stimulated output, suggesting that lobeline provides a selective inhibition of amphetamine effects. It has been suggested that this reduction occurs via increased dopamine metabolism and a reduction in the dopamine available for reverse transport through the DAT (Miller et al., 2001). Thus, by taking a VMAT2 inhibitor, dopamine-releasing drugs such as amphetamine have less of a rewarding or euphoric effect. These studies suggest that lobeline and its analogs have potential for therapeutic use in addiction. However, long-term reductions in VMAT2 function through pharmacological (e.g. reserpine and tetrabenazine) and genetic (e.g. VMAT2-deficient mice) manipulations have been shown to increase vulnerability to neurodegeneration, reduce locomotion, and dramatically alter affective behaviors (Freis, 1954; Pettibone et al., 1984; Fumagalli et al., 1999; Caudle et al., 2007; Guillot et al., 2008b; Taylor et al., 2009). Based on these findings, a targeted VMAT2-inhibitor should be pursued cautiously and, perhaps, for only brief treatment periods.

Neuroprotection via elevated VMAT2 function.

Even the most subtle alterations in intracellular dopamine levels can alter METH neurotoxicity (Thomas et al., 2008). The data presented here suggest that a positive modulator of VMAT2 may be highly beneficial in preventing cellular toxicity in dopamine neurons. Additionally, these findings suggest that elevated VMAT2 function does not enhance the rewarding effects of METH, a critical distinction that could have confounded the therapeutic potential of a positive VMAT2 modulator. VMAT2 modulation may be especially relevant to dopamine neurons, which are often considered to be vulnerable to insult (Guillot and Miller, 2009). Evidence also suggests that METH-mediated toxicity may elevate the risk of other dopaminergic dysfunction based on emerging evidence that METH and amphetamine users have up to a 3-fold increase in the likelihood of developing Parkinson's disease throughout their lifetime (Callaghan et al., 2012; Curtin et al., 2014). In hypodopaminergic states like Parkinson's disease or the METH-treated brain, increasing vesicle function would provide two therapeutic benefits: restoration of dopaminergic signaling and protection against cytosolic neurotoxicity.

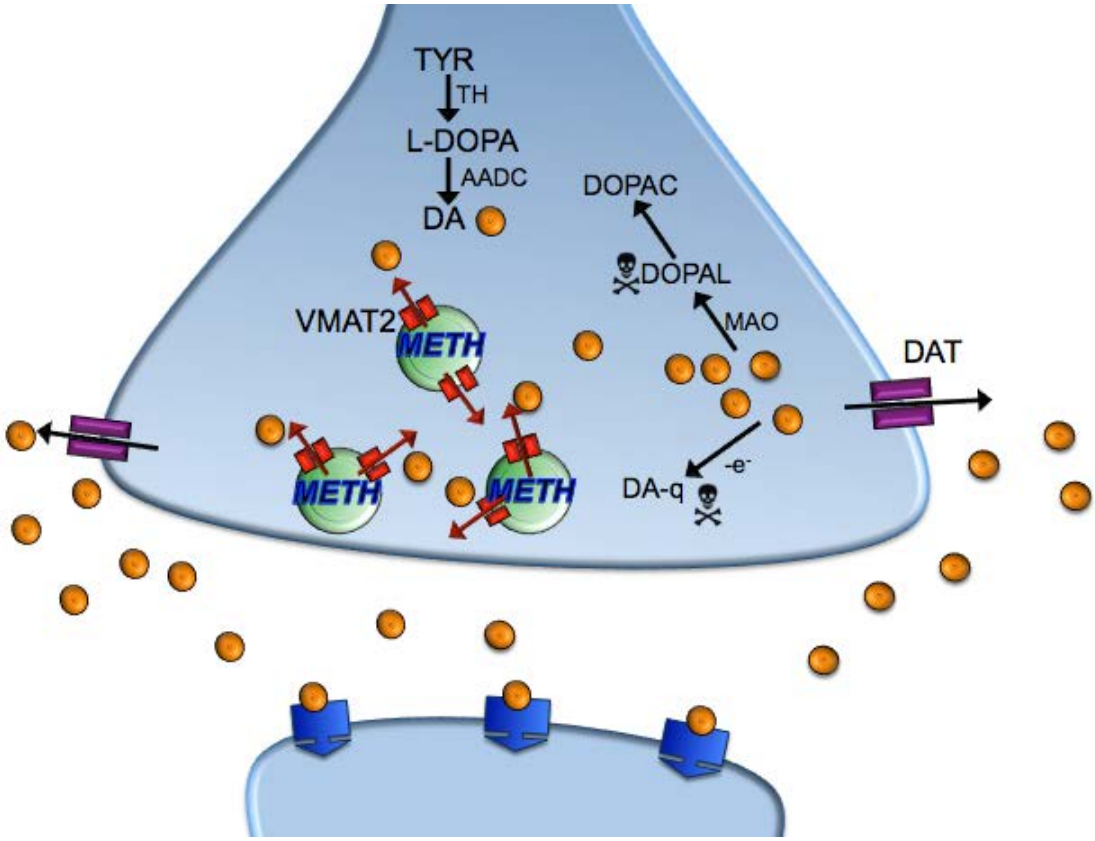
TYR
TH
L-DOPA
AADC
DA
DOPAC
DOPAL
MAO
VMAT2
METH
METH
METH
DAT
-e⁻
DA-q

Figure 5.1 Schematic for methamphetamine toxicity in a dopaminergic terminal.

METH causes a disruption of dopamine compartmentalization at the synaptic terminal. METH enters dopaminergic terminals via the DAT and depletes vesicular dopamine stores. This results in a large increase in cytosolic dopamine. Cytosolic dopamine, when not sequestered into the vesicular compartment, is vulnerable to oxidation and conversion to neurotoxic species, including the formation of dopamine-quinones and cysteinyl adducts. Additionally, METH promotes dopamine synthesis via upregulation of TH function and opposes dopamine degradation via reductions in MAO activity. The large amount of cytosolic dopamine causes an efflux of dopamine via the DAT. This dopamine efflux results in a flood of extracellular dopamine, which acts on postsynaptic receptors and causes the psychostimulant effects of the compound.

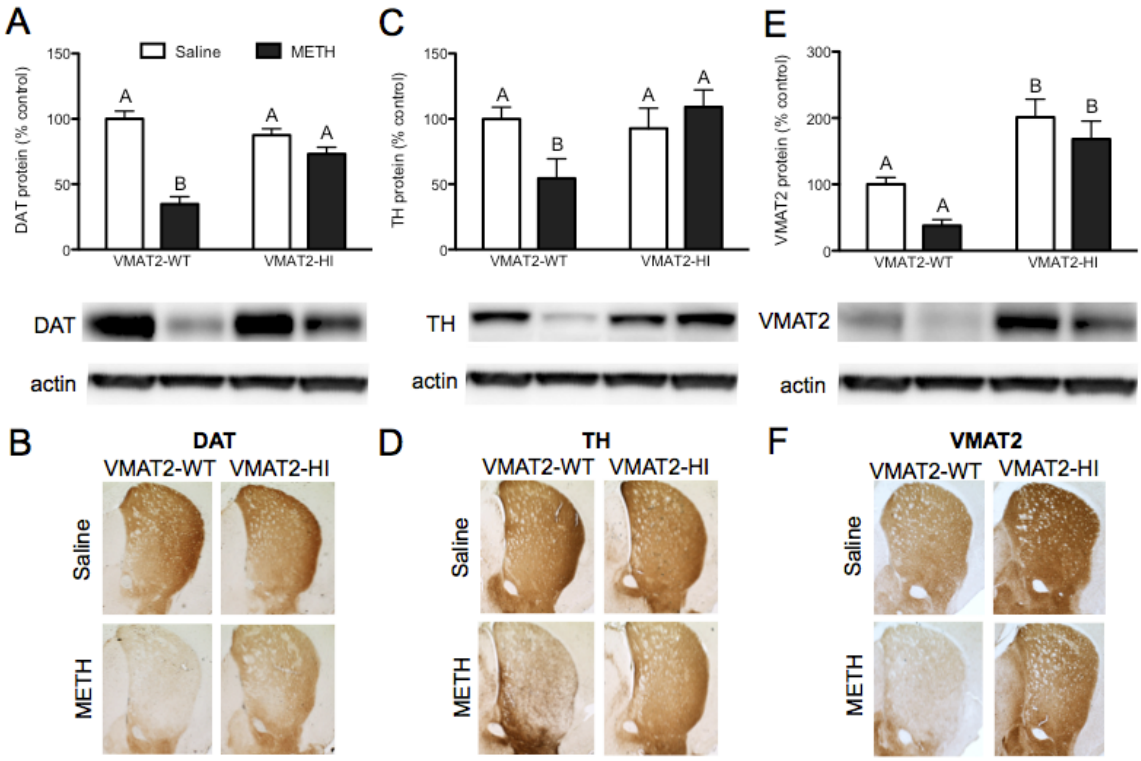
A
Saline
METH
DAT protein (% control)
150
100
50
0
A
B
A
A
VMAT2-WT
VMAT2-HI
C
TH protein (% control)
150
100
50
0
A
B
A
A
VMAT2-WT
VMAT2-HI
E
VMAT2 protein (% control)
300
200
100
0
A
A
B
B
VMAT2-WT
VMAT2-HI
DAT
actin
TH
actin
VMAT2
actin
B
DAT
VMAT2-WT
VMAT2-HI
Saline
METH
D
TH
VMAT2-WT
VMAT2-HI
Saline
METH
F
VMAT2
VMAT2-WT
VMAT2-HI
Saline
METH

Figure 5.2. VMAT2-HI mice are significantly protected from METH toxicity.

Male wildtype and VMAT2-HI mice were treated with 4 injections of either saline or 10 mg/kg methamphetamine every 2 hours and sacrificed 48 hours after the final injection. **(A-D)** Wildtype animals show significant losses in DAT and TH levels. VMAT2-HI mice are significantly protected from losses in both DAT ($p < 0.01$) and TH ($p < 0.05$) following METH. (**E-F**) Wildtype mice also show a trend towards VMAT2 protein loss following METH, while VMAT2-HI mice maintain a VMAT2 level greater than wildtype even following METH. Data are presented as % of saline-treated wildtype mice. Different letters at the tops of bars indicate differences of at least $p < 0.05$ as determined by a two-way ANOVA with Bonferroni post-hoc tests ($n = 6$).

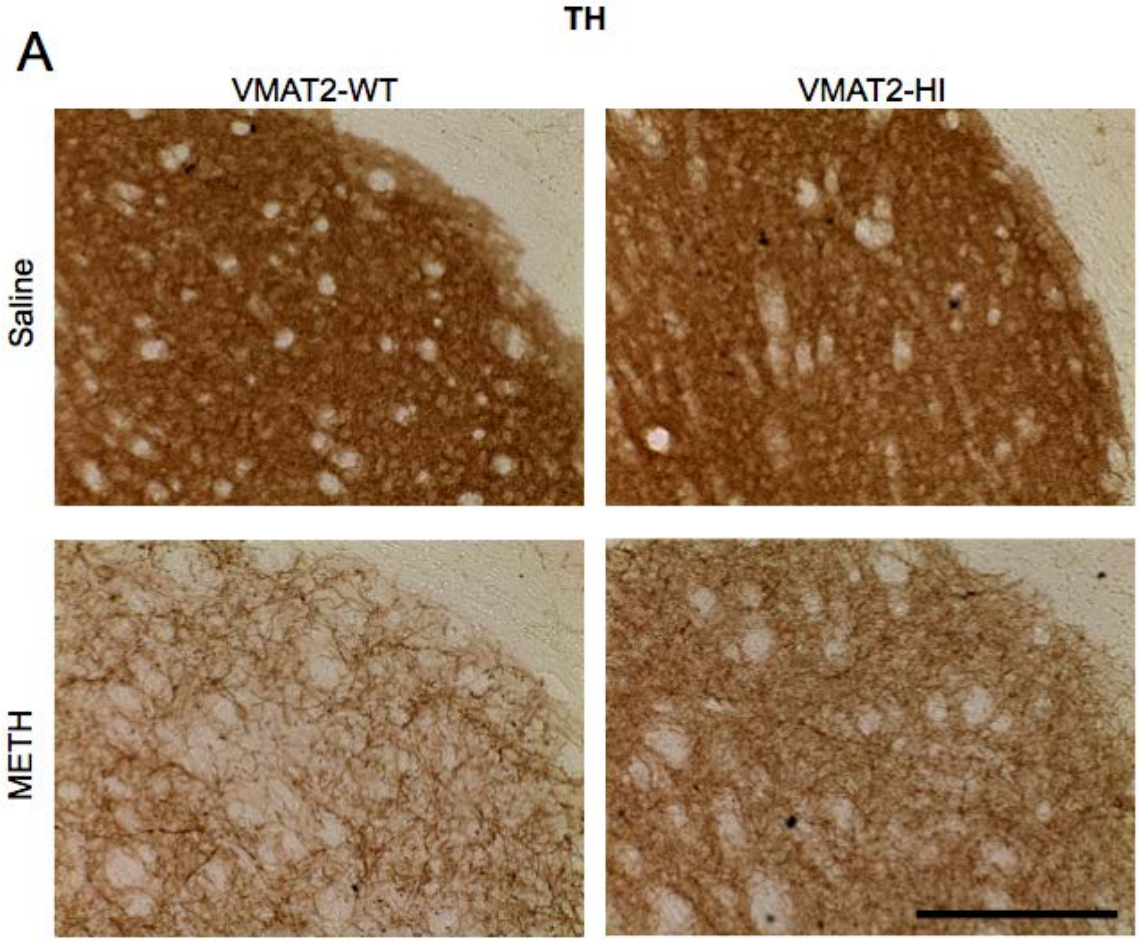
A
TH
VMAT2-WT
VMAT2-HI
Saline
METH

Figure 5.3. Higher magnification of TH-positive terminals in METH-treated mice of both genotypes.

VMAT2-HI mice are protected from the loss of TH+ fibers in the striatum. Representative images of dorsolateral striatum pictured with cortex on the right side of each image. Scale bar = 200 μm.

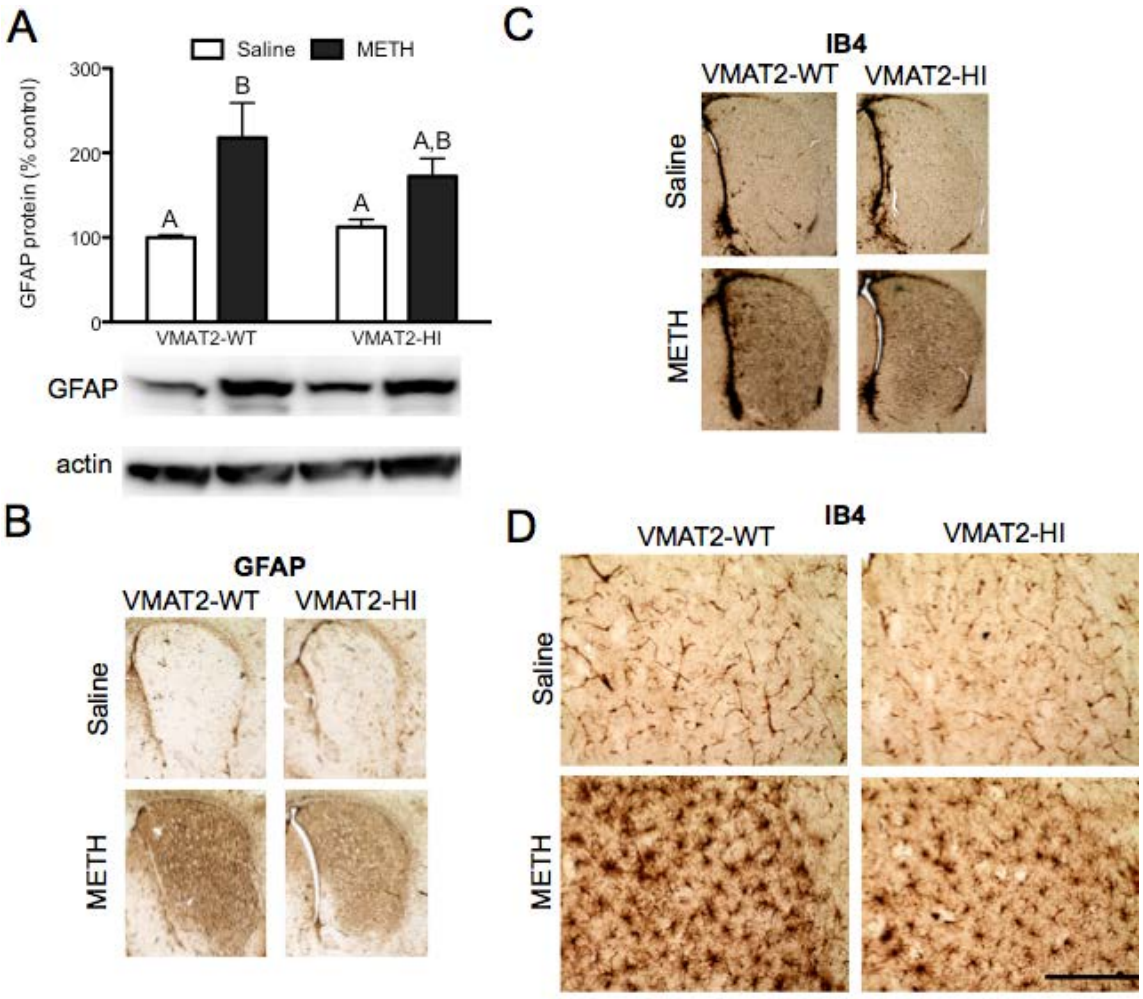
A
Saline
METH
GFAP protein (% control)
300
200
100
0
A
B
A
A,B
VMAT2-WT
VMAT2-HI
GFAP
actin
B
GFAP
VMAT2-WT
VMAT2-HI
Saline
METH
C
IB4
VMAT2-WT
VMAT2-HI
Saline
METH
D
IB4
VMAT2-WT
VMAT2-HI
Saline
METH

Figure 5.4. VMAT2-HI mice are protected from the inflammatory cascade following METH treatment.

(A-B) VMAT2-HI mice show a significantly smaller increase in astrogliosis as indicated by GFAP expression (n = 6). Different letters above the bars indicate difference of $p < 0.05$. Data are presented as % of saline-treated wildtype mice. (C-D) VMAT2-HI mice show less ramified microglia as shown by IB4 staining. Representative images of dorsolateral striatum pictured with corpus callosum in the upper right corner of each image. Scale bar = 200 μm.

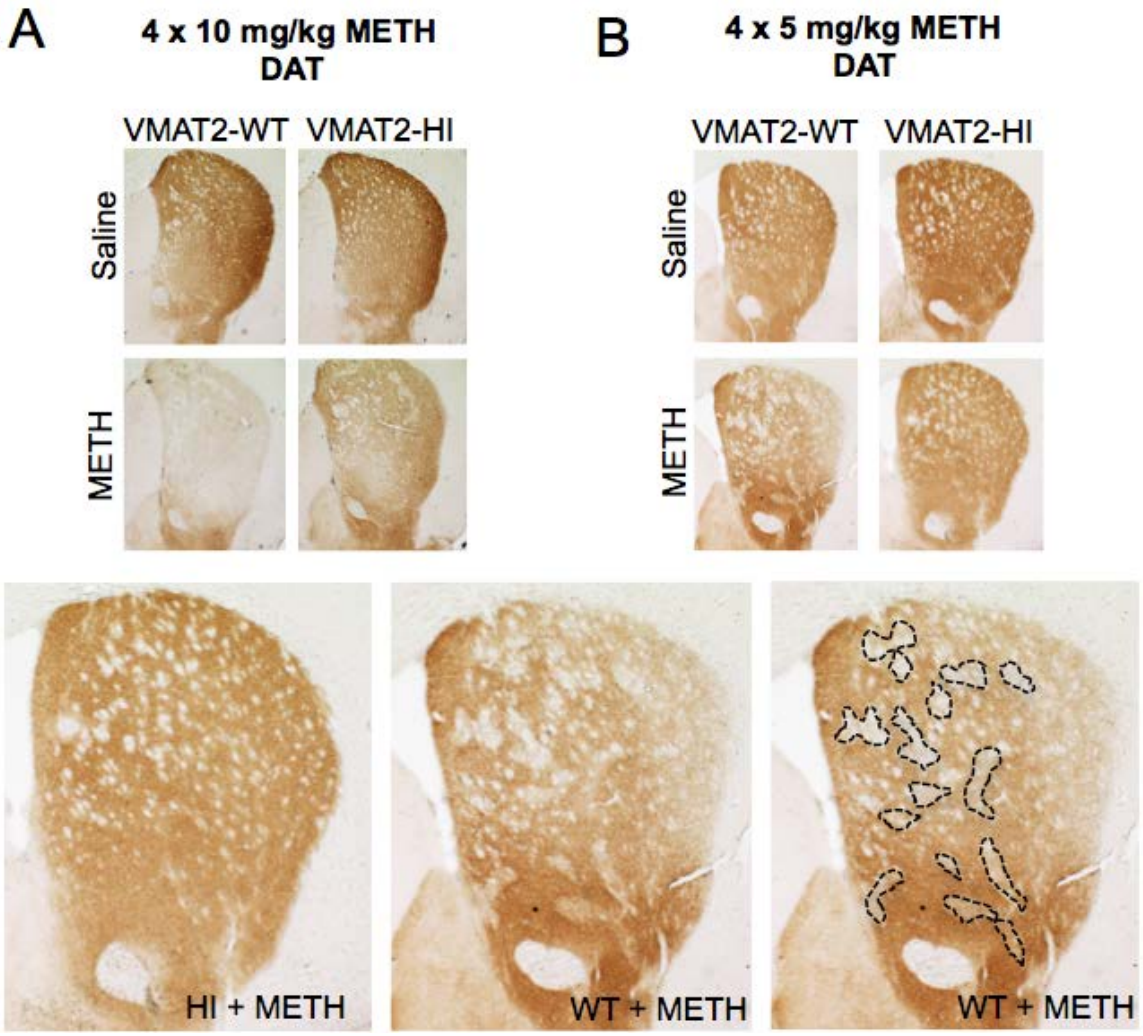
A
4 x 10 mg/kg METH
DAT
VMAT2-WT
VMAT2-HI
Saline
METH
B
4 x 5 mg/kg METH
DAT
VMAT2-WT
VMAT2-HI
Saline
METH
HI + METH
WT + METH
WT + METH

Figure 5.5. Preferential loss of dopamine markers in the striosomes of both genotypes.

(A-B) No difference in TH+ cells ($p > 0.05$) or Nissl+ cells ($p > 0.05$) between the genotypes following a 4 x 10 mg/kg METH dose ($n = 6$). (C) Representative images of TH staining of the midbrain with and without METH treatment. Dashed lines emphasize striosome-specific loss of TH labeling.

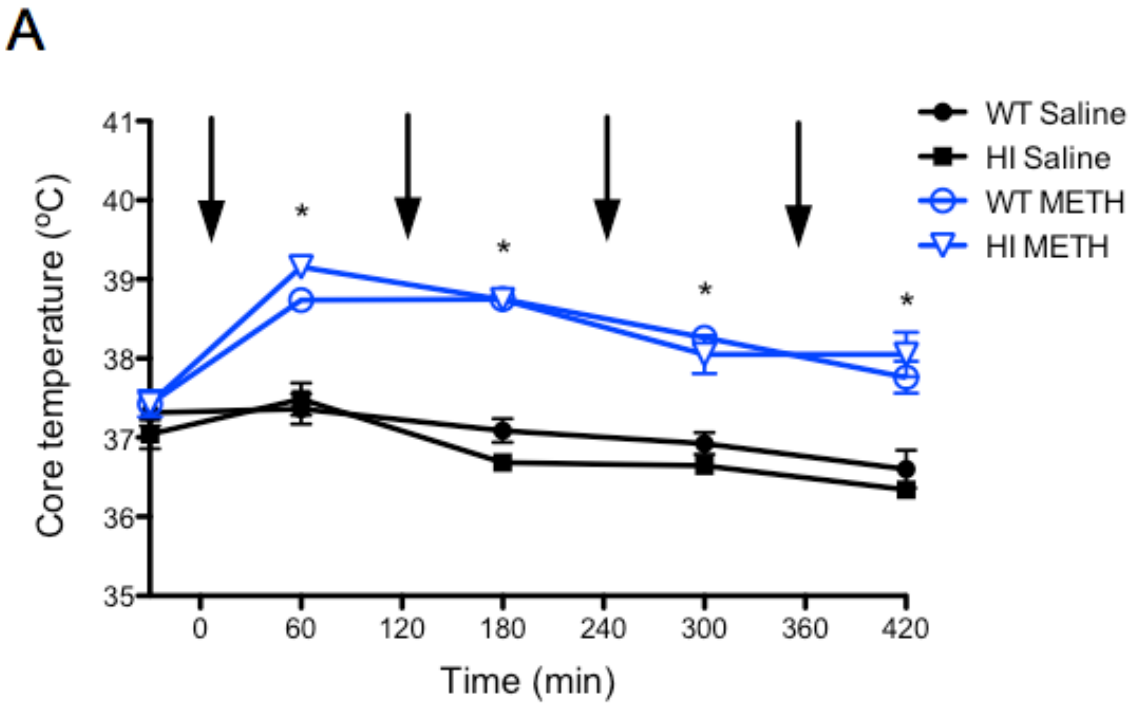
A
Core temperature (°C)
41
40
39
38
37
36
35
0
60
120
180
240
300
360
420
Time (min)
*
*
*
*
WT Saline
HI Saline
WT METH
HI METH

Figure 5.6. Increased VMAT2 level does not alter the hyperthermic response following METH treatment.

Core temperatures taken 1 hour post each METH injection (injections indicated by arrows). While there was a significant increase in core temperature in both genotypes, there was no difference between the hyperthermic profiles between wildtype and VMAT2-HI mice ($p > 0.05$) ($n = 12$).

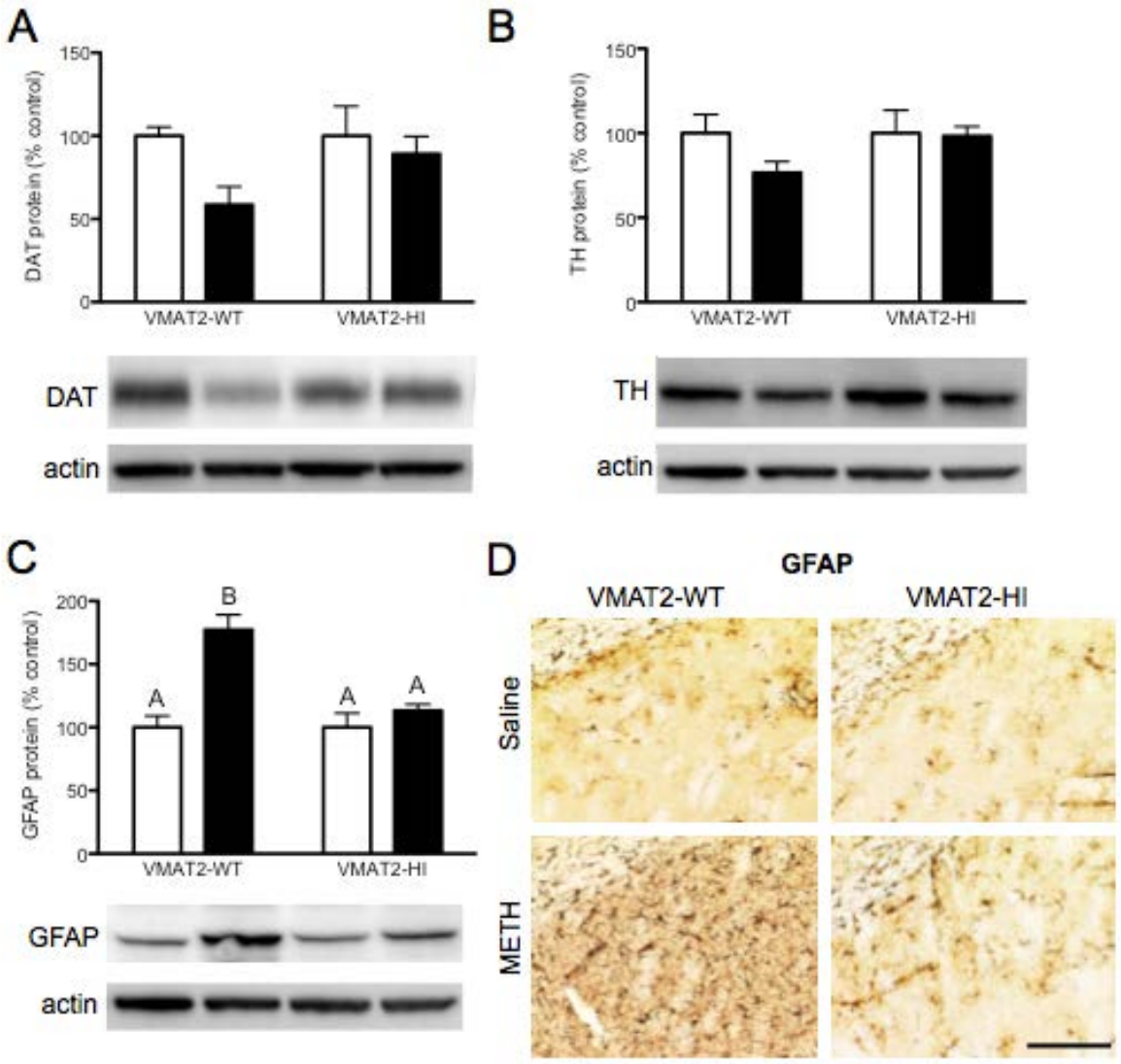
A
DAT protein (% control)
150
100
50
0
VMAT2-WT
VMAT2-HI
DAT
actin
B
TH protein (% control)
150
100
50
0
VMAT2-WT
VMAT2-HI
TH
actin
C
GFAP protein (% control)
200
150
100
50
0
A
B
A
A
VMAT2-WT
VMAT2-HI
GFAP
actin
D
GFAP
VMAT2-WT
VMAT2-HI
Saline
METH

Figure 5.7. VMAT2-HI mice are also protected from methamphetamine toxicity at a lower dose 4 x 5 mg/kg METH.

(A-B) Wildtype mice show trends towards dopaminergic terminal loss in both DAT and TH. (C-D) VMAT2-HI mice show no increase in GFAP, while wildtype mice present a robust inflammatory response ($n = 5$). Different letters indicate difference of $p < 0.05$. Data are presented as % of saline-treated wildtype mice. Dorsolateral striatum pictured with corpus callosum in the upper right corner of each image. Scale bar = 200 μm.

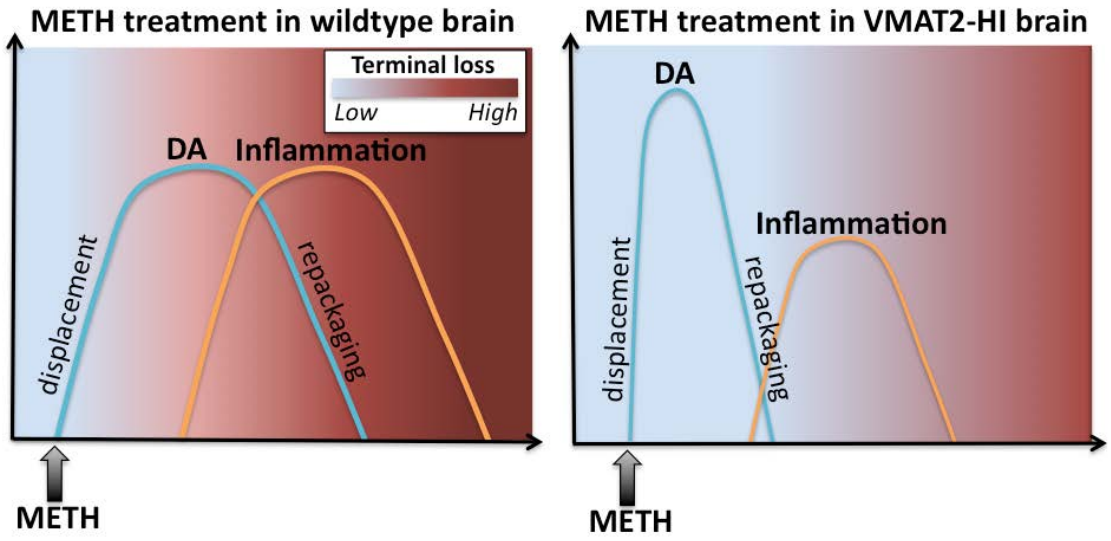
METH treatment in wildtype brain
Terminal loss
Low
High
DA
Inflammation
displacement
repackaging
METH
METH treatment in VMAT2-HI brain
DA
Inflammation
displacement
repackaging
METH

Figure 5.8. Hypothetical interaction of VMAT2 function and methamphetamine.

While the timeline and exact mechanism of the compound's toxicity are unknown, it is clear that METH displaces dopamine in neuronal terminals by both depleting vesicular stores and reversing DAT transport (blue line). Though the work presented here did not describe METH-induced dopamine measurements by microdialysis, we assume that VMAT2-HI mice would 1) release more DA following METH application due to their elevated dopamine levels and 2) sequester and repackage this displaced dopamine more quickly than their wildtype littermates. If one assumes that the toxicity of METH is dependent on the perisistent accumulation of cytosolic dopamine, these dynamics may explain the reduced toxicity shown in the VMAT2-HI mice (red background gradient). We have also shown that the inflammatory response following METH is also lessened in the VMAT2-HI mice (orange line). Based on previous accounts in the literature, we also know that this dopamine displacement induces an inflammatory cascade, which may explain the protection shown in the VMAT2-HI mice.

CHAPTER VI: NEURONAL VULNERABILITY AND LEVODOPA HANDLING IN VMAT2 GENOTYPES

Introduction

The vesicular monoamine transporter 2 (VMAT2; SLC18A2) is located on both synaptic and dense core vesicles to allow for the vesicular packaging of the monoamine neurotransmitters: dopamine, norepinephrine, serotonin, and histamine. As a 12-transmembrane H^+-ATPase antiporter, VMAT2 is evolutionarily related to a family of toxin extruding transporters (TEXANs), which explains its ability to also sequester neuronal toxicants from the cytosol into vesicles. In fact, the initial cloning of VMAT was the result of the discovery of resistance to the dopaminergic toxicant 1-methyl-4-phenyl-1,2,3,6-tetrahydropyridine or MPTP (Erickson et al., 1992; Liu et al., 1992a, 1992b). Additionally, the packaging of cytosolic dopamine by VMAT2 is particularly important since dopamine left unpackaged is susceptible to the formation of reactive oxygen species and dopamine-quinones (Sulzer and Zecca, 1999). Thus, through its sequestration of cytosolic dopamine, VMAT2 also opposes this endogenous toxicity.

In mice, genetic knockout of VMAT2 is fatal (Takahashi et al., 1997; Wang et al., 1997b). We previously reported that VMAT2-deficient mice, which have a 95% reduction in VMAT2 expression, exhibit progressive catecholaminergic degeneration, dysregulated dopamine homeostasis, α-synuclein accumulation, and both motor and nonmotor behavioral deficits reminiscent of Parkinson's disease (Caudle et al., 2007; Taylor et al., 2009, 2014). Reduced VMAT2 levels in mice increase neuronal vulnerability to a variety of toxicants, including MPTP and methamphetamine (Takahashi et al., 1997; Gainetdinov et al., 1998; Fumagalli et al., 1999; Staal et al., 2000; Mooslehner et al., 2001; Guillot et al., 2008b). Most recently, mice with elevated VMAT2 levels were shown to have enhanced dopaminergic output and resistance to both MPTP and methamphetamine (Lohr

et al., 2014, 2015). Unfortunately, the VMAT2-deficient mice described previously were of a mixed genetic background consisting of both C57BL/6 and 129SV strains (Caudle et al., 2007; Guillot et al., 2008b; Taylor et al., 2009, 2011), whereas the VMAT2-HI mice were bred onto a pure C57BL/6 strain. It is well established that background strain of mice greatly influences neurochemical, pharmacological, and behavioral outcomes. Thus, studying the effects of altered vesicular function in mice with varying levels of VMAT2 requires that these animals are on the same background strain. Here we describe the first genotypic continuum of vesicular function using VMAT2-LO, wildtype, and VMAT2-HI mice on a pure C57BL/6 background. We show that reduced vesicular function results in both progressive neurodegeneration and an increased vulnerability to the dopaminergic toxicant, MPTP. Conversely, elevated vesicular function opposes these deficits.

Finally, since VMAT2 level dictates dopamine storage capacity, we examined the handling of exogenously applied dopamine in mice with varying VMAT2 levels both with and without dopaminergic terminal loss. To address this question, we measured stimulated dopamine release from striatal slices of lesioned and unlesioned VMAT2 mice following L-DOPA application. We predicted that increased VMAT2 level would better package dopamine from this exogenous source. Here we show that elevated VMAT2 levels preserves of stimulated dopamine release following a neurotoxic lesion and, surprisingly, even alter neurochemical handling of the excess dopamine.

Methods

Back-crossing of the VMAT2-LO mice

The VMAT2-deficient mice previously described by our lab (Caudle et al., 2007; Guillot et al., 2008b; Taylor et al., 2009, 2014) had been outbred to reintroduce the α-synuclein gene, which had been spontaneously deleted from the original VMAT2-deficient strain (Ka1) originally described by other groups (Mooslehner et al., 2001; Specht and Schoepfer, 2001). These α-synuclein-positive VMAT2-deficient mice were maintained on a C57BL/6 and 129SV mixed genetic background in our lab. For the current study, these mixed background VMAT2-deficient mice were backcrossed to Charles River C57BL/6 mice for 4 generations using a marker assisted selection (i.e. "speed congenic") approach. Mouse genomes were assessed at the DartMouseTM Speed Congenic Core Facility at Dartmouth Medical School. DartMouse uses the Illumina, Inc. (San Diego, CA) GoldenGate Genotyping Assay to interrogate 1449 SNPs spread throughout the genome. The raw SNP data were analyzed using DartMouse's SNaP-MapTM and Map-SynthTM software, allowing the determination for each mouse of the genetic background at each SNP location. These backcrossed VMAT2-deficient mice on a congenic for a C57BL/6 background are referred to as VMAT2-LO hereafter. Mice were 1 year old upon testing, except in the aging study where mice were 22 month old. Wildtype mice from both VMAT2-LO and VMAT2-HI colonies were used.

VMAT2-HI mice

BAC transgenic VMAT2-overexpressing mice were generated as previously described (Lohr et al., 2014). Mice were 1 year old upon testing.

MPTP injection schedules

Male mice of the varying genotypes were injected (s.c.) with either MPTP-HCl (M0896, Sigma,) or saline (0.9%). The lesion consisted of two injections of 10 mg/kg

MPTP (freebase) with an interinjection interval of 10 hours. Mice were killed 7 days after the final dose for immunochemical and voltammetry analyses.

Western blotting

Western blots were performed as previously described (Caudle et al., 2007). Primary antibodies used were: polyclonal rabbit anti-VMAT2 serum (Covance1:20,000), rat anti-DAT (Millipore, 1:5,000), rabbit anti-TH (Millipore, 1:1,000), mouse anti-GFAP (1:5,000) and mouse anti-β-actin (Sigma, 1:5,000). The appropriate HRP-linked secondary antibodies (Jackson ImmunoResearch, 1:5,000) were used. Analysis was calibrated to coblotted standards of pooled sample from wildtype samples. Rabbit polyclonal anti-VMAT2 serum was raised against a peptide in the C-terminal region of mouse VMAT2 (CTQNNVQPYPVGDDEESESD) by Covance Custom Immunology Services.

Immunohistochemistry

Immunohistochemistry was performed as previously described (Caudle et al., 2007). Primary antibodies used were: polyclonal rabbit anti-VMAT2 serum (1:50,000), rat anti-DAT (1:1,000), mouse anti-GFAP (1:1,000) or rabbit anti-TH (1:1,000). The appropriate biotinylated secondary antibodies (Jackson ImmunoResearch, 1:200) were used. All images were acquired with NeuroLucida (MicroBrightField).

Fast-scan cyclic voltammetry in striatal slice

Slice FSCV was performed as previously described (Kile et al., 2012). A five-recording survey of four different dorsal striatal release sites was taken for each animal with a 5-minute rest interval between each synaptic stimulation (2.31 V). Application of waveform, stimulus, and current monitoring was controlled by TarHeel CV [University of North Carolina (UNC)] using a custom potentiostat (UEI, UNC Electronics Shop). The

waveform for dopamine detection consisted of a −0.4 V holding potential versus an Ag/AgCl (In Vivo Metric) reference electrode. The applied voltage ramp goes from −0.4 V to 1.0 V and back to -0.4 V at a rate of 600 V/s at 60 Hz. Maximal release at striatal sites in a slice was averaged. Carbon-fiber microelectrodes were calibrated with dopamine standards using a flow-cell injection system. Kinetic constants were extracted using nonlinear regression analysis of release and uptake of dopamine.

L-DOPA fast-scan cyclic voltammetry

The applied voltage ramp and recording parameters were the same as described above. Both saline and MPTP-lesioned wildtype, VMAT2-LO, and VMAT2-HI animals were used in these experiments. Following incubation in oxygenated HEPES aCSF (30° C), five recordings were taken from a single stable dorsolateral striatal site for two different sets of stimulation parameters. Stimulation 1 was 1 pulse applied at 60 Hz (2.31 V) with 5 minutes of rest in between stimulations. Afterwards, stimulation set 2 was applied with 4 pulses applied at 10 Hz with 10 minutes of rest between stimulations. After these baseline recordings, HEPES aCSF with 100 μM L-DOPA (Sigma) and 1.7 mM ascorbate was applied to the slice for 1 hour followed by a 1 hour washout with HEPES aCSF. Following the washout period, recordings were taken again with both stimulation parameter sets.

[^{3}H]-WIN binding

[^{3}H]-WIN 35,428 (83 Ci/mmol) was obtained from PerkinElmer Life Sciences. Bilateral striata were dissected from wildtype and VMAT2-HI mice following rapid decapitation. Tissue was homogenized in homogenization buffer using a glass-teflon homogenizer at 1000 rpm for 10-12 strokes. Following, a 10 minute spin at 48000 x g, the pellet was resuspended and the spin was repeated three times. The final pellet was

then resuspended in DAT binding buffer at a ratio of 1 bilateral striatum per 1 mL. These crude striatal synaptosomes were incubated with a single concentration (10 nM) of [3H]-WIN 35,428 in 25 mM sodium phosphate buffer for 1 hour at 4°C. Incubations were terminated by rapid vacuum filtration onto GF/B filter paper, and radioactivity was determined by liquid scintillation counting. Nonspecific binding was determined using the addition of 10 μM nomifensine, and specific binding was calculated as the total binding minus nonspecific binding (incubated with nomifensine). After determination of protein concentrations, binding to DAT was calculated as fmol/mg protein and expressed as raw values.

Statistical analysis

All data were analyzed in GraphPad Prism. Differences were analyzed using two-way ANOVA (with treatment and genotype as factors) with Bonferroni post hoc tests. Outliers were defined by the Grubbs' test for outliers ($\alpha = 0.05$). All errors shown are SEM.

Results

Reduced VMAT2 causes loss of dopamine terminal integrity in aged mice on a C57BL/6 genetic background.

The newly generated VMAT2-LO mice were shown to be >97% for the desired C57BL/6 background. These VMAT2-LO mice showed significantly reduced vesicular uptake in isolated vesicles (**Fig. 6.1**) and reduced VMAT2 levels (>90% loss) as measured by immunoblotting (**Fig. 6.2**). VMAT2-LO mice also show a significant loss of striatal DAT levels, a marker of dopamine terminal integrity, at 22 months of age, replicating previous results that showed that impaired vesicular storage results in progressive degeneration of the nigrostriatal pathway (~30% loss, LO vs. WT, $p < 0.05$) (**Fig**. **6.2**) (Caudle et al., 2007).

VMAT2 level modulates MPTP toxicity in mice on a C57BL/6 genetic background.

Male VMAT2-LO show exacerbated MPTP toxicity in the striatum following a 2 x 10 mg/kg MPTP dosing regimen. This increased toxicity was shown by greater losses of striatal DAT levels following MPTP in the VMAT2-LO mice compared to the other genotypes (**Fig. 6.3**). Conversely, mice with elevated VMAT2 levels show a protection from MPTP toxicity by these measures (83% vs. 77% vs. 48% DAT loss, LO, WT, HI, respectively). Similar trends were also seen in protection from striatal TH loss (72% vs. 67% vs. 49% loss, LO, WT, HI, respectively). Immunoblotting results were further confirmed with immunohistochemical analysis of DAT and TH in the striatum (**Fig. 6.4**). A trend towards decreased DAT levels was also seen in saline-treated male VMAT2-LO mice at 12 months of age compared to wildtype mice (**Fig. 6.3**).

VMAT2 level modifies stimulated dopamine release following MPTP treatment.

We next examined the effects of varying VMAT2 levels on stimulated dopamine release both with and without a toxic lesion (**Fig. 6.5)**. At baseline, VMAT2 level dictates the amplitude of stimulated dopamine release (**Fig. 6.6, left**). VMAT2-LO mice show the smallest baseline release (0.47 μM DAmax) and VMAT2-HI mice show the largest release (2.52 μM DAmax), with dopamine release levels wildtype mice falling in between the genotypes (1.75 μM DAmax).

VMAT2 level modifies stimulated dopamine release following MPTP treatment.

Following a 2 x 10 mg/kg MPTP lesion, all of the VMAT2 genotypes show significant decreases in peak stimulated dopamine release compared to control mice (~60% decrease in DAmax compared to untreated for all genotypes) (**Fig. 6.6, right**). However, VMAT2-HI mice show a significantly preserved peak dopamine release following this MPTP dosing regimen (1.06 μM DAmax vs. 0.69 μM vs. 0.21 μM, LO, WT, HI; $p < 0.05$).

VMAT2 level modifies L-DOPA induced increases in dopamine release.

Next we examined the effect of varying VMAT2 levels (both with and without lesioning) on handling exogenously applied dopamine. Following acute L-DOPA application, we show differences in the neurochemical dopamine handling between the VMAT2 genotypes. Following L-DOPA application, VMAT2-LO mice show the largest increase in peak DA release with a 91% increase in DAmax from baseline (0.9 μM DAmax) (**Fig. 6.7**). Wildtype mice show a significant 73% increase in stimulated dopamine release when L-DOPA is applied (3.0 μM DAmax), and VMAT2-HI mice show the smallest increase in release with only a 64% increase from baseline (4.1 μM DAmax).

L-DOPA treatment in the VMAT2 genotypes resulted in varying levels of extracellular dopamine following stimulation based on measurements of the area under the curve (AOC) of the release trace. VMAT2-LO mice show small L-DOPA-induced increases in AOC, presumably due their low storage capacity at baseline (baseline = 0.793 ± 0.043; L-DOPA = 8.952 ± 0.502 for a 1028% increase from baseline). Surprisingly, L-DOPA treatment in the VMAT2-HI mice induced a smaller AOC than in wildtype mice (VMAT2-HI: baseline = 1.676 ± 0.0247; L-DOPA = 15.099 ± 4.327; for a 1149% increase from baseline) (Wildtype: baseline = 0.907 ± 0.085; L-DOPA = 23.793 ± 8.035; for a 2523% increase from baseline).

VMAT2 level modifies movement of extracellular dopamine.

In addition to differences in peak dopamine release, the VMAT2 genotypes also showed changes in levels and the movement of extracellular dopamine via indirect measures. This altered handling of the newly synthesized dopamine is reflected by the rate constant tau, which is the time at which the trace falls to ~63.3% of its maximum. Tau was significantly smaller in the VMAT2-HI mice than that of the other genotypes (**Fig. 6.8**) (LO = 16.49 ± 2.58 s, WT = 8.59 ± 2.74 s, HI = 2.86 ± 0.96 s; $p < 0.01$). The size of the release trace and clearance of extracellular dopamine can also be reflected by the measure of half-width of the trace, which is the time that it takes for the trace to reach half of its total width. The half-width is also significantly smaller in the VMAT2-HI mice following L-DOPA compared to both VMAT2-LO and wildtype mice (LO = 14.67 ± 1.84 s, WT = 6.74 ± 1.08 s, HI = 3.31 ± 0.83 s; $p < 0.01$). The VMAT2-HI mice also showed increased peak release and faster extracellular dopamine clearance using larger stimulation parameters (4 pulses, 10 Hz) (**Fig. 6.9-6.10**).

No change in total DAT levels in the VMAT2-HI mice.

Due to the suggestion that there may be a change in DAT-mediated uptake of exogenously applied dopamine in the VMAT2-HI mice, we measured total DAT levels in the striatum of both wildtype and VMAT2-HI mice. VMAT2-HI mice have no significant change in total DAT levels as measured by immunoblotting (**Fig. 6.11**) and immunohistochemistry (Lohr et al., 2014). Additionally, synaptosomal levels of the DAT are unchanged between the genotypes as measured by [^{3}H]-WIN-35,428 binding (**Fig. 6.12**).

Discussion

Here we show that VMAT2 protein level modifies vulnerability to MPTP intoxication and L-DOPA handling in mice of the same C57BL/6 genetic background. These mice of varying VMAT2 levels provide important tools to assess vesicular function on a continuum in vivo.

VMAT2 as a mediator of toxicity

Previous work has shown that VMAT2 acts as a modifier of dopaminergic toxicity (Guillot and Miller, 2009). Using our newly backcrossed VMAT2-LO mice, we confirmed that reduced VMAT2 levels reduce vesicular uptake and result in progressive terminal loss with aging (**Fig. 6.1-6.2**). The current study also showed that VMAT2-LO mice exhibit significant decreases in DAT levels following a low 2 x 10 mg/kg MPTP dose, whereas VMAT2-HI mice show a preservation of these protein levels **(Fig. 6.3-6.4)**. These data provide new insight into VMAT2's fine control of neurotoxic outcomes, even at a mild MPTP dose. Furthermore, stimulated dopamine release appears to be significantly decreased in the VMAT2-LO mice following MPTP treatment to a practically undetectable level **(Fig. 6.6)**. While wildtype and VMAT2-HI mice also have decreased stimulated dopamine release following a mild MPTP lesion, the peak dopamine release in these genotypes remains significantly greater than that of the VMAT2-LO mice **(Fig. 6.6)**. VMAT2-HI mice also have the highest dopamine release after MPTP treatment. These data provide evidence that VMAT2 modifies MPTP toxicity in a protein level-dependent manner and that these indicators of degeneration correlate to neurotransmitter output as measured by voltammetry. These results also confirm previously published reports on the negative effects of reduced vesicular function on toxicological outcomes (Takahashi et al.,

1997; Gainetdinov et al., 1998; Fumagalli et al., 1999; Caudle et al., 2007; Guillot et al., 2008b) and beneficial effects of elevated VMAT2 levels (Lohr et al., 2014, 2015). Furthermore, the consistent genetic background of the VMAT2-LO, wildtype, and VMAT2-HI mice will provide additional power when assessing VMAT2 function in future neurochemical and behavioral assays.

VMAT2 as a modifier of L-DOPA handling

The current study also suggests that augmented vesicular function may modify the handling of L-DOPA-derived dopamine release in a striatal slice. Following L-DOPA treatment, all of the VMAT2 genotypes show large increases in their peak dopamine release compared to baseline stimulated release. As expected, the VMAT2-LO mice have the smallest peak release after L-DOPA treatment, and the VMAT2-HI mice have the largest peak dopamine release (**Fig. 6.7**). Surprisingly, the VMAT2-HI mice actually have a smaller total area under the release curve compared to wildtype mice. This led us to analyze the kinetics of the release traces, which reflect the clearance of dopamine from the extracellular space following stimulation.

It has previously been shown that VMAT2-HI mice have enhanced stimulated dopamine release at baseline (Lohr et al., 2014). In this untreated state, the VMAT2-HI mice have no change in the DAT-mediated uptake of dopamine back into the presynaptic neuron following stimulation as measured by tau or half-width. However, it appears that VMAT2-HI mice have modified DAT-mediated uptake after the application of a massive amount of newly synthesized dopamine from L-DOPA treatment. Here we show that VMAT2-LO mice have the slowest extracellular dopamine clearance, and VMAT2-HI mice have faster clearance of extracellular dopamine by these measures (**Fig. 6.8, 6.10**).

This change in dopamine handling in the VMAT2-HI mice preserves a more typical time course of dopamine release and reuptake, similar to baseline release traces. Based on our verification of the unchanged DAT levels in the VMAT2-HI mice (**Fig. 6.11-6.12**), we attribute change in tau and half-width to alterations of the movement of dopamine through the DAT.

Implications for L-DOPA-induced dyskinesias

Several therapeutic strategies have been used to enhance dopamine neurotransmitter signaling in diseases of deficient dopamine like Parkinson's disease. While L-DOPA treatment does not halt the progression of the neurodegeneration in Parkinson's disease, it remains the best intervention to restore movement in affected individuals (Cheshire et al., 2015). However, L-DOPA is also notorious due to its deleterious side effects. The tricky pharmacokinetics of the drug and fluctuations of endogenous dopamine levels throughout the circadian cycle add additional layers of complexity to the therapy. The most notable side effect of L-DOPA treatment is uncontrolled movements termed L-DOPA-induced dyskinesias (LIDs) (Jenner, 2008). LIDs become more common and dramatic the longer the patient is on L-DOPA and tend to limit the therapeutic window for the drug over time.

There are a variety of hypotheses to describe the mechanism by which LIDs occur. Some have speculated that these undesirable movements occur because of the temporal dysregulation of dopamine release and uptake following the loss of dopaminergic innervation in the putamen (Jenner, 2008; Crittenden and Graybiel, 2011; Cenci, 2014). These changes may result in massive sensitization of post-synaptic receptors over time. In the presence of a huge flood of dopamine derived from L-DOPA treatment, these receptors

would become excessively activated, perhaps resulting in the aberrant motor movements of dyskinesias.

Most promisingly, it has been suggested that LIDs are due to unregulated dopamine release from formerly serotonin-releasing neurons (Carta et al., 2008; Mosharov et al., 2014; Cheshire et al., 2015). In this scenario, the massive loss of dopaminergic innervation in the striatum in Parkinson's disease leaves no place for dopamine to be stored. Thus, serotonergic terminals take up, package, and release the newly synthesized dopamine. Since serotonergic terminals lack the proper synaptic inputs and neuromodulatory connections that dopamine neurons previously held, this aberrant dopamine release is thought to result in uncoordinated neurotransmission and, perhaps, dyskinesias. Though it is unclear as to why these dyskinetic symptoms arise in Parkinson's disease patients over time, most would agree that LIDs develop due to the improper handling of dopamine in a brain that lacks the neurons that formerly produced the transmitter (Cenci, 2014). A method to protect those dopamine-producing neurons and, perhaps, allow them to better handle large floods of dopamine may be an avenue to modify the severity of LIDs.

Possible mechanisms for altered extracellular dopamine uptake

There are three possible mechanisms that may explain the ability of elevated vesicular function via overexpression of VMAT2 to modify tau in the presence of excess dopamine. First, it is possible that DAT function is being dictated by a concentration gradient across the plasma membrane. Following stimulation, a flood of extracellular dopamine is released from the neuron. Wildtype mice would have a large dopamine concentration in the cytoplasm because they are unable to store the massive amount of dopamine. Thus, the difference between the cytoplasmic and extracellular dopamine

concentrations would be minimal, resulting in reduced DAT function and an increase in tau. In contrast, VMAT2-HI mice would better store this newly synthesized dopamine, leaving a low concentration of cytosolic dopamine. In this case, when stimulation occurs and dopamine is released, there would be very high extracellular dopamine content, and relatively low cytosolic dopamine concentration, creating a greater driving force across the DAT and faster dopamine clearance.

The second option is also based on the dopamine concentration gradient across the DAT, but this scenario uses the ability of the DAT to reverse transport directions. The DAT is able to reverse transport and cause an efflux of dopamine when cytosolic dopamine concentrations become high. The best known example of this is when amphetamines are applied to dopamine neurons (Sulzer et al., 2005). Amphetamines deplete vesicular stores, elevating cytosolic dopamine concentrations, and this high concentration gradient (high cytosolic dopamine, low extracellular dopamine) causes DAT to reverse transport directions, dumping dopamine into the extracellular space (Pifl et al., 1995). Similarly, wildtype mice that are unable to store excess dopamine may have high cytosolic dopamine levels, resulting in DAT-mediated dopamine efflux. In voltammetry, this would be recorded as a slower recovery of the signal to baseline and an increase in tau and half-width. In contrast, VMAT2-HI mice would have lower cytosolic dopamine levels because of their ability to store dopamine, resulting in less DAT-mediated dopamine efflux. This reduced efflux would be recorded as a faster recovery of the signal and decrease tau and half-width. There has been previous evidence that increases to cytosolic dopamine levels will increase DAT-mediated efflux. MPP+, the metabolite of MPTP, displaces dopamine into the cytosol and induces a stimulation-independent efflux of dopamine, much like an

amphetamine-like compound (Choi et al., 2015). Additionally, it is known that compounds that inhibit VMAT2, and presumably elevate cytosolic dopamine, can also reduce DAT function (Meyer et al., 2011).

Finally, it is possible that vesicular function modifies DAT-mediated plasmalemmal uptake by a direct interaction between DAT and the synaptic vesicle. The DAT has been shown to interact with known vesicle associated proteins, including syntaxin (Lee et al., 2004). In this way, it is possible that the dopamine shuttled into the presynaptic terminal via DAT may be directly or more efficiently packaged into synaptic vesicle pools near the transporter. However, such an interaction is undocumented in the literature thus far.

Benefits of increased VMAT2 function

In the current study, we demonstrated that vesicular storage acts on a continuum with a large range of amplitudes of neurochemical output. For the first time, we are able to assess genetic changes to vesicular function using mice of the same C57BL/6 genetic background. As expected, VMAT2 level opposes dopaminergic toxicity following MPTP exposure and enhances dopamine release both with and without lesioning. Interestingly, it also appears that changes to vesicular neurotransmitter storage modify the handling of an exogenously applied flood of dopamine by L-DOPA treatment. In a disorder like Parkinson's disease, which is defined by a vulnerability to insult, decreased dopamine output, and dysfunctional handling of L-DOPA, enhancing vesicle filling could preserve and improve the output of dopaminergic circuitry.

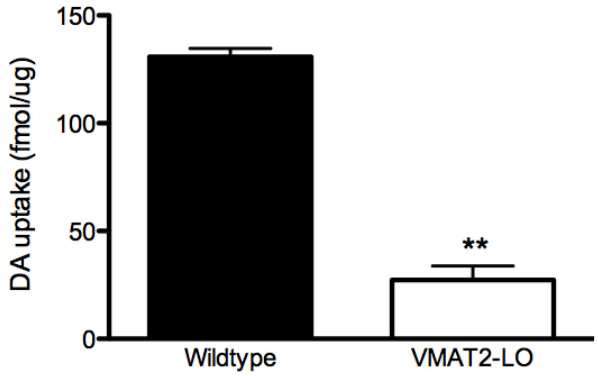
150
100
50
0
DA uptake (fmol/ug)
**
Wildtype
VMAT2-LO

Figure 6.1. C57BL/6 VMAT2-LO mice have significantly reduced vesicular uptake. VMAT2-LO mice show an 80% reduction in [^{3}H]-dopamine uptake in isolated vesicles compared to wildtype littermates ($p < 0.01$, $n = 2$-3). Radioactive uptake was normalized to protein level using a BCA protein assay (Pierce).

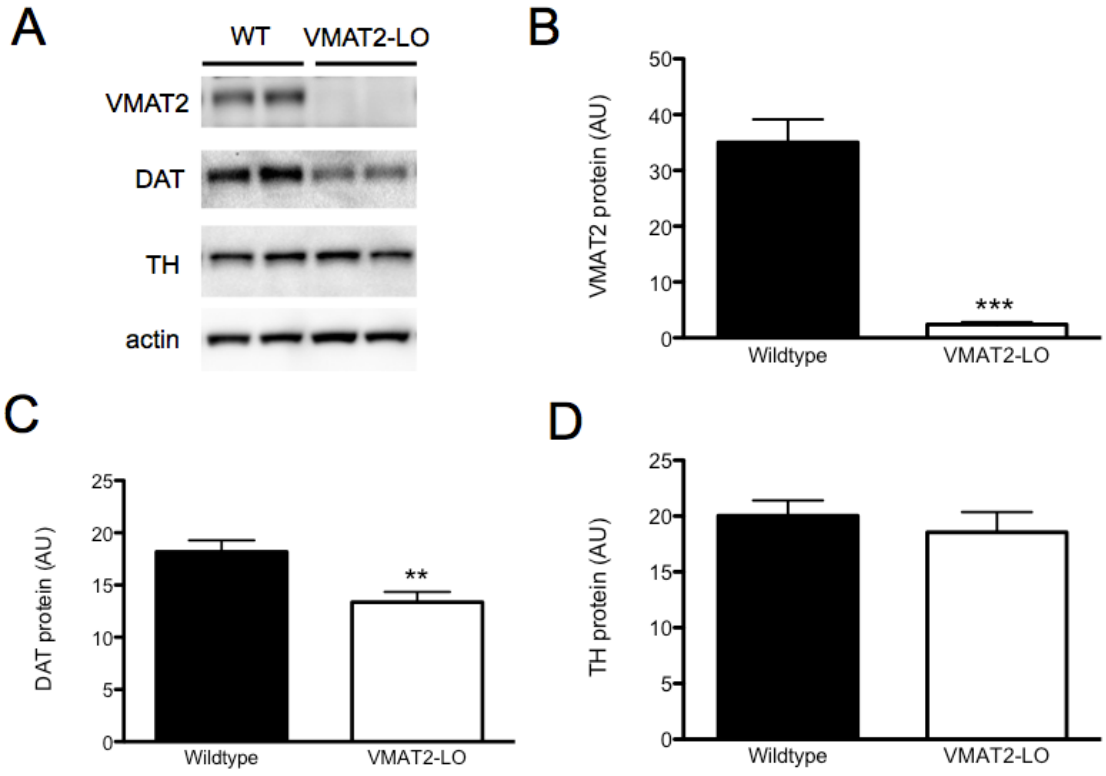
A
WT
VMAT2-LO
VMAT2
DAT
TH
actin
B
VMAT2 protein (AU)
50
40
30
20
10
0
***
Wildtype
VMAT2-LO
C
DAT protein (AU)
25
20
15
10
5
0
**
Wildtype
VMAT2-LO
D
TH protein (AU)
25
20
15
10
5
0
Wildtype
VMAT2-LO

Figure 6.2. C57BL/6 VMAT2-LO mice show progressive loss of the dopamine terminal marker DAT when aged.

At 22 months of age, back-crossed VMAT2-LO mice show significant reductions in DAT level in the striatum, as measured by immunoblotting (n = 10). These results show that the progressive degenerative phenotype that was originally described in VMAT2-deficient mice holds true when these animals are inbred on C57BL/6 (Caudle et al., 2007).

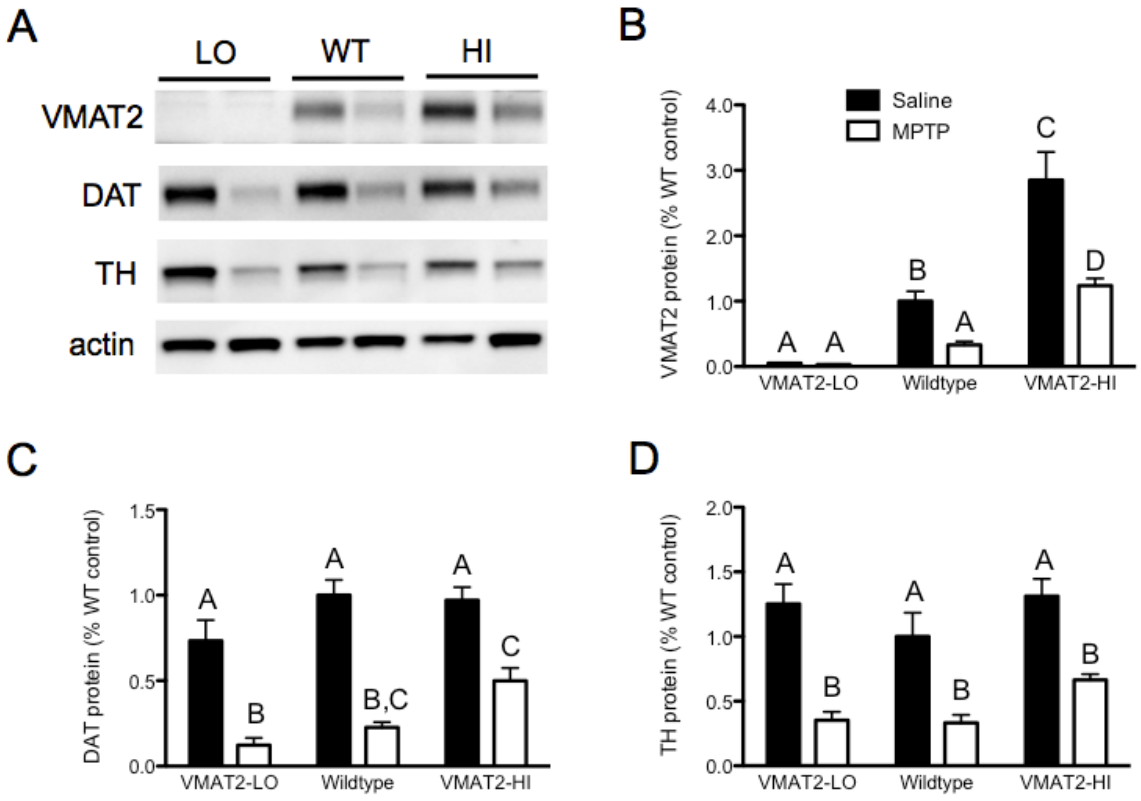
A
LO
WT
HI
VMAT2
DAT
TH
actin
B
Saline
MPTP
VMAT2 protein (% WT control)
4.0
3.0
2.0
1.0
0.0
A A
B
A
C
D
VMAT2-LO
Wildtype
VMAT2-HI
C
DAT protein (% WT control)
1.5
1.0
0.5
0.0
A
B
A
B,C
A
C
VMAT2-LO
Wildtype
VMAT2-HI
D
TH protein (% WT control)
2.0
1.5
1.0
0.5
0.0
A
B
A
B
A
B
VMAT2-LO
Wildtype
VMAT2-HI

Figure 6.3. VMAT2 level modifies vulnerability to dopamine terminal marker loss following MPTP.

(A) Representative immunoblotting of VMAT2 and dopaminergic markers DAT and TH, with actin loading control. (B) VMAT2 levels vary with genotypes as expected and show similar losses following a mild 2 x 10 mg/kg MPTP treatment. (C-D) VMAT2-LO mice show a larger decrease in dopaminergic markers DAT and TH, compared to wildtype and VMAT2-HI mice. VMAT2-HI mice show a protection from these losses, and DAT and TH levels following MPTP falls in between the two genotypes in wildtype mice. Different letters above the bars indicate differences of at least $p < 0.05$ as indicated by a two-way ANOVA and Bonferroni posthoc tests ($n = 4$-6).

A

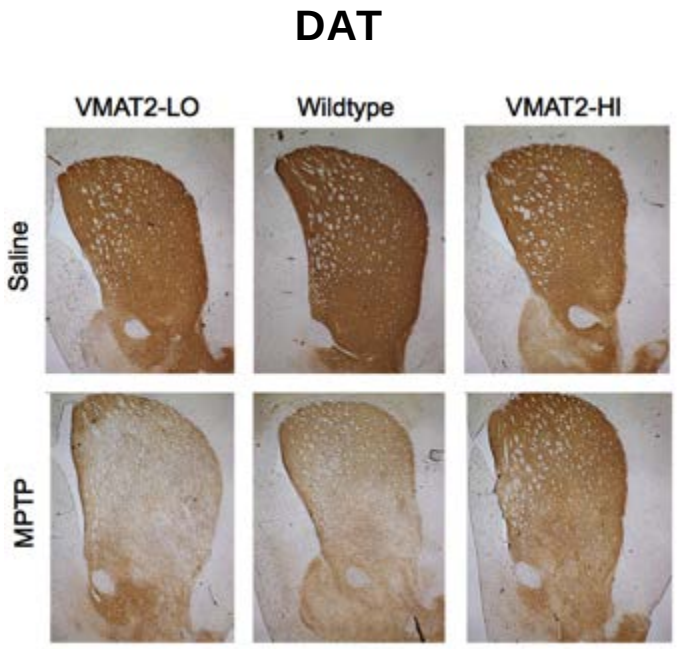
DAT
VMAT2-LO
Wildtype
VMAT2-HI
Saline
MPTP

B

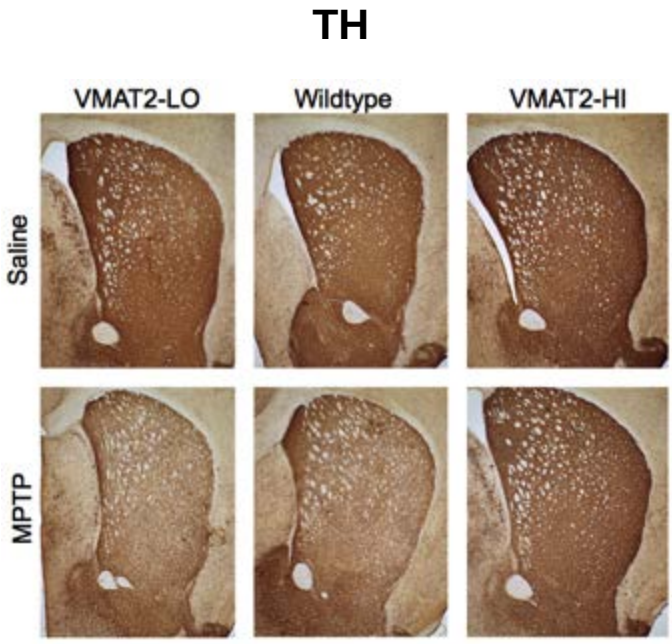
TH
VMAT2-LO
Wildtype
VMAT2-HI
Saline
MPTP

Figure 6.4. VMAT2 level modifies vulnerability to dopamine terminal marker loss following MPTP.

Representative immunohistochemical labeling of dopaminergic markers DAT (A) and TH (B). VMAT2 levels vary with genotypes as expected and show similar losses following a mild 2 x 10 mg/kg MPTP treatment. VMAT2-LO mice show a larger decrease in dopaminergic markers DAT and TH, compared to wildtype and VMAT2-HI mice. VMAT2-HI mice show a protection from these losses, and DAT and TH levels following MPTP falls in between the two genotypes in wildtype mice.

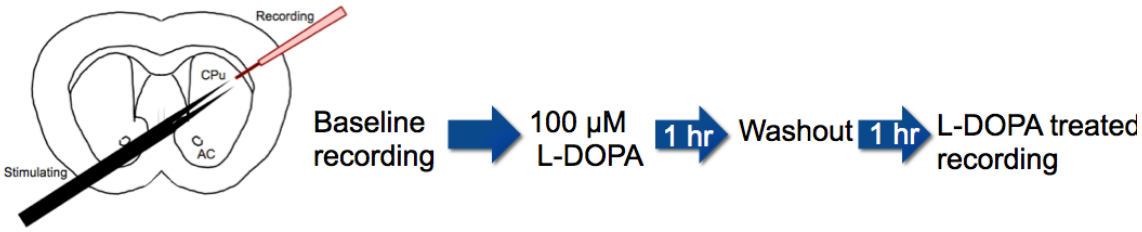
Recording
CPu
AC
Stimulating
Baseline recording
100 µM L-DOPA
1 hr
Washout
1 hr
L-DOPA treated recording

Figure 6.5. Fast-scan cyclic voltammetry experimental design.

Lesioned animals were treated with 2 x 10 mg/kg MPTP 7 days prior to voltammetry. Striatal slices were bathed in oxygenated aCSF containing 100 μM L-DOPA, washed out for 60 minutes, and then recordings began. Stimulations were given at two intensities (1 p, 60 Hz; 4 p, 10 Hz)

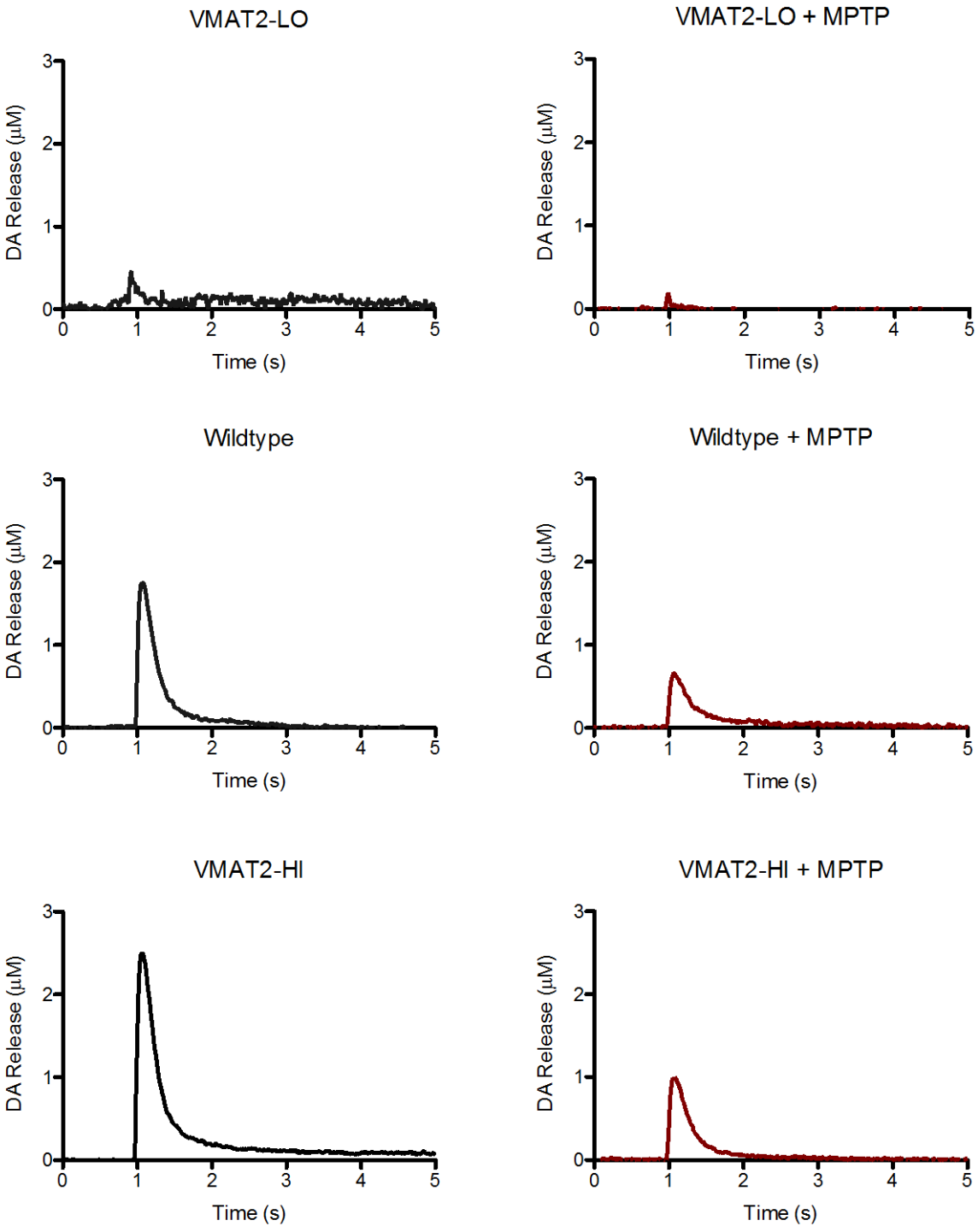
VMAT2-LO
VMAT2-LO + MPTP
Wildtype
Wildtype + MPTP
VMAT2-HI
VMAT2-HI + MPTP
DA Release (µM)
Time (s)
0
1
2
3
4
5

Figure 6.6. VMAT2 level modifies stimulated dopamine (1p) release with and without MPTP lesioning.

(Left) VMAT2-LO mice show the smallest release (0.47 μM DAmax). Wildtype mice have 1.75 μM DAmax. VMAT2-HI mice show the largest release (2.52 μM DAmax). (Right) Following a 2 x 10 mg/kg MPTP lesion, all of the VMAT2 genotypes show significant decreases in peak stimulated dopamine release compared to controls mice (all ~60% decrease in DAmax compared to baselines). VMAT2-HI mice show a significantly preserved peak dopamine release following this dosing regimen (1.06 μM DAmax vs. 0.69 μM vs. 0.21 μM, LO, WT, HI) (n = 4).

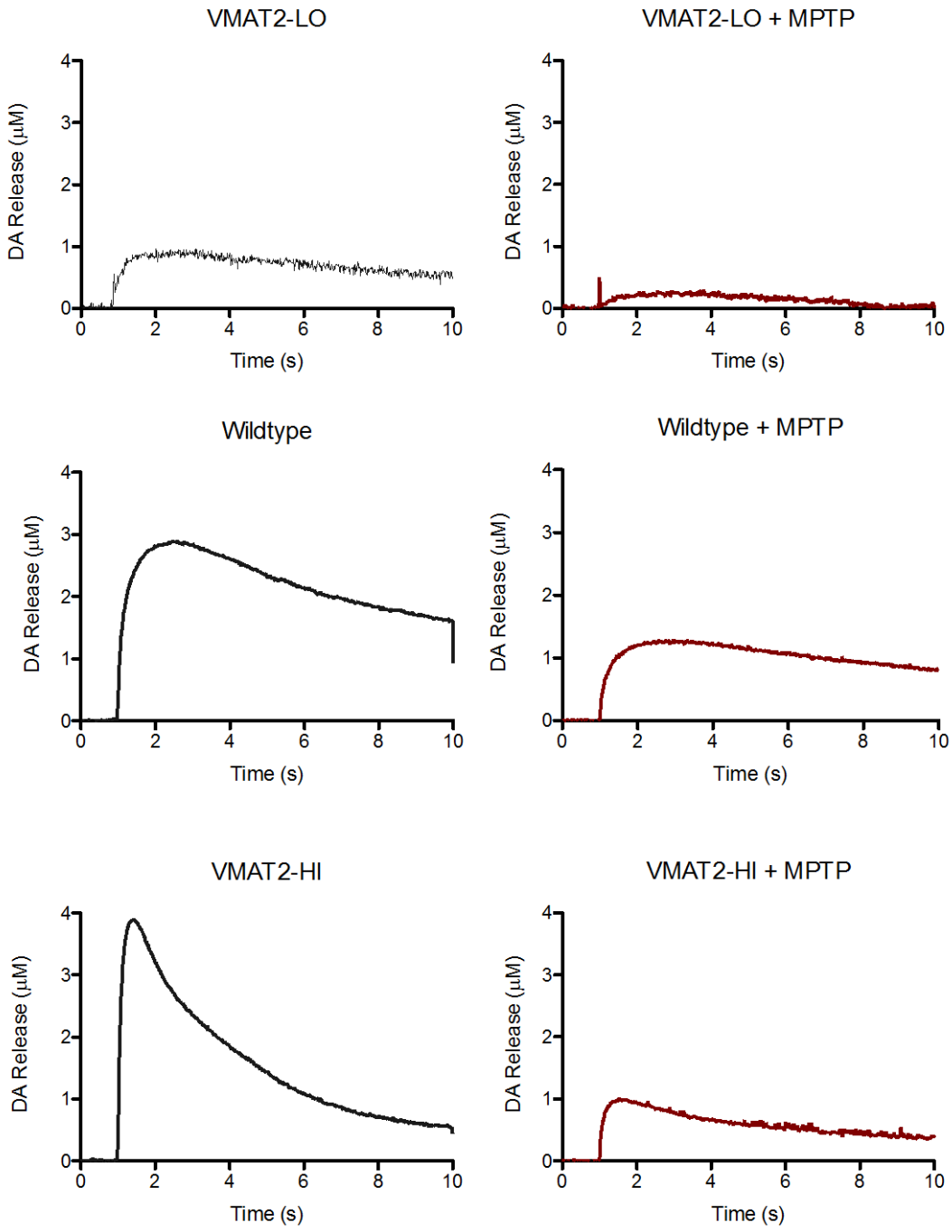
VMAT2-LO
VMAT2-LO + MPTP
Wildtype
Wildtype + MPTP
VMAT2-HI
VMAT2-HI + MPTP
DA Release (μM)
Time (s)
0
1
2
3
4
0
2
4
6
8
10

Figure 6.7. VMAT2 level alters dopamine dynamics following L-DOPA application in unlesioned and MPTP-lesioned mice.

Dopamine release (μM) vs. time traces taken from fast-scan cyclic voltammetry after L-DOPA application in both untreated (left) and MPTP-treated (right) mice. All three genotypes (VMAT2-LO, wildtype, and VMAT2-HI) showed increases in DAmax following L-DOPA application, compared to baseline values seen in Fig. 6.6 (n = 4-6). The fall time of the release traces appeared to be particularly affected between the genotypes.

A

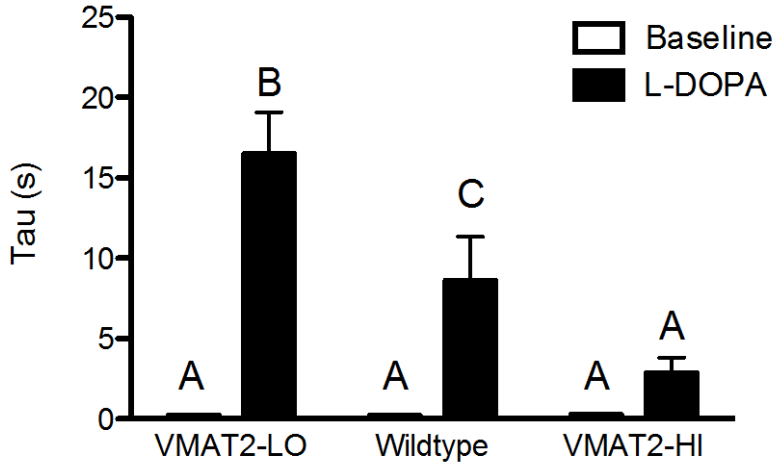
Baseline
L-DOPA
Tau (s)
25
20
15
10
5
0
B
C
A
A
A
A
VMAT2-LO
Wildtype
VMAT2-HI

B

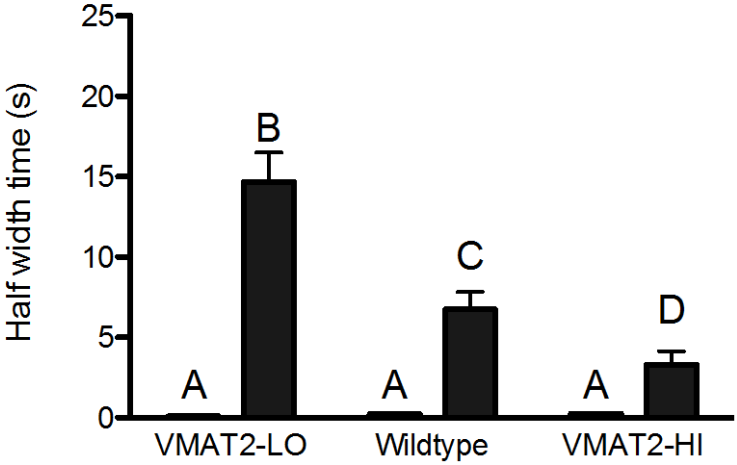
Half width time (s)
25
20
15
10
5
0
B
C
D
A
A
A
VMAT2-LO
Wildtype
VMAT2-HI

Figure 6.8. VMAT2 levels alter dopamine dynamics following L-DOPA application in unlesioned mice.

With increased VMAT2 level, movement of dopamine from the extracellular space appears to be increased. VMAT2-HI mice show a significant decrease in both the rate constant, tau, and half-width, all of which reflects the steeper fall of the release traces in this genotype compared to wildtype and VMAT2-LO mice. Different letters above the bars indicate differences of at least $p < 0.05$ as indicated by a two-way ANOVA and Bonferroni posthoc tests ($n = 4$-6).

4 pulse stimulation

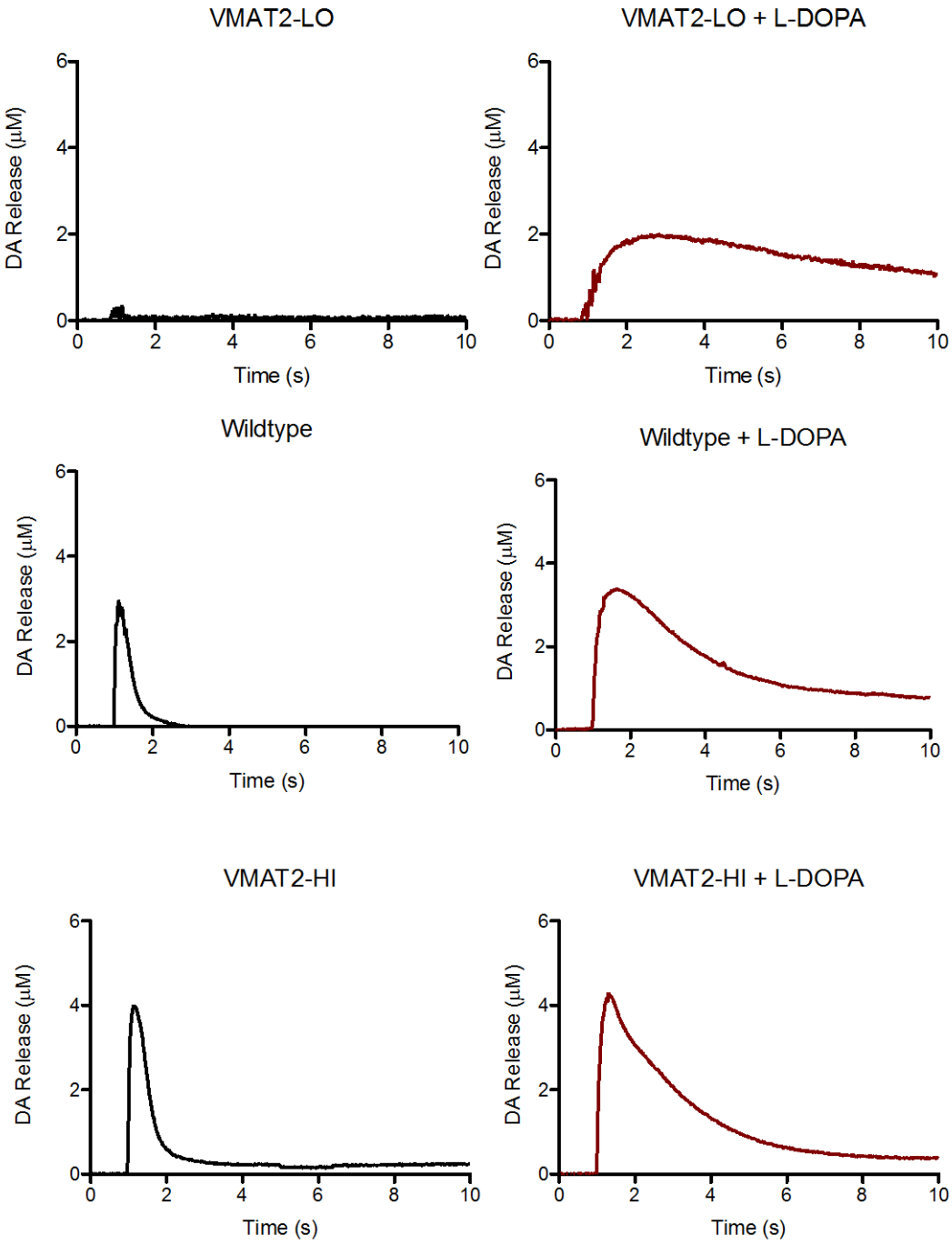

Figure 6.9. VMAT2 levels alter neurochemical output following L-DOPA application in unlesioned mice even with a more intense 4-pulse stimulation.

Both wildtype and VMAT2-HI mice show increases in DAmax following L-DOPA application (n = 6). VMAT2-HI mice also show a significant decrease in the area under the curve, half-width, and rate constant tau, all of which reflects the steeper fall of the release traces in this genotype. Different letters above the bars indicate differences of at least $p < 0.05$ as indicated by a two-way ANOVA and Bonferroni posthoc tests.

4 pulse stimulation

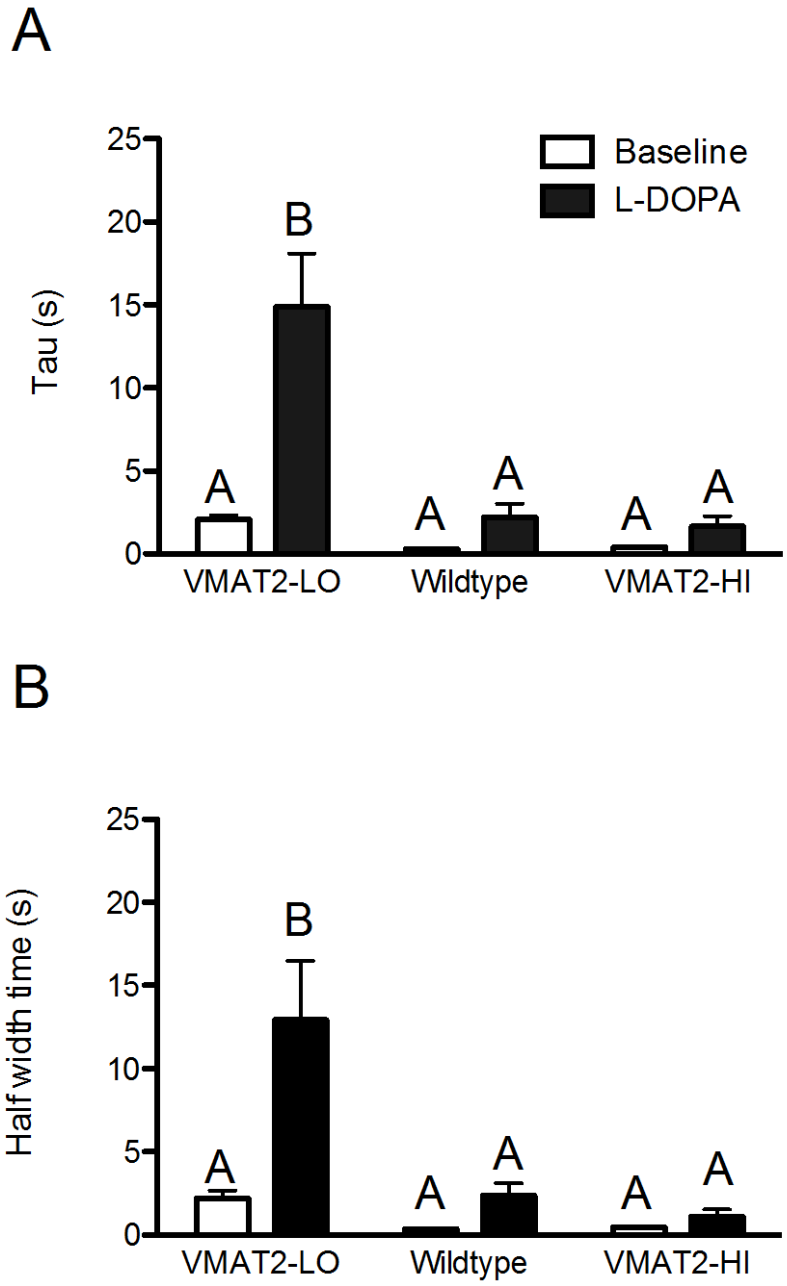

Figure 6.10. VMAT2 level alters dopamine dynamics following L-DOPA application in unlesioned mice even with a more intense 4-pulse stimulation.

With increased VMAT2 level, movement of dopamine from the extracellular space appears to be increased. VMAT2-HI mice show a significant decrease in both the rate constant, tau, and half-width, all of which reflects the steeper fall of the release traces in this genotype compared to wildtype and VMAT2-LO mice. Different letters above the bars indicate differences of at least $p < 0.05$ as indicated by a two-way ANOVA and Bonferroni posthoc tests ($n = 4$-6).

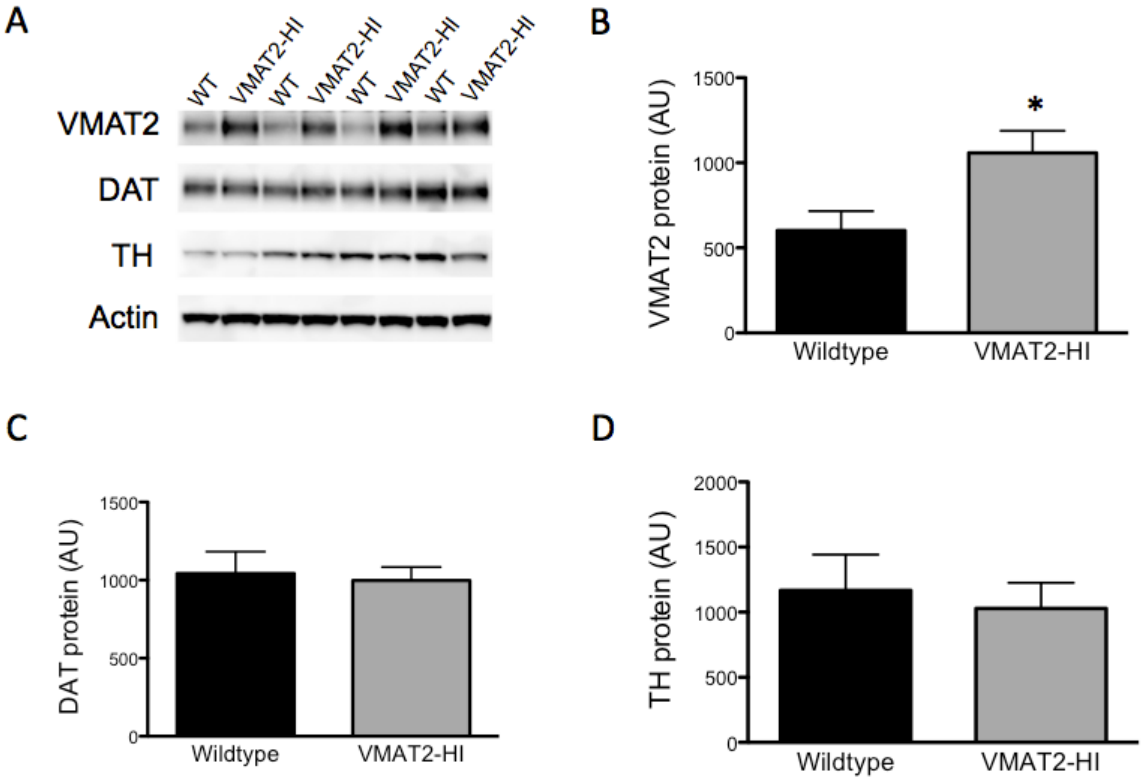
A
WT
VMAT2-HI
WT
VMAT2-HI
WT
VMAT2-HI
WT
VMAT2-HI
VMAT2
DAT
TH
Actin
B
VMAT2 protein (AU)
1500
1000
500
0
*
Wildtype
VMAT2-HI
C
DAT protein (AU)
1500
1000
500
0
Wildtype
VMAT2-HI
D
TH protein (AU)
2000
1500
1000
500
0
Wildtype
VMAT2-HI

Figure 6.11. There are no changes in DAT expression in synaptosomes prepared from wildtype and VMAT2-HI mice.

(A) Representative immunoblotting of VMAT2 and dopaminergic markers DAT and TH between wildtype and VMAT2-HI mice from synaptosomal preparations. (B) VMAT2 level is significantly increased in the VMAT2-HI mice. (C,D) There are no differences in the expression levels of DAT and TH between wildtype and VMAT2-HI mice.

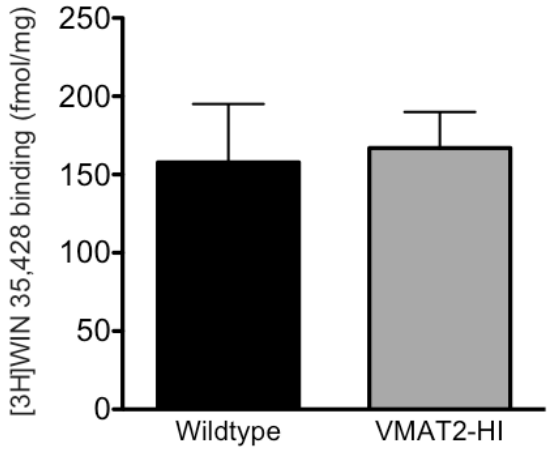
[3H]WIN 35,428 binding (fmol/mg)
250
200
150
100
50
0
Wildtype
VMAT2-HI

Figure 6.12. There is no change in synaptosomal DAT binding between wildtype and VMAT2-HI mice.

Using isolated synaptosomal preparations from bilateral dissected striatal homogenates, [^{3}H]-WIN-35,428 binding showed no significant differences between genotypes ($p > 0.05$; $n = 4$). Radioactive counts were normalized to protein concentration using a BCA protein assay (Pierce).

CHAPTER VII: SUMMARY AND FUTURE DIRECTIONS

Conclusions

This discussion has been previously published:

Lohr KM, Miller GW (2014) VMAT2 and Parkinson's disease: harnessing the dopamine vesicle. *Expert Rev Neurother. 14(10)*:1115–7.

Despite a movement away from dopamine-focused Parkinson's disease (PD) research, a recent surge of evidence now suggests that altered vesicular storage of dopamine may contribute to the demise of the nigral neurons in this disease. Human studies demonstrate that the vesicular monoamine transporter 2 (VMAT2; SLC18A2) is dysfunctional in Parkinson's disease brain. Moreover, studies with transgenic mice suggest that there is an untapped reserve capacity of the dopamine vesicle that could be unbridled by increasing VMAT2 function. Therapeutic manipulation of VMAT2 level or function has the potential to improve efficacy of dopamine derived from administered levodopa, increase dopamine neurotransmission from remaining midbrain dopamine neurons and protect against neurotoxic insults. Thus, the development of drugs to enhance the storage of release of dopamine may be a fruitful avenue of research for PD.

Parkinson's disease (PD) is a dramatic and progressive movement disorder where quick fluid motions are replaced by slowness and leaden rigidity. Nearly 60 years ago, Ehringer and Hornykievicz identified the depletion of dopamine as a central hallmark to the disease (Ehringer and Hornykievicz, 1960). In the following decades, a great deal of effort has been exerted to restore dopamine function in PD. More recently, some have suggested that the study of dopamine-mediated dysfunction in Parkinson's disease is an elusive and unrewarding pursuit, likening these dopamine-centric research strategies to beating a dead horse (Ahlskog, 2007). We agree that Parkinson's disease is much more

than just a dopaminergic disorder; however, it is impossible to dismiss the selective degeneration of nigral dopamine neurons and the efficacy of levodopa (L-DOPA) therapies in Parkinson's disease. After all, L-DOPA remains the primary treatment for millions of Parkinson's disease patients and continues to provide awakenings in disease sufferers. In light of recent evidence from both animal and clinical studies, we argue that this proverbial horse that is synaptic dopamine handling in the pathogenesis of Parkinson's disease is not dead, nor is it ready to be put out to pasture.

Dopamine handling and Parkinson's disease

L-DOPA restores the underlying dopamine deficit in the Parkinson's disease brain, addressing the primary motor symptoms of the disease with striking effectiveness in most patients. L-DOPA is converted to dopamine by dopa decarboxylase in the neuronal cytosol; this new dopamine is then packaged into synaptic vesicles, tiny storage compartments for neurotransmitter, so that the dopamine can be released into the synapse for neurotransmission. However, the treatment window of L-DOPA is often limited due to the eventual onset of side effects, such as dyskinesias. As it stands today, the research community is at a loss as to why L-DOPA-induced dyskinesias appear throughout the course of treatment, and clinicians often delay escalation of L-DOPA doses to widen this treatment window. We pose the question now: what if dopamine neurons could more efficiently package, store and release this newly made dopamine? Since most of the brain's dopamine is stored in synaptic vesicles, improvements to dopamine packaging into the vesicle could more efficiently use L-DOPA and extend the treatment window.

A few key players in the neuron terminal mediate these dopamine dynamics, perhaps the most important of which is the focus of this piece: the vesicular monoamine

transporter 2 (VMAT2; SLC18A2). VMAT2 as a wrangler of synaptic dopamine VMAT2 is an H+-ATPase antiporter that packages monoamines (dopamine, norepinephrine, serotonin, epinephrine and histamine) into small synaptic and dense core vesicles for their subsequent release from the neuron (Liu and Edwards, 1997). Through this transmitter storage, VMAT2 also acts to sequester potentially harmful cytosolic dopamine. Dopamine molecules left unpackaged are vulnerable to the creation of reactive oxygen species including hydroxyl radicals, superoxide, hydrogen peroxide and also dopamine-quinones that can result in function-altering cysteinyl adducts on cellular proteins (Sulzer and Zecca, 1999). Interestingly, VMAT2 is evolutionarily related to a family of toxin-extruding antiporters found in bacteria (Schuldiner et al., 1995), so it is no surprise that VMAT2 levels have been shown to modify dopamine neuron vulnerability to additional toxic insults, including those by 1-methyl-4-phenyl- 1,2,3,6-tetrahydropyridin (MPTP) and methamphetamine (Guillot and Miller, 2009).

Mouse models of altered VMAT2 function

The modulation of synaptic vesicle filling and function is perhaps best represented in mouse models of varying VMAT2 levels. Although a complete loss of VMAT2 is lethal (Fon et al., 1997; Takahashi et al., 1997; Wang et al., 1997b), mice with a 95% reduction in VMAT2 (VMAT2-deficient mice) survive into adulthood. However, these VMAT2-deficient animals experience dramatic dopamine depletion, progressive loss of in dopamine neurons and α-synuclein accumulation (Caudle et al., 2007). Thus, reductions in vesicular storage are detrimental to the dopamine system. Luckily, the converse is also true: increased vesicular function is beneficial to the dopamine system. Mice with elevated VMAT2 levels (VMAT2-HI) have an increased capacity for the storage of dopamine in

their neurons, which results in increased total dopamine levels, increased dopamine release and protection from neurotoxic insult by MPTP and methamphetamine (Lohr et al., 2014, 2015). This means that a small molecule capable of enhancing VMAT2 function may increase neuronal dopamine output, while also protecting those cells from intracellular stressors. These findings from the VMAT2-HI mice provide a crucial stepping stone to understanding the uppermost limits of the dopamine vesicle, suggesting that VMAT2 modulation may be a viable therapeutic approach to address deficits in neurotransmitters like dopamine.

VMAT2 function in human disease

Multiple groups have reported the importance of vesicular function in human parkinsonism. Over 50 years after the key finding from the Ehringer and Hornykievicz (Ehringer and Hornykievicz, 1960), Pifl et al. reported that post-mortem Parkinson's disease brains show dramatically reduced VMAT2-mediated vesicular filling, greater than what could be explained by terminal loss alone (Pifl et al., 2014). This demonstrates that impaired packaging of dopamine into vesicles may be a key player in the disease process. These results also complement recent findings, including higher cytosolic dopamine turnover in Parkinson's disease patients (Goldstein et al., 2013) and a familial VMAT2 mutation that dramatically reduces vesicular filling and causes an infantile parkinsonian condition with profound motor and cognitive impairments (Rilstone et al., 2013). Additionally, there is mounting evidence that increased VMAT2 level or function protects against Parkinson's disease. Glatt et al. demonstrated that a gain in VMAT2 function protects against the development of Parkinson's disease (Glatt et al., 2006). Brighina et al. associated two SNPs in the promoter region of the VMAT2 gene with a reduced

Parkinson's disease risk, suggesting that increases to VMAT2 level confer protection to the disease (Brighina et al., 2013). Thus, vesicular function may oppose the vulnerability of midbrain dopamine neurons to other factors that influence Parkinson's disease outcome, whether genetic (Parkinson's disease -associated mutations) or environmental (toxic insult).

Therapeutic potential of vesicular modulation

It is time to revisit the idea of optimizing the function of existing dopamine neurons in the PD brain (Osherovich, 2014). By manipulating vesicular filling through increased VMAT2 level or function, the benefits in a Parkinson's disease patient would be threefold: improved efficacy of newly synthesized dopamine via L-DOPA treatment, increased dopamine neurotransmission from remaining dopamine neurons and protection from either exogenous or endogenous neurotoxic insults. With the latest work from our lab and others, it appears to be more plausible than ever before to take advantage of the malleable nature of the synaptic dopamine vesicle. Interestingly, the VMAT2-HI mice mentioned above also show improved outcomes on measures of depressive and anxiety-like behaviors, both of which are likely mediated by monoamines beyond just dopamine. Thus, it is possible that a VMAT2-targeted therapeutic strategy may have beneficial effects in other monoamine-deficient diseases like depression, for example. Alternatively, ligands that are also selective for plasma membrane transporters (DAT on dopamine neurons, SERT on serotonin neurons or NET on norepinephrine neurons) would allow for more transmitter system-specific VMAT2 modulation. Finally, one must not forget that other mediators of vesicular dopamine storage may provide alternate targets for the development of therapeutics. In this

way, our understanding of the benefits of increased VMAT2 function could serve as a proxy for another vesicular protein target.

Future Directions

To screen for a compound that positively modulates vesicular function

As mentioned previously, both reserpine and tetrabenazine allow for pharmacological VMAT2 inhibition. The data presented here suggests that upregulating function of the existing transporter would be advantageous. However, due to the lack of crystallization of the protein, the structure of VMAT2 remains unknown (Wimalasena, 2011). This makes positive allosteric modulators of VMAT2 extremely difficult to create. Despite the challenges presented by the creation of these compounds, the field has made progress towards screening for VMAT2 modulators. Fluorescent false neurotransmitters, commercially available compounds that fluoresce specifically when localized to the acidic intravesicular compartment, are now available (Hu et al., 2013). These dopamine-like compounds allow for a large scale high throughput screen for VMAT2 ligands through both novel compounds and known chemical libraries (Bernstein et al., 2012).

To examine the effects of modified vesicular storage on various stages of the vesicle cycle

Vesicles fill up a large percentage of the total area of the synaptic terminal. Within the terminal, vesicles are organized into specific vesicular pools based on where they fall in the synaptic vesicle cycle. Vesicular pools are regulated by neuronal activity and by interactions between vesicles and other proteins (Rizzoli and Betz, 2005). Though the terminology of the three main vesicular pools has varied in recent years, the field has reached a general consensus on the naming of these populations based on their size and proximity to the active zone (Alabi and Tsien, 2012). A small subset of synaptic vesicles (estimated between 6-10 vesicles or about 5% of total synaptic vesicles) remains docked

at the presynaptic membrane ready for release upon an action potential. These vesicles comprise the readily releasable pool (RRP) of vesicles. Upon an action potential in the neuron, calcium channels located near the RRP of vesicles open, resulting in a large influx of calcium (Südhof, 2004). This calcium interacts with the SNARE complex of proteins responsible for the docking of the vesicle, specifically the calcium-sensing protein synaptotagmin, and triggers the fusion and release of the vesicular contents into the synaptic cleft through exocytosis (Südhof and Rizo, 2011; Leitz and Kavalali, 2015). This process occurs rapidly on a millisecond time scale with every neuronal signaling event. The recycling pool, a larger vesicular population consisting of between 17-20 vesicles (~10% of total vesicles), resides slightly farther away from the plasma membrane. Recycling pool vesicles are shuttled into the RRP upon neuronal stimulation when RRP vesicles are depleted and reenter the vesicle cycle. Finally, the largest population of vesicles is the resting or reserve pool (>100 vesicles or ~85% of total vesicles), which resides farthest away from the active zone.

Once a vesicle has fused to the synaptic membrane and released its contents, there are a few different options for the transition between exocytosis and endocytosis. First, vesicles can “kiss and stay” where, once fused to the membrane, the vesicle releases its contents but does not endocytose (Edwards, 2007). Instead, the vesicle is immediately refilled and is ready for the next calcium influx. Alternatively, the “kiss and run” vesicle phenomena is characterized by fusion, release, and then local reacidification, refilling, and recycling into the reserve pool (Harata et al., 2006; Smith et al., 2008; Alabi and Tsien, 2013). Finally, vesicles can be coated with clathrin and recycled via the endosomal pathway (Saheki and De Camilli, 2012). Interestingly, recent evidence has suggested that

a variety of disease-related proteins are interacting with vesicular trafficking and the vesicle cycle (see Chapter I). Based on the emerging evidence linking VMAT2 to human diseases, it would be beneficial to examine whether the enlargement of synaptic vesicles in the VMAT2-HI mice changes distribution of vesicular pools. The electron microscopy analysis performed in previous studies has shown that the VMAT2-HI mice have no change in the total number of vesicles (Lohr et al., 2014), but the delineations between different vesicular pools have yet to be determined.

To investigate the ability of VMAT2 levels to rescue Parkinson's disease pathology in an α-synuclein mouse model

VMAT2 mediates cytosolic toxicity by packaging of dopamine, preventing its toxic oxidation. α-Synuclein levels also alter cytosolic toxicity, synaptic transmission and vesicle clustering and endocytosis (Volles and Lansbury, 2002; Cooper et al., 2006; Guo et al., 2008; Busch et al., 2014). α-Synuclein accumulation induces intracellular oxidative stress and dopamine-mediated toxicity, which also increases accumulation of α-synuclein (Conway, 2001; Perez et al., 2002; Xu et al., 2002). Pitx3-A53T mutant α-synuclein knock-in mice show Lewy body-like inclusions in the SNpc, progressive degeneration of dopaminergic midbrain neurons and profound motor impairment (Lin et al., 2012). The connection between VMAT2 levels and α-synuclein remain unclear, yet these experiments would provide evidence for a link between dopamine homeostasis as mediated by VMAT2 and the cytotoxic accumulation of α-synuclein. Our lab has already shown that VMAT2-LO mice show increased α-synuclein accumulation (Caudle et al., 2007). Further, viral α-synuclein overexpression in VMAT2-deficient mice leads to a significant increase in nigral cell loss (Ulusoy et al., 2012). This continuous feedback of intracellular stress may be modified by VMAT2, as VMAT2 is a key player in intracellular dopamine dynamics.

Results from this study would ultimately show if VMAT2 levels attenuate deficits in an α-synuclein model of PD, suggesting possible interaction between α-synuclein and vesicular filling. I would hypothesize that increased VMAT2 levels will reduce the cytosolic toxicity seen in the Pitx3-A53T mice, resulting in reduced dopamine cell loss, α-synuclein accumulation and reduced severity of the parkinsonian phenotype in these mice.

To examine the interaction of the vesicle with other proteins of interest

The synaptic vesicle, though small in the scale of the entire neuron or even the entire synaptic terminal, contains many proteins critical for vesicular filling, fusion, and release events. Indeed, almost every protein located within the synaptic terminal of a neuron serves a purpose in this process leading to neurotransmission (Südhof, 2013). There is also growing evidence for the importance of presynaptic function in a variety of human diseases, including Alzheimer's disease, autism, bipolar disorder, depression, epilepsy, Huntington's disease, Parkinson's disease, dystonia, and schizophrenia (Waites and Garner, 2011). Thus, it is possible that the results presented here may serve as a proxy for other mediators of vesicular dopamine storage. By immunoprecipitating VMAT2 from brain homogenate in both mouse and human tissue samples, one could assess interacting partners by immunoblotting and mass spectrometry. The data presented in these studies suggest that manipulations to the efficiency of the vesicle are indeed possible, and the identification of other interacting proteins may provide targets that are even more ideal for the development of therapeutics.

Final Thoughts

In conclusion, the delicate balance of dopamine in the neuronal terminal is a complicated game of keeping the neurotransmitter in the right place at the right time. Too much dopamine left unpackaged, and the cytosolic environment becomes precarious. With too little dopamine in the system, the neurons lose signaling efficacy, which manifests itself as a parkinsonism-like behavior. Luckily, there appears to be a 'dopamine sweet spot' where one can take advantage of an additional vesicular capacity, thereby perhaps improving L-DOPA efficacy, increasing transmitter output and protecting cells from toxic insult. Based on the latest clinical findings on vesicular storage and Parkinson's disease risk, mouse models of varying VMAT2 levels may better reflect the human spectrum of vesicular filling and dopamine homeostasis than we previously realized. With the recent focus on newly uncovered genetic associations with Parkinson's disease, there has been movement away from dopamine towards mechanistic descriptions of these disease-causing mutations. However, the recent findings discussed here suggest that modulation of dopamine circuits holds great potential for answering long-held questions about Parkinson's disease and other disorders. Furthermore, the synaptic vesicle and the proteins bound within its membrane stand as ideal targets for this manipulation.

APPENDIX

1. In vivo fast-scan cyclic voltammetry

Introduction

Similar to the neurochemical characterization described in the VMAT2-HI mice in Chapter II, here we describe the initial attempts to perform in vivo fast-scan cyclic voltammetry in the VMAT2-HI mice and wildtype littermates. These studies were performed in the months leading up to the ex vivo slice approaches.

Methods

VMAT2-HI and wildtype mice less than 6 months old were used in these experiments. Voltammetry was performed as previously published (Kile et al., 2010, 2012). Following urethane anesthetization (Sigma, 30 mg/kg, i.p.) and placement into the stereotax, a double-pronged stainless steel stimulating electrodes was placed in the medial forebrain bundle of the mouse using Bregma coordinates. Stimulation parameters were initially 60 Hz, 24 p, and 350 μA (bipolar) with 5 minute stimulation intervals. A carbon fiber microelectrode was placed into the center of the striatum for recording dopamine release. A signal was considered stable after three recordings with <10% variability. Nomifensine (Sigma, 1 mg/kg, i.p.) was injected after the baseline recordings and the stimulation set was repeated. Electrodes were calibrated using a flow-cell injection system and known dopamine standards.

Results

Preliminary studies examining stimulated dopamine release in anesthetized mice showed that the VMAT2-HI mice have elevated dopamine release in the striatum compared to wildtype littermates (**Fig. 7.1. top row**, n = 1). Additionally, both genotypes show a large increase in dopamine release following treatment with the DAT inhibitor nomifensine

(1 mg/kg, bottom row). The percent increase also appears to be similar between the genotypes.

Discussion

These data suggest that the VMAT2-HI mice show increased stimulated dopamine release even in an intact brain. It should be noted that this is only preliminary data. Furthermore, the values for released dopamine are large compared to previously reported values in the literature. There are multiple possible reasons for such large concentrations. First, the stimulation parameters applied here are large compared to the slice preparations described in Chapter II. The stimulation is also applied to the medial forebrain bundle, which stimulates dopamine release from presumably every midbrain dopamine neuron in the circuit. Furthermore, the stimulation is applied almost selectively to dopamine neurons, so there is little to no stimulation to other neuron types, perhaps limiting any feedback inhibition on dopamine release. Finally, it is possible that the calibration methods initially used on these experiments were inaccurate compared to the newer calibration techniques used in the later slice preparations.

The laboratory switched to the ex vivo slice approach due to technical issues with the in vivo preparations. The largest issues arose from electrical noise within the recording system, inaccuracy in hitting the Bregma coordinates for the medial forebrain bundle, and depth of urethane anesthesia. Despite these challenges, in vivo fast-scan cyclic voltammetry allows both for systemic administration of drugs (more closely mimics doses used in behavioral testing) and assessment of intact brain circuitry. However, for the purposes of the characterization of the VMAT2-HI mice, the intact circuits were unnecessary.

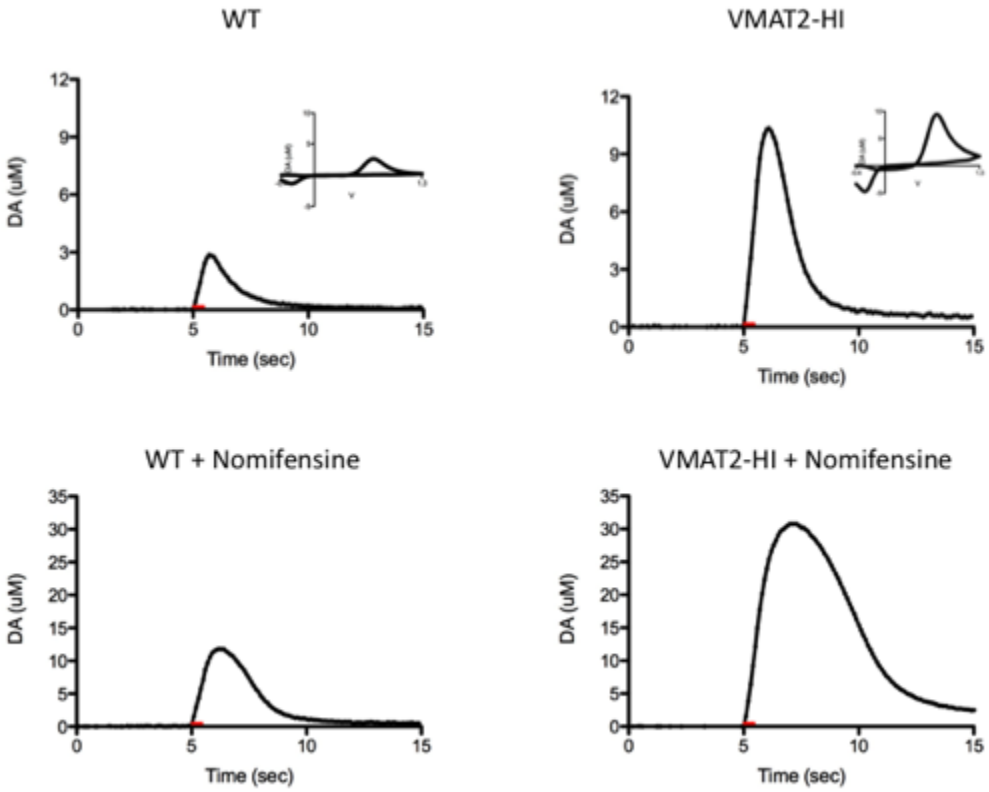
WT
VMAT2-HI
WT + Nomifensine
VMAT2-HI + Nomifensine
DA (uM)
Time (sec)
0
3
6
9
12
15
20
25
30
35
5
10

Figure 7.1. VMAT2-HI mice show increased stimulated dopamine release in vivo. Preliminary studies examining stimulated dopamine release in anesthetized mice showed that the VMAT2-HI mice have elevated dopamine release in the striatum compared to wildtype littermates (top row, n = 1). Additionally, both genotypes show a large increase in dopamine release following treatment with the DAT inhibitor nomifensine (1 mg/kg, bottom row). The percent increase between baseline and nomifensine also appears to be similar between the genotypes.

2. Amphetamine-induced redistribution of VMAT2

Introduction

Previous studies have shown that amphetamine administration redistributes VMAT2 protein from the vesicular protein fraction to the plasma membrane (Riddle et al., 2007). Based on our interest in the effects of amphetamine-like compounds in our mice, we separated brain homogenates from both wildtype and VMAT2-HI mice and examined the ratio of VMAT2 redistribution between the genotypes. Because we saw a small elevation in locomotor activity with amphetamine treatment (Chapter III) and protection from methamphetamine toxicity (Chapter IV), a differential redistribution of the protein may explain some of these results.

Methods

Six month old male VMAT2-HI and wildtype mice were treated with 3 mg/kg d-amphetamine (i.p., free base, Sigma) and sacrificed 90 minute after the injection (n = 2). Brains were homogenized and separated using differential centrifugation into vesicular and membrane fractions. VMAT2 levels were analyzed using immunoblotting as previously published (Caudle et al., 2007). All results were compared by two-way ANOVA with Bonferroni posthoc tests.

Results

As expected, VMAT2-HI mice have significantly increased VMAT2 expression in both the vesicular and membrane fractions (**Fig. 7.2,** $p < 0.01$). Both wildtype and VMAT2-HI mice show small reductions in VMAT2 expression in the vesicular fraction following a 3 mg/kg amphetamine injection. Wildtype mice show a 30.9% decrease in vesicular VMAT2 ($p < 0.05$), compared to a 22.3% trend towards a decrease in the VMAT2-HI mice (ns). Both genotypes also have trends toward increased VMAT2 expression in the

membrane fraction following amphetamine treatment, though these values were not significant. No significant differences were shown in the ratio of vesicular to membrane VMAT2 levels between the genotypes**.**

Discussion

VMAT2-HI mice appear to have the same percentage of amphetamine-induced redistribution of VMAT2 protein as wildtype mice. This suggests that the altered locomotor and neurotoxicological outcomes seen in the VMAT2-HI mice are not due to modifications of the redistribution phenomenon. It is worth noting that this VMAT2 redistribution in response to amphetamine is specific to monoaminergic neurons. This suggests that the changes in compartmentalization of dopamine following amphetamine treatment may mediate this effect, though the exact mechanisms are unclear. Additionally, the amphetamine-induced reductions in vesicular VMAT2 are actually the opposite effects seen in methylphenidate treatment, which has been postulated to be a part of the differential effects of these drugs in the treatment of psychiatric disorders such as attention deficit disorders (Riddle et al., 2006).

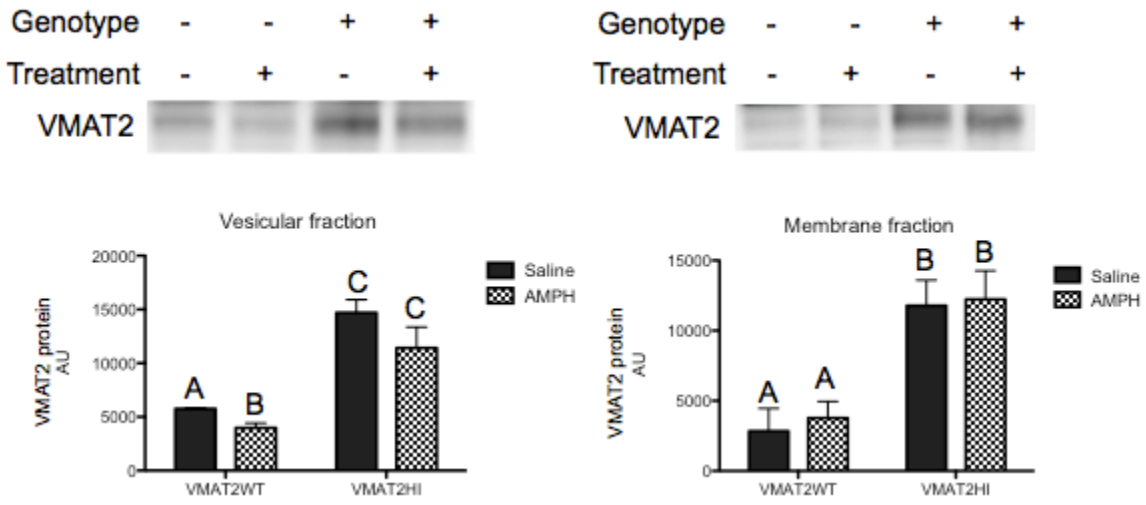
Genotype - - + +
Treatment - + - +
VMAT2
Genotype - - + +
Treatment - + - +
VMAT2
Vesicular fraction
VMAT2 protein AU
20000
15000
10000
5000
0
A
B
C
C
VMAT2WT
VMAT2HI
Saline
AMPH
Membrane fraction
VMAT2 protein AU
15000
10000
5000
0
A
A
B
B
VMAT2WT
VMAT2HI
Saline
AMPH

Figure 7.2. VMAT2-HI mice exhibit similar VMAT2 redistribution following amphetamine treatment.

For genotype labeling, - is wildtype and + is VMAT2-HI. For treatment labeling, - is saline injection and + is 3 mg/kg amphetamine injection. As expected, VMAT2 levels were elevated in both fractions in the VMAT2-HI mice. A single 3 mg/kg amphetamine treatment induces a redistribution of VMAT2 from the vesicular fraction to the membrane fraction 90 minutes following the injection. No significant differences were shown in the ratio of vesicular to membrane VMAT2 levels between the genotypes**.** Different letters above the bars indicate differences of $p < 0.05$.

References

Aghajanian GK, Rosecrans JA, Sheard MH (1967) Serotonin: Release in the Forebrain by Stimulation of Midbrain Raphe. Science (80-) 156:402–403.

Ahlskog JE (2007) Beating a dead horse: dopamine and Parkinson disease. Neurology 69:1701–1711.

Alabi AA, Tsien RW (2012) Synaptic vesicle pools and dynamics. Cold Spring Harb Perspect Biol 4:a013680.

Alabi AA, Tsien RW (2013) Perspectives on kiss-and-run: role in exocytosis, endocytosis, and neurotransmission. Annu Rev Physiol 75:393–422.

Albers DS, Sonsalla PK (1995) Methamphetamine-induced hyperthermia and dopaminergic neurotoxicity in mice: pharmacological profile of protective and nonprotective agents. J Pharmacol Exp Ther 275:1104–1114.

Alter SP, Lenzi GM, Bernstein AI, Miller GW (2013) Vesicular integrity in Parkinson's disease. Curr Neurol Neurosci Rep 13:362.

Anderson DG, Mariappan SVS, Buettner GR, Doorn JA (2011) Oxidation of 3,4-dihydroxyphenylacetaldehyde, a toxic dopaminergic metabolite, to a semiquinone radical and an ortho-quinone. J Biol Chem 286:26978–26986.

Anwar S, Peters O, Millership S, Ninkina N, Doig N, Connor-Robson N, Threlfell S, Kooner G, Deacon RM, Bannerman DM, Bolam JP, Chandra SS, Cragg SJ, Wade-Martins R, Buchman VL (2011) Functional alterations to the nigrostriatal system in mice lacking all three members of the synuclein family. J Neurosci 31:7264–7274.

Axelrod J, Weinshilboum R (1972) Catecholamines. N Engl J Med:237–242 Available at: http://www.nejm.org/doi/full/10.1056/NEJM197208032870508 [Accessed July 10, 2015].

Bannon MJ, Roth RH (1983) Pharmacology of mesocortical dopamine neurons. Pharmacol Rev 35:53–68.

Belluzzi E, Greggio E, Piccoli G (2012) Presynaptic dysfunction in Parkinson's disease: a focus on LRRK2. Biochem Soc Trans 40:1111–1116.

Bemis JC, Seegal RF (2004) PCB-induced inhibition of the vesicular monoamine transporter predicts reductions in synaptosomal dopamine content. Toxicol Sci 80:288–295.

Ben-Shachar D, Zuk R, Glinka Y (1995) Dopamine neurotoxicity: inhibition of mitochondrial respiration. J Neurochem 64:718–723.

Beninger RJ (1983) The role of dopamine in locomotor activity and learning. Brain Res 287:173–196.

Bernstein AI, Stout KA, Miller GW (2012) A fluorescent-based assay for live cell, spatially resolved assessment of vesicular monoamine transporter 2-mediated neurotransmitter transport. J Neurosci Methods 209:357–366.

Bezard E, Gross CE, Fournier MC, Dovero S, Bloch B, Jaber M (1999) Absence of MPTP-induced neuronal death in mice lacking the dopamine transporter. Exp Neurol 155:268–273.

Birkmayer W, Hornykiewicz O (1961) [The L-3,4-dioxyphenylalanine (DOPA)-effect in Parkinson-akinesia]. Wien Klin Wochenschr 73:787–788.

Blesa J, Przedborski S (2014) Parkinsonâ€™s disease: animal models and dopaminergic cell vulnerability. Front Neuroanat 8:155.

Bolam JP, Pissadaki EK (2012) Living on the edge with too many mouths to feed: why dopamine neurons die. Mov Disord 27:1478–1483.

Bradner JM, Suragh TA, Wilson WW, Lazo CR, Stout KA, Kim HM, Wang MZ, Walker DI, Pennell KD, Richardson JR, Miller GW, Caudle WM (2013) Exposure to the polybrominated diphenyl ether mixture DE-71 damages the nigrostriatal dopamine system: role of dopamine handling in neurotoxicity. Exp Neurol 241:138–147.

Breuer O, Lawhorn C, Miller T, Smith DM, Brown LL (2005) Functional architecture of the mammalian striatum: mouse vascular and striosome organization and their anatomic relationships. Neurosci Lett 385:198–203.

Brighina L, Riva C, Bertola F, Saracchi E, Fermi S, Goldwurm S, Ferrarese C (2013) Analysis of vesicular monoamine transporter 2 polymorphisms in Parkinson's disease. Neurobiol Aging 34:1712.e9–e13.

Brooks WJ, Jarvis MF, Wagner GC (1989) Astrocytes as a primary locus for the conversion MPTP into MPP+. J Neural Transm 76:1–12.

Bruns D, Riedel D, Klingauf J, Jahn R (2000) Quantal release of serotonin. Neuron 28:205–220.

Burke WJ, Kumar VB, Pandey N, Panneton WM, Gan Q, Franko MW, O'Dell M, Li SW, Pan Y, Chung HD, Galvin JE (2008) Aggregation of alpha-synuclein by DOPAL, the monoamine oxidase metabolite of dopamine. Acta Neuropathol 115:193–203.

Burke WJ, Li SW, Williams EA, Nonneman R, Zahm DS (2003) 3,4-Dihydroxyphenylacetaldehyde is the toxic dopamine metabolite in vivo: implications for Parkinson's disease pathogenesis. Brain Res 989:205–213.

Busch DJ, Oliphint PA, Walsh RB, Banks SML, Woods WS, George JM, Morgan JR (2014) Acute increase of α-synuclein inhibits synaptic vesicle recycling evoked during intense stimulation. Mol Biol Cell 25:3926–3941.

Calabresi P, Picconi B, Tozzi A, Ghiglieri V, Di Filippo M (2014) Direct and indirect pathways of basal ganglia: a critical reappraisal. Nat Neurosci 17:1022–1030.

Callaghan RC, Cunningham JK, Sykes J, Kish SJ (2012) Increased risk of Parkinson's disease in individuals hospitalized with conditions related to the use of methamphetamine or other amphetamine-type drugs. Drug Alcohol Depend 120:35–40.

Cannon JR, Greenamyre JT (2011) The role of environmental exposures in neurodegeneration and neurodegenerative diseases. Toxicol Sci 124:225–250.

Carlsson A (1972) Biochemical and pharmacological aspects of Parkinsonism. Acta Neurol Scand Suppl 51:11–42.

Carlsson A (1976) The contribution of drug research to investigating the nature of endogenous depression. Pharmakopsychiatr Neuropsychopharmakol 9:2–10.

Carlsson A, Lindqvist M, Magnusson T, Waldeck B (1958) On the presence of 3-hydroxytyramine in brain. Science 127:471.

Carta M, Carlsson T, Muñoz A, Kirik D, Björklund A (2008) Serotonin-dopamine interaction in the induction and maintenance of L-DOPA-induced dyskinesias. Prog Brain Res 172:465–478.

Cartier EA, Parra LA, Baust TB, Quiroz M, Salazar G, Faundez V, Egaña L, Torres GE (2010) A biochemical and functional protein complex involving dopamine synthesis and transport into synaptic vesicles. J Biol Chem 285:1957–1966.

Caudle WM, Colebrooke RE, Emson PC, Miller GW (2008a) Altered vesicular dopamine storage in Parkinson's disease: a premature demise. Trends Neurosci 31:303–308.

Caudle WM, Colebrooke RE, Emson PC, Miller GW (2008b) Altered vesicular dopamine storage in Parkinson's disease: a premature demise. Trends Neurosci 31:303–308.

Caudle WM, Guillot TS, Lazo C, Miller GW (2012) Parkinson's disease and the environment: beyond pesticides. Neurotoxicology 33:585.

Caudle WM, Richardson JR, Wang MZ, Taylor TN, Guillot TS, McCormack AL, Colebrooke RE, Di Monte D a, Emson PC, Miller GW (2007) Reduced vesicular storage of dopamine causes progressive nigrostriatal neurodegeneration. J Neurosci 27:8138–8148.

Cenci MA (2014) Presynaptic Mechanisms of l-DOPA-Induced Dyskinesia: The Findings, the Debate, and the Therapeutic Implications. Front Neurol 5:242.

Chang H-Y, Grygoruk A, Brooks ES, Ackerson LC, Maidment NT, Bainton RJ, Krantz DE (2006a) Overexpression of the Drosophila vesicular monoamine transporter increases motor activity and courtship but decreases the behavioral response to cocaine. Mol Psychiatry 11:99–113.

Chang H-Y, Grygoruk A, Brooks ES, Ackerson LC, Maidment NT, Bainton RJ, Krantz DE (2006b) Overexpression of the Drosophila vesicular monoamine transporter increases motor activity and courtship but decreases the behavioral response to cocaine. Mol Psychiatry 11:99–113.

Chaudhry FA, Boulland J-L, Jenstad M, Bredahl MKL, Edwards RH (2008) Pharmacology of neurotransmitter transport into secretory vesicles. Handb Exp Pharmacol:77–106.

Cheshire P, Ayton S, Bertram KL, Ling H, Li A, McLean C, Halliday GM, O'Sullivan SS, Revesz T, Finkelstein DI, Storey E, Williams DR (2015) Serotonergic markers in Parkinson's disease and levodopa-induced dyskinesias. Mov Disord.

Choi SJ, Panhelainen A, Schmitz Y, Larsen KE, Kanter E, Wu M, Sulzer D, Mosharov E V (2015) Changes in Neuronal Dopamine Homeostasis following 1-Methyl-4-phenylpyridinium (MPP+) Exposure. J Biol Chem 290:6799–6809.

Cirnaru MD, Marte A, Belluzzi E, Russo I, Gabrielli M, Longo F, Arcuri L, Murru L, Bubacco L, Matteoli M, Fedele E, Sala C, Passafaro M, Morari M, Greggio E, Onofri F, Piccoli G (2014) LRRK2 kinase activity regulates synaptic vesicle trafficking and neurotransmitter release through modulation of LRRK2 macro-molecular complex. Front Mol Neurosci 7:49.

Colliver TL, Pyott SJ, Achalabun M, Ewing AG (2000) VMAT-mediated changes in quantal size and vesicular volume. J Neurosci 20:5276–5282.

Colpaert F (1987) Pharmacological characteristics of tremor, rigidity and hypokinesia induced by reserpine in rat. Neuropharmacology 26:1431–1440.

Conway KAR (2001) Kinetic Stabilization of the Alpha-Synuclein Protofibril by a Dopamine-Alpha-Synuclein Adduct. Science (80-) 294:1346.

Cookson MR (2012) Parkinsonism due to mutations in PINK1, parkin, and DJ-1 and oxidative stress and mitochondrial pathways. Cold Spring Harb Perspect Med 2:a009415.

Cooper AA, Gitler AD, Cashikar A, Haynes CM, Hill KJ, Bhullar B, Liu K, Xu K, Strathearn KE, Liu F, Cao S, Caldwell KA, Caldwell GA, Marsischky G, Kolodner RD, Labaer J, Rochet J-C, Bonini NM, Lindquist S (2006) Alpha-synuclein blocks ER-Golgi traffic and Rab1 rescues neuron loss in Parkinson’s models. Science 313:324–328.

Cragg SJ, Rice ME (2004) DAncing past the DAT at a DA synapse. Trends Neurosci 27:270–277.

Creese I, Burt DR, Snyder SH (1976) Dopamine receptor binding predicts clinical and pharmacological potencies of antischizophrenic drugs. Science (80-) 192:481–483.

Crittenden JR, Graybiel AM (2011) Basal Ganglia disorders associated with imbalances in the striatal striosome and matrix compartments. Front Neuroanat 5:59.

Cubells JF, Rayport S, Rajendran G, Sulzer D (1994) Methamphetamine neurotoxicity involves vacuolation of endocytic organelles and dopamine-dependent intracellular oxidative stress. J Neurosci 14:2260–2271.

Curtin K, Fleckenstein AE, Robison RJ, Crookston MJ, Smith KR, Hanson GR (2014) Methamphetamine/amphetamine abuse and risk of Parkinson’s disease in Utah: A population-based assessment. Drug Alcohol Depend.

Daniels RW, Collins CA, Gelfand M V, Dant J, Brooks ES, Krantz DE, DiAntonio A (2004) Increased expression of the Drosophila vesicular glutamate transporter leads to excess glutamate release and a compensatory decrease in quantal content. J Neurosci 24:10466–10474.

Dauer W, Przedborski S (2003) Parkinson's disease: mechanisms and models. Neuron 39:889–909.

Doty RL (2012) Olfaction in Parkinson's disease and related disorders. Neurobiol Dis 46:527–552.

Dwoskin LP, Crooks PA (2002) A novel mechanism of action and potential use for lobeline as a treatment for psychostimulant abuse. Biochem Pharmacol 63:89–98.

Edwards RH (2007) The neurotransmitter cycle and quantal size. Neuron 55:835–858.

Egashira N, Abe M, Shirakawa A, Niki T, Mishima K, Iwasaki K, Oishi R, Fujiwara M (2012) Effects of mood stabilizers on marble-burying behavior in mice : Involvement of GABAergic system. Psychopharmacology (Berl).

Ehringer H, Hornykievicz O (1960) [Distribution of noradrenaline and dopamine (3-hydroxytyramine) in the human brain and their behavior in diseases of the extrapyramidal system.]. Klin Wochenschr 38:1236–1239.

Eiden LE, Weihe E (2011) VMAT2: a dynamic regulator of brain monoaminergic neuronal function interacting with drugs of abuse. Ann NY Acad Sci 1216:86–98.

Eisenberg J, Asnis GM, van Praag HM, Vela RM (1988) Effect of tyrosine on attention deficit disorder with hyperactivity. J Clin Psych 49:193–195.

Eisenhofer G, Kopin IJ, Goldstein DS (2004a) Catecholamine metabolism: a contemporary view with implications for physiology and medicine. Pharmacol Rev 56:331–349.

Eisenhofer G, Kopin IJ, Goldstein DS (2004b) Leaky catecholamine stores: undue waste or a stress response coping mechanism? Ann NY Acad Sci 1018:224–230.

Erickson JD, Eiden LE (1993) Functional identification and molecular cloning of a human brain vesicle monoamine transporter. J Neurochem 61:2314–2317.

Erickson JD, Eiden LE, Hoffman BJ (1992) Expression cloning of a reserpine-sensitive vesicular monoamine transporter. Proc Natl Acad Sci 89:10993–10997.

Escanilla O, Yuhas C, Marzan D, Linster C (2009) Dopaminergic modulation of olfactory bulb processing affects odor discrimination learning in rats. Behav Neurosci 123:828–833.

Fibiger HC, Phillips AG (1988) Mesocorticolimbic dopamine systems and reward. Ann N Y Acad Sci 537:206–215.

Fon EA, Pothos EN, Sun BC, Killeen N, Sulzer D, Edwards RH (1997) Vesicular transport regulates monoamine storage and release but is not essential for amphetamine action. Neuron 19:1271–1283.

Frazer A, Hensler JG (1999) Serotonin Involvement in Physiological Function and Behavior.

Freis ED (1954) Mental depression in hypertensive patients treated for long periods with large doses of reserpine. N Engl J Med 251:1006–1008.

Fumagalli F, Gainetdinov RR, Valenzano KJ, Caron MG (1998) Role of dopamine transporter in methamphetamine-induced neurotoxicity: evidence from mice lacking the transporter. J Neurosci 18:4861–4869.

Fumagalli F, Gainetdinov RR, Wang YM, Valenzano KJ, Miller GW, Caron MG (1999) Increased methamphetamine neurotoxicity in heterozygous vesicular monoamine transporter 2 knock-out mice. J Neurosci 19:2424–2431.

Gainetdinov RR, Fumaga, 99lli F, Wang Y, Jones SR, Levey AI, Miller GW, Caron MG (1998) Increased MPTP Neurotoxicity in Vesicular Monoamine Transporter 2 Heterozygote Knockout Mice. J Neurochem 70:1973–1978.

Glatt CE, Wahner AD, White DJ, Ruiz-linares A (2006) Gain-of-function haplotypes in the vesicular monoamine transporter promoter are protective for Parkinson disease in women. Hum Mol Gen 15:299–305.

Goldberg M (2005) Nigrostriatal Dopaminergic Deficits and Hypokinesia Caused by Inactivation of the Familial Parkinsonism-Linked Gene DJ-1. Neuron:489–496 Available at: http://www.sciencedirect.com.proxy.library.emory.edu/science/article/pii/S0896627305000796 [Accessed June 2, 2013].

Goldstein DS, Sullivan P, Holmes C, Miller GW, Alter S, Strong R, Mash DC, Kopin IJ, Sharabi Y (2013) Determinants of buildup of the toxic dopamine metabolite DOPAL in Parkinson's disease. J Neurochem 126:591–603.

Goldstein, Sullivan P, Holmes C, Kopin IJ, Basile MJ, Mash DC (2011) Catechols in post-mortem brain of patients with Parkinson disease. Eur J Neurol 18:703–710.

Gong LW, Hafez I, Alvarez de Toledo G, Lindau M (2003) Secretory vesicles membrane area is regulated in tandem with quantal size in chromaffin cells. J Neurosci 23:7917–7921.

Graham DG (1978) Oxidative pathways for catecholamines in the genesis of neuromelanin and cytotoxic quinones. Molec Pharm 14:633–643.

Granado N, Ares-Santos S, O'Shea E, Vicario-Abejón C, Colado MI, Moratalla R (2010) Selective vulnerability in striosomes and in the nigrostriatal dopaminergic pathway after methamphetamine administration : early loss of TH in striosomes after methamphetamine. Neurotox Res 18:48–58.

Guilarte TR, Nihei MK, McGlothan JL, Howard AS (2003) Methamphetamine-induced deficits of brain monoaminergic neuronal markers: distal axotomy or neuronal plasticity. Neuroscience 122:499–513.

Guillot TS, Miller GW (2009) Protective actions of the vesicular monoamine transporter 2 (VMAT2) in monoaminergic neurons. Mol Neurobiol 2:149–170.

Guillot TS, Richardson JR, Wang MZ, Li YJ, Taylor TN, Ciliax BJ, Zachrisson O, Mercer A, Miller GW (2008a) PACAP38 increases vesicular monoamine transporter 2 (VMAT2) expression and attenuates methamphetamine toxicity. Neuropeptides 42:423–434.

Guillot TS, Shepherd KR, Richardson JR, Wang MZ, Li Y, Emson PC, Miller GW (2008b) Reduced vesicular storage of dopamine exacerbates methamphetamine-induced neurodegeneration and astrogliosis. J Neurochem 106:2205–2217.

Guo JT, Chen AQ, Kong Q, Zhu H, Ma CM, Qin C (2008) Inhibition of vesicular monoamine transporter-2 activity in alpha-synuclein stably transfected SH-SY5Y cells. Cell Mol Neurobiol 28:35–47.

Haber SN (2014) The place of dopamine in the cortico-basal ganglia circuit. Neuroscience 282:248–257.

Harata NC, Aravanis AM, Tsien RW (2006) Kiss-and-run and full-collapse fusion as modes of exo-endocytosis in neurosecretion. J Neurochem 97:1546–1570.

Hatcher JM, Pennell KD, Miller GW (2008) Parkinson's disease and pesticides: a toxicological perspective. Trends Pharmacol Sci 29:322–329.

Hatcher-Martin JM, Gearing M, Steenland K, Levey AI, Miller GW, Pennell KD (2012) Association between polychlorinated biphenyls and Parkinson's disease neuropathology. Neurotoxicology 33:1298–1304.

Hess A, Desiderio C, McAuliffe WG (1990) Acute neuropathological changes in the caudate nucleus caused by MPTP and methamphetamine: immunohistochemical studies. J Neurocytol 19:338–342.

Hildebrand JG, Shepherd GM (1997) Mechanisms of olfactory discrimination: converging evidence for common principles across phyla. Annu Rev Neurosci 20:595–631.

Hornykiewicz O (1966) Dopamine (3-hydroxytyramine) and brain function. Pharmacol Rev 18:925–964.

Hornykiewicz O (2002) Dopamine miracle: from brain homogenate to dopamine replacement. Mov Disord 17:501–508.

Howell LL, Kimmel HL (2008) Monoamine transporters and psychostimulant addiction. Biochem Pharmacol 75:196–217.

Hu G, Henke A, Karpowicz RJ, Sonders MS, Farrimond F, Edwards R, Sulzer D, Sames D (2013) New fluorescent substrate enables quantitative and high-throughput examination of vesicular monoamine transporter 2 (VMAT2). ACS Chem Biol 8:1947–1954.

Javitch JA, D'Amato RJ, Strittmatter SM, Snyder SH (1985) Parkinsonism-inducing neurotoxin, N-methyl-4-phenyl-1,2,3,6 -tetrahydropyridine: uptake of the metabolite N-methyl-4-phenylpyridine by dopamine neurons explains selective toxicity. Proc Natl Acad Sci U S A 82:2173–2177.

Jenner P (2003) Oxidative Stress in Parkinson's Disease. Ann Neurol:26–38.

Jenner P (2008) Molecular mechanisms of L-DOPA-induced dyskinesia. Nat Rev Neurosci 9:665–677.

Kahlig KM, Galli A (2003) Regulation of dopamine transporter function and plasma membrane expression by dopamine, amphetamine, and cocaine. Eur J Pharmacol 479:153–158.

Kanner BI, Schuldiner S (1987) Mechanism of transport and storage of neurotransmitters. CRC Crit Rev Biochem 22:1–38.

Kaur D, Yantiri F, Rajagopalan S, Kumar J, Mo JQ, Boonplueang R, Viswanath V, Jacobs R, Yang L, Beal MF, DiMonte D, Volitaskis I, Ellerby L, Cherny RA, Bush AI, Andersen JK (2003) Genetic or pharmacological iron chelation prevents MPTP-induced neurotoxicity in vivo: a novel therapy for Parkinson's disease. Neuron 37:899–909.

Kebabian JW, Petzold GL, Greengard P (1972) Dopamine-sensitive adenylate cyclase in caudate nucleus of rat brain, and its similarity to the "dopamine receptor". Proc Natl Acad Sci U S A 69:2145–2149.

Kile BM, Guillot TS, Venton BJ, Wetsel WC, Augustine GJ, Wightman RM (2010) Synapsins differentially control dopamine and serotonin release. J Neurosci 30:9762–9770.

Kile BM, Walsh PL, McElligott ZA, Bucher ES, Guillot TS, Salahpour A, Caron MG, Wightman RM (2012) Optimizing the temporal resolution of fast-scan cyclic voltammetry. ACS Chem Neurosci 3:285–292.

Kirshner N (1962) Uptake of catecholamines by a particulate fraction of the adrenal medulla. Science (80-) 135:107–108.

Kirshner N, Rorie M, Kamin (1963) Inhibition of dopamine uptake in vitro by reserpine administered in vivo. J Pharmacol Exp Ther 141:285–289.

Kitada T, Pisani A, Porter DR, Yamaguchi H, Tscherter A, Martella G, Bonsi P, Zhang C, Pothos EN, Shen J (2007) Impaired dopamine release and synaptic plasticity in the striatum of PINK1-deficient mice. Proc Natl Acad Sci U S A 104:11441–11446.

Klawans HL, Goodman RM, Paulson GW, Barbeau A (1972) Levodopa in the presymptomatic diagnosis of Huntington's chorea. Lancet 2:49.

Kolisnyk B, Guzman MS, Raulic S, Fan J, Magalhães AC, Feng G, Gros R, Prado VF, Prado MAM (2013) ChAT-ChR2-EYFP mice have enhanced motor endurance but show deficits in attention and several additional cognitive domains. J Neurosci 33:10427–10438.

Koob GF (1992) Neural mechanisms of drug reinforcement. Ann N Y Acad Sci 654:171–191.

Krebs CE, Karkheiran S, Powell JC, Cao M, Makarov V, Darvish H, Di Paolo G, Walker RH, Shahidi GA, Buxbaum JD, De Camilli P, Yue Z, Paisán-Ruiz C (2013) The Sac1 domain of SYNJ1 identified mutated in a family with early-onset progressive Parkinsonism with generalized seizures. Hum Mutat 34:1200–1207.

Krishnan V, Nestler EJ (2008) The molecular neurobiology of depression. Nature 455:894–902.

Kristal BS, Conway AD, Brown AM, Jain JC, Ulluci PA, Li SW, Burke WJ (2001) Selective dopaminergic vulnerability: 3,4-dihydroxyphenylacetaldehyde targets mitochondria. Free Radic Biol Med 30:924–931.

Kuhar MJ, Couceyro PR, Lambert PD (1999) Biosynthesis of Catecholamines.

Kuhn DM, Arthur RE, Thomas DM, Elferink LA (2001) Tyrosine Hydroxylase Is Inactivated by Catechol-Quinones and Converted to a Redox-Cycling Quinoprotein. J Neurochem 73:1309–1317.

Kuhn DM, Francescutti-Verbeem DM, Thomas DM (2006) Dopamine quinones activate microglia and induce a neurotoxic gene expression profile: relationship to methamphetamine-induced nerve ending damage. Ann N Y Acad Sci 1074:31–41.

Langston JW, Ballard P, Tetrud JW, Irwin I (1983) Chronic Parkinsonism in humans due to a product of meperidine-analog synthesis. Science 219:979–980.

Larsen KE, Fon EA, Hastings TG, Edwards RH, Sulzer D (2002) Methamphetamine-Induced Degeneration of Dopaminergic Neurons Involves Autophagy and Upregulation of Dopamine Synthesis. J Neurosci 22:8951–8960.

LaVoie MJ, Card JP, Hastings TG (2004) Microglial activation precedes dopamine terminal pathology in methamphetamine-induced neurotoxicity. Exp Neurol 187:47–57.

LaVoie MJ, Hastings TG (1999) Dopamine quinone formation and protein modification associated with the striatal neurotoxicity of methamphetamine: Evidence against a role for extracellular dopamine. J Neurosci 19:1484–1491.

Lawal HO, Chang H-Y, Terrell AN, Brooks ES, Pulido D, Simon AF, Krantz DE (2010) The Drosophila vesicular monoamine transporter reduces pesticide-induced loss of dopaminergic neurons. Neurobiol Dis 40:102–112.

Lawal HO, Krantz DE (2013) SLC18: Vesicular neurotransmitter transporters for monoamines and acetylcholine. Mol Aspects Med 34:360–372.

Lee K-H, Kim M-Y, Kim D-H, Lee Y-S (2004) Syntaxin 1A and Receptor for Activated C Kinase Interact with the N-Terminal Region of Human Dopamine Transporter. Neurochem Res 29:1405–1409.

Leitz J, Kavalali ET (2015) Ca2+ Dependence of Synaptic Vesicle Endocytosis. Neuroscientist.

Lerche S, Seppi K, Behnke S, Liepelt-Scarfone I, Godau J, Mahlknecht P, Gaenslen A, Brockmann K, Srulijes K, Huber H, Wurster I, Stockner H, Kiechl S, Willeit J, Gasperi A, Fassbender K, Poewe W, Berg D (2014) Risk factors and prodromal markers and the development of Parkinson's disease. J Neurol 261:180–187.

Lessin AW, Parkes MW (1957) The hypothermic and sedative action of reserpine in the mouse. J Pharm Pharmacol 9:657–662.

Lin X, Parisiadou L, Sgobio C, Liu G, Yu J, Sun L, Shim H, Gu X-L, Luo J, Long C-X, Ding J, Mateo Y, Sullivan PH, Wu L-G, Goldstein DS, Lovinger D, Cai H (2012) Conditional Expression of Parkinson's Disease-Related Mutant α-Synuclein in the Midbrain Dopaminergic Neurons Causes Progressive Neurodegeneration and Degradation of Transcription Factor Nuclear Receptor Related 1. J Neurosci 32:9248–9264.

Liu Y, Edwards RH (1997) The role of vesicular transport proteins in synaptic transmission and neural degeneration. Annu Rev Neurosci 20:125–156.

Liu Y, Peter D, Roghani A, Schuldiner S, Privé GG, Eisenberg D, Brecha N, Edwards RH (1992a) A cDNA that suppresses MPP+ toxicity encodes a vesicular amine transporter. Cell 70:539–551.

Liu Y, Roghani A, Edwards RH (1992b) Gene transfer of a reserpine-sensitive mechanism of resistance to N-methyl-4-phenylpyridinium. Proc Natl Acad Sci 89:9074–9078.

Lohr KM, Bernstein AI, Stout KA, Dunn AR, Lazo CR, Alter SP, Wang M, Li Y, Fan X, Hess EJ, Yi H, Vecchio LM, Goldstein DS, Guillot TS, Salahpour A, Miller GW (2014) Increased vesicular monoamine transporter enhances dopamine release and opposes Parkinson disease-related neurodegeneration in vivo. Proc Natl Acad Sci 111:9977–9982.

Lohr KM, Stout KA, Dunn AR, Wang M, Salahpour A, Guillot TS, Miller GW (2015) Increased Vesicular Monoamine Transporter 2 (VMAT2; Slc18a2) Protects against Methamphetamine Toxicity. ACS Chem Neurosci 6:790–799.

Lotharius J, Barg S, Wiekop P, Lundberg C, Raymon HK, Brundin P (2002) Effect of mutant alpha-synuclein on dopamine homeostasis in a new human mesencephalic cell line. J Biol Chem 277:38884–38894.

Lotharius J, O'Malley KL (2000) The parkinsonism-inducing drug 1-methyl-4-phenylpyridinium triggers intracellular dopamine oxidation. A novel mechanism of toxicity. J Biol Chem 275:38581–38588.

Lotharius, O'Malley KL (2001) Role of mitochondrial dysfunction and dopamine-dependent oxidative stress in amphetamine-induced toxicity. Ann Neurol 49:79–89.

Masoud ST, Vecchio LM, Bergeron Y, Hossain MM, Nguyen LT, Bermejo MK, Kile B, Sotnikova TD, Siesser WB, Gainetdinov RR, Wightman RM, Caron MG, Richardson JR, Miller GW, Ramsey AJ, Cyr M, Salahpour A (2015) Increased expression of the dopamine transporter leads to loss of dopamine neurons, oxidative stress and l-DOPA reversible motor deficits. Neurobiol Dis 74:66–75.

Mattammal MB, Haring JH, Chung HD, Raghu G, Strong R (1995) An endogenous dopaminergic neurotoxin: implication for Parkinson's disease. Neurodegeneration 4:271–281.

Medina L, Figueredo-Cardenas G, Reiner A (1996) Differential abundance of superoxide dismutase in interneurons versus projection neurons and in matrix versus striosome neurons in monkey striatum. Brain Res 708:59–70.

Meyer AC, Horton DB, Neugebauer NM, Wooters TE, Nickell JR, Dwoskin LP, Bardo MT (2011) Tetrabenazine inhibition of monoamine uptake and methamphetamine behavioral effects: locomotor activity, drug discrimination and self-administration. Neuropharmacology 61:849–856.

Miller DB, O'Callaghan JP (1994) Environment-, drug- and stress-induced alterations in body temperature affect the neurotoxicity of substituted amphetamines in the C57BL/6J mouse. J Pharmacol Exp Ther 270:752–760.

Miller DK, Crooks PA, Teng L, Witkin JM, Munzar P, Goldberg SR, Acri JB, Dwoskin LP (2001) Lobeline Inhibits the Neurochemical and Behavioral Effects of Amphetamine. J Pharmacol Exp Ther 296:1023–1034.

Miller GW, Erickson JD, Perez JT, Penland SN, Mash DC, Rye DB, Levey AI (1999a) Immunochemical analysis of vesicular monoamine transporter (VMAT2) protein in Parkinson's disease. Exp Neurol 156:138–148.

Miller GW, Gainetdinov RR, Levey AI, Caron MG (1999b) Dopamine transporters and neuronal injury. Trends Pharmacol Sci 20:424–429.

Miller GW, Staley JK, Heilman CJ, Perez JT, Mash DC, Rye DB, Levey AI (1997) Immunochemical analysis of dopamine transporter protein in Parkinson's disease. Ann Neurol 41:530–539.

Moore KE, Wuerthele SM (1979) Regulation of nigrostriatal and tuberoinfundibular-hypophyseal dopaminergic neurons. Prog Neurobiol 13:325–359.

Moore RY, Halaris AE, Jones BE (1978) Serotonin neurons of the midbrain raphe: ascending projections. J Comp Neurol 180:417–438.

Mooslehner KA, Chan PM, Xu W, Liu L, Smadja C, Humby T, Allen ND, Wilkinson LS, Emson PC (2001) Mice with very low expression of the vesicular monoamine transporter 2 gene survive into adulthood: potential mouse model for parkinsonism. Mol Cell Biol 21:5321–5331.

Morais VA, Verstreken P, Roethig A, Smet J, Snellinx A, Vanbrabant M, Haddad D, Frezza C, Mandemakers W, Vogt-Weisenhorn D, Van Coster R, Wurst W, Scorrano L, De Strooper B (2009) Parkinson's disease mutations in PINK1 result in decreased Complex I activity and deficient synaptic function. EMBO Mol Med 1:99–111.

Moriyama Y, Futai M (1990) H(+)-ATPase, a primary pump for accumulation of neurotransmitters, is a major constituent of brain synaptic vesicles. Biochem Biophys Res Commun 173:443–448.

Mosharov E V, Borgkvist A, Sulzer D (2014) Presynaptic Effects of Levodopa and Their Possible Role in Dyskinesia. Mov Disord.

Mosharov E V, Larsen KE, Kanter E, Phillips K a, Wilson K, Schmitz Y, Krantz DE, Kobayashi K, Edwards RH, Sulzer D (2009) Interplay between cytosolic dopamine, calcium, and alpha-synuclein causes selective death of substantia nigra neurons. Neuron 62:218–229.

Nagy PM, Aubert I (2012) Overexpression of the vesicular acetylcholine transporter increased acetylcholine release in the hippocampus. Neuroscience 218:1–11.

Nemani VM, Lu W, Berge V, Nakamura K, Onoa B, Lee MK, Chaudhry FA, Nicoll RA, Edwards RH (2010) Increased expression of alpha-synuclein reduces neurotransmitter release by inhibiting synaptic vesicle reclustering after endocytosis. Neuron 65:66–79.

Nestler EJ, Hyman SE (2010) Animal models of neuropsychiatric disorders. Nat Neurosci 13:1161–1169.

Nickell JR, Krishnamurthy S, Norrholm S, Deaciuc G, Siripurapu KB, Zheng G, Crooks PA, Dwoskin LP (2010) Lobelane inhibits methamphetamine-evoked dopamine release via inhibition of the vesicular monoamine transporter-2. J Pharmacol Exp Ther 332:612–621.

O'Callaghan JP, Miller DB (1994) Neurotoxicity profiles of substituted amphetamines in the C57BL/6J mouse. J Pharmacol Exp Ther 270:741–751.

Obeso JA, Rodriguez MC, DeLong MR (1997) Basal ganglia pathophysiology. A critical review. Adv Neurol 74:3–18.

Olanow CW, Tatton WG (1999) Etiology and pathogenesis of Parkinson's disease. Annu Rev Neurosci 22:123–144.

Osamu Suzuki, Hideki Hattori, Minoru Asano, Masakazu Oya, Yoshinao Katsumata (1980) Inhibition of monoamine oxidase by d-methamphetamine. Biochem Pharmacol 29:2071–2073.

Osherovich L (2014) Priming the PD pump. Sci Exch 7.

Papp M, Willner P, Muscat R (1991) An animal model of anhedonia: attenuation of sucrose consumption and place preference conditioning by chronic unpredictable mild stress. Psychopharmacology (Berl) 104:255–259.

Park SU, Ferrer J V, Javitch JA, Kuhn DM (2002) Peroxynitrite inactivates the human dopamine transporter by modification of cysteine 342: potential mechanism of neurotoxicity in dopamine neurons. J Neurosci 22:4399–4405.

Parsons SM, Prior C, Marshall IG (1993) Acetylcholine transport, storage, and release. Int Rev Neurobiol 35:279–390.

Patel J, Mooslehner K a., Chan PM, Emson PC, Stamford J a. (2003) Presynaptic control of striatal dopamine neurotransmission in adult vesicular monoamine transporter 2 (VMAT2) mutant mice. J Neurochem 85:898–910.

Pellow S, Chopin P, File SE, Briley M (1985) Validation of open:closed arm entries in an elevated plus-maze as a measure of anxiety in the rat. J Neurosci Methods 14:149–167.

Perez RG, Waymire JC, Lin E, Liu JJ, Guo F, Zigmond MJ (2002) A role for alpha-synuclein in the regulation of dopamine biosynthesis. J Neurosci 22:3090–3099.

Peter D, Jimenez J, Liu Y, Kim J, Edwards RH (1994) The chromaffin granule and synaptic vesicle amine transporters differ in substrate recognition and sensitivity to inhibitors. J Biol Chem 269:7231–7237.

Peter D, Liu Y, Sternini C, de Giorgio R, Brecha N, Edwards RH (1995) Differential expression of two vesicular monoamine transporters. J Neurosci 15:6179–6188.

Pettibone DJ, Totaro JA, Pflueger AB (1984) Tetrabenazine-induced depletion of brain monoamines: Characterization and interaction with selected antidepressants. Eur J Pharmacol 102:425–430.

Piccoli G, Condliffe SB, Bauer M, Giesert F, Boldt K, De Astis S, Meixner A, Sarioglu H, Vogt-Weisenhorn DM, Wurst W, Gloeckner CJ, Matteoli M, Sala C, Ueffing M (2011) LRRK2 controls synaptic vesicle storage and mobilization within the recycling pool. J Neurosci 31:2225–2237.

Pifl C, Drobny H, Reither H, Hornykiewicz O, Singer EA (1995) Mechanism of the dopamine-releasing actions of amphetamine and cocaine: plasmalemmal dopamine transporter versus vesicular monoamine transporter. Mol Pharmacol 47:368–373.

Pifl C, Rajput A, Reither H, Blesa J, Cavada C, Obeso JA, Rajput AH, Hornykiewicz O (2014) Is Parkinson’s Disease a vesicular dopamine storage disorder? Evidence from a study in isolated synaptic vesicles of human and nonhuman primate striatum. J Neurosci 34:8210–8218.

Porsolt RD (1979) Animal model of depression. Biomedicine 30:139–140.

Porter JC, Kedzierski W, Aguila-Mansilla N, Jorquera BA, González HA (1990) The tuberoinfundibular dopaminergic neurons of the brain: hormonal regulation. Adv Exp Med Biol 274:1–23.

Portig PJ, Vogt M (1969) Release to the cerebral ventricles of substances with possible transmitter function in the caudate nucleus. J Physiol 204:687–715.

Pothos EN (2002) Regulation of dopamine quantal size in midbrain and hippocampal neurons. Brain Behav Res 130:203–207.

Pothos EN, Larsen KE, Krantz DE, Liu Y, Haycock JW, Setlik W, Gershon MD, Edwards RH, Sulzer D (2000) Synaptic vesicle transporter expression regulates vesicle phenotype and quantal size. J Neurosci 20:7297–7306.

Przedborski S, Jackson-lewis V, Naini AB, Petzinger G, Miller R, Akram M (2001) The parkinsonian toxin (MPTP): a technical review of its utility and safety. :1265–1274.

Quinn GP, Shore PA, Brodie BB (1959) Biochemical and pharmacological studies of RO 1-9569 (tetrabenazine), a nonindole tranquilizing agent with reserpine-like effects. J Pharmacol Exp Ther 127:103–109.

Rabinovic AD, Lewis DA, Hastings TG (2000) Role of oxidative changes in the degeneration of dopamine terminals after injection of neurotoxic levels of dopamine. Neuroscience 101:67–76.

Ransom BR, Kunis DM, Irwin I, Langston JW (1987) Astrocytes convert the parkinsonism inducing neurotoxin, MPTP, to its active metabolite, MPP+. Neurosci Lett 75:323–328.

Rees JN, Florang VR, Eckert LL, Doorn JA (2009) Protein reactivity of 3,4-dihydroxyphenylacetaldehyde, a toxic dopamine metabolite, is dependent on both the aldehyde and the catechol. Chem Res Toxicol 22:1256–1263.

Reimer RJ, Fon EA, Edwards RH (1998) Vesicular neurotransmitter transport and the presynaptic regulation of quantal size. Curr Opin Neurobiol 8:405–412.

Ricaurte GA, Guillery RW, Seiden LS, Schuster CR, Moore RY (1982) Dopamine nerve terminal degeneration produced by high doses of methylamphetamine in the rat brain. Brain Res 235:93–103.

Ricaurte GA, Seiden LS, Schuster CR (1984) Further evidence that amphetamines produce long-lasting dopamine neurochemical deficits by destroying dopamine nerve fibers. Brain Res 303:359–364.

Rice ME, Cragg SJ (2008) Dopamine spillover after quantal release: rethinking dopamine transmission in the nigrostriatal pathway. Brain Res Rev 58:303–313.

Richardson JR, Caudle WM, Guillot TS, Watson JL, Nakamaru-Ogiso E, Seo BB, Sherer TB, Greenamyre JT, Yagi T, Matsuno-Yagi A, Miller GW (2007) Obligatory role for complex I inhibition in the dopaminergic neurotoxicity of 1-methyl-4-phenyl-1,2,3,6-tetrahydropyridine (MPTP). Toxicol Sci 95:196–204.

Richardson JR, Miller GW (2004) Acute exposure to aroclor 1016 or 1260 differentially affects dopamine transporter and vesicular monoamine transporter 2 levels. Toxicol Lett 148:29–40.

Riddle EL, Fleckenstein AE, Hanson GR (2006) Mechanisms of methamphetamine-induced dopaminergic neurotoxicity. AAPS J 8:E413–E418.

Riddle EL, Hanson GR, Fleckenstein AE (2007) Therapeutic doses of amphetamine and methylphenidate selectively redistribute the vesicular monoamine transporter-2. Eur J Pharmacol 571:25–28.

Rilstone J, Alkhater R, Minassian B (2013) Brain dopamine-serotonin vesicular transport disease and its treatment. New Engl J Med:543–550.

Ritz MC, Lamb RJ, Goldberg SR, Kuhar MJ (1988) Cocaine self-administration appears to be mediated by dopamine uptake inhibition. Prog Neuropsychopharmacol Biol Psychiatry 12:233–239.

Rizzoli SO, Betz WJ (2005) Synaptic vesicle pools. Nat Rev Neurosci 6:57–69.

Rossetti ZL, Sotgiu A, Sharp DE, Hadjiconstantinou M, Neff NH (1988) 1-Methyl-4-phenyl-1,2,3,6-tetrahydropyridine (MPTP) and free radicals in vitro. Biochem Pharmacol 37:4573–4574.

Rudnick G, Steiner-Mordoch SS, Fishkes H, Stern-Bach Y, Schuldiner S (1990) Energetics of reserpine binding and occlusion by the chromaffin granule biogenic amine transporter. Biochemistry 29:603–608.

Saadat KS, Elliott JM, Colado MI, Green a R (2006) The acute and long-term neurotoxic effects of MDMA on marble burying behaviour in mice. J Psychopharmacol 20:264–271.

Saheki Y, De Camilli P (2012) Synaptic vesicle endocytosis. Cold Spring Harb Perspect Biol 4:a005645.

Salahpour A, Ramsey AJ, Medvedev IO, Kile B, Sotnikova TD, Holmstrand E, Ghisi V, Nicholls PJ, Wong L, Murphy K, Sesack SR, Wightman RM, Gainetdinov RR,

Caron MG (2008) Increased amphetamine-induced hyperactivity and reward in mice overexpressing the dopamine transporter. Proc Natl Acad Sci U S A 105:4405–4410.

Sang T-K, Chang H-Y, Lawless GM, Ratnaparkhi A, Mee L, Ackerson LC, Maidment NT, Krantz DE, Jackson GR (2007) A Drosophila model of mutant human parkin-induced toxicity demonstrates selective loss of dopaminergic neurons and dependence on cellular dopamine. J Neurosci 27:981–992.

Schank JR, Liles LC, Weinshenker D (2008) Norepinephrine signaling through beta-adrenergic receptors is critical for expression of cocaine-induced anxiety. Biol Psychiatry 63:1007–1012.

Schapira AH (1994) Evidence for mitochondrial dysfunction in Parkinson's disease--a critical appraisal. Mov Disord 9:125–138.

Schuldiner S, Shirvan A, Linial M (1995) Vesicular neurotransmitter transporters: from bacteria to humans. Physiol Rev 75:369–392.

Seeman P, Chau-Wong M, Tedesco J, Wong K (1976) Dopamine receptors in human and calf brains, using [3H]apomorphine and an antipsychotic drug. Proc Natl Acad Sci U S A 73:4354–4358.

Shimosato K, Ohkuma S (2000) Simultaneous Monitoring of Conditioned Place Preference and Locomotor Sensitization Following Repeated Administration of Cocaine and Methamphetamine. Pharmacol Biochem Behav 66:285–292.

Simons CJP, van Winkel R (2013) Intermediate phenotype analysis of patients, unaffected siblings, and healthy controls identifies VMAT2 as a candidate gene for psychotic disorder and neurocognition. Schiz Bull 39:848–856.

Smith SM, Renden R, von Gersdorff H (2008) Synaptic vesicle endocytosis: fast and slow modes of membrane retrieval. Trends Neurosci 31:559–568.

Solovieff N, Roberts AL, Ratanatharathorn A, Haloosim M, De Vivo I, King AP, Liberzon I, Aiello A, Uddin M, Wildman DE, Galea S, Smoller JW, Purcell SM, Koenen KC (2014) Genetic Association Analysis of 300 Genes Identifies a Risk Haplotype in SLC18A2 for Posttraumatic Stress Disorder in two Independent Samples. Neuropsychopharmacology.

Song C, Hyun, Fan X, Exeter CJ, Hess EJ, Jinnah HA (2012) Functional analysis of dopaminergic systems in a DYT1 knock-in mouse model of dystonia. Neurobiol Dis 48:66–78.

Song H, Ming G, Fon E, Bellocchio E, Edwards RH, Poo M (1997) Expression of a Putative Vesicular Acetylcholine Transporter Facilitates Quantal Transmitter Packaging. Neuron 18:815–826.

Sotnikova TD, Beaulieu J-M, Gainetdinov RR, Caron MG (2006) Molecular biology, pharmacology and functional role of the plasma membrane dopamine transporter. CNS Neurol Disord Drug Targets 5:45–56.

Specht CG, Schoepfer R (2001) Deletion of the alpha-synuclein locus in a subpopulation of C57BL/6J inbred mice. BMC Neurosci 2:11.

Staal RG, Hogan KA, Liang CL, German DC, Sonsalla PK (2000) In vitro studies of striatal vesicles containing the vesicular monoamine transporter (VMAT2): rat versus mouse differences in sequestration of 1-methyl-4-phenylpyridinium. J Pharmacol Exp Ther 293:329–335.

Südhof TC (2004) The synaptic vesicle cycle. Annu Rev Neurosci 27:509–547.

Südhof TC (2013) Neurotransmitter release: the last millisecond in the life of a synaptic vesicle. Neuron 80:675–690.

Südhof TC, Rizo J (2011) Synaptic vesicle exocytosis. Cold Spring Harb Perspect Biol 3:a005637 – .

Sulzer D (2007) Multiple hit hypotheses for dopamine neuron loss in Parkinson’s disease. Trends Neurosci 30:244–250.

Sulzer D, Chen TK, Yau Yi Lau, Kristensen H, Rayport S, Ewing A (1995) Amphetamine redistributes dopamine from synaptic vesicles to the cytosol and promotes reverse transport. J Neurosci 15:4102–4108.

Sulzer D, Pothos E, Sung HM, Maidment NT, Hoebel BG, Rayport S (1992) Weak base model of amphetamine action. Ann N Y Acad Sci 654:525–528.

Sulzer D, Rayport S (1990) Amphetamine and other psychostimulants reduce pH gradients in midbrain dopaminergic neurons and chromaffin granules: a mechanism of action. Neuron 5:797–808.

Sulzer D, Sonders MS, Poulsen NW, Galli A (2005) Mechanisms of neurotransmitter release by amphetamines: a review. Prog Neurobiol 75:406–433.

Sulzer D, Zecca L (1999) Intraneuronal dopamine-quinone synthesis: A review. Neurotox Res 1:181–195.

Swerdlow NR, Koob GF (1987a) Dopamine, schizophrenia, mania, and depression: Toward a unified hypothesis of cortico-striatopallido-thalamic function. Behav Brain Sci 10:197–208.

Swerdlow NR, Koob GF (1987b) Dopamine, schizophrenia, mania, and depression: Toward a unified hypothesis of cortico-striatopallido-thalamic function. Behav Brain Sci 10:197–208.

Takahashi N, Miner LL, Sora I, Ujike H, Revay RS, Kostic V, Jackson-Lewis V, Przedborski S, Uhl GR (1997) VMAT2 knockout mice: heterozygotes display reduced amphetamine-conditioned reward, enhanced amphetamine locomotion, and enhanced MPTP toxicity. Proc Natl Acad Sci 94:9938–9943.

Tanner CM, Ottman R, Goldman SM, Ellenberg J, Chan P, Mayeux R, Langston JW (1999) Parkinson disease in twins: an etiologic study. JAMA 281:341–346.

Taylor TN, Alter SP, Wang M, Goldstein DS, Miller GW (2014) Reduced vesicular storage of catecholamines causes progressive degeneration in the locus ceruleus. Neuropharmacology 76:97–105.

Taylor TN, Caudle WM, Miller GW (2011) VMAT2-Deficient Mice Display Nigral and Extranigral Pathology and Motor and Nonmotor Symptoms of Parkinson's Disease. Parkinsons Dis 2011:124165.

Taylor TN, Caudle WM, Shepherd KR, Noorian A, Jackson CR, Iuvone PM, Weinshenker D, Greene JG, Miller GW (2009) Nonmotor symptoms of Parkinson's disease revealed in an animal model with reduced monoamine storage capacity. J Neurosci 29:8103–8113.

Thiriet N, Gennequin B, Lardeux V, Chauvet C, Decressac M, Janet T, Jaber M, Solinas M (2011) Environmental enrichment does not reduce the rewarding and neurotoxic effects of methamphetamine. Neurotox Res 19:172–182.

Thomas DM, Francescutti-Verbeem DM, Kuhn DM (2008) The newly synthesized pool of dopamine determines the severity of methamphetamine-induced neurotoxicity. J Neurochem 105:605–616.

Thomas DM, Walker PD, Benjamins JA, Geddes TJ, Kuhn DM (2004) Methamphetamine neurotoxicity in dopamine nerve endings of the striatum is associated with microglial activation. J Pharmacol Exp Ther 311:1–7.

Torres B, Ruoho AE (2014) N-terminus regulation of VMAT2 mediates methamphetamine-stimulated efflux. Neuroscience 259:194–202.

Travis ER, Wang YM, Michael DJ, Caron MG, Wightman RM (2000) Differential quantal release of histamine and 5-hydroxytryptamine from mast cells of vesicular monoamine transporter 2 knockout mice. Proc Natl Acad Sci 97:162–167.

Ugarte Y, Rau KS, Riddle EL, Hanson GR, Fleckenstein AE (2003) Methamphetamine rapidly decreases mouse vesicular dopamine uptake: role of hyperthermia and dopamine D2 receptors. Eur J Pharmacol 472:165–171.

Uhl GR (1998) Hypothesis: the role of dopaminergic transporters in selective vulnerability of cells in Parkinson's disease. Ann Neurol 43:555–560.

Ulusoy A, Björklund T, Buck K, Kirik D (2012) Dysregulated dopamine storage increases the vulnerability to α-synuclein in nigral neurons. Neurobiol Dis 47:367–377.

Usami Y, Hatano T, Imai S, Kubo S, Sato S, Saiki S, Fujioka Y, Ohba Y, Sato F, Funayama M, Eguchi H, Shiba K, Ariga H, Shen J, Hattori N (2011) DJ-1 associates with synaptic membranes. Neurobiol Dis 43:651–662.

Vardy E, Arkin IT, Gottschalk KE, Kaback HR, Schuldiner S (2004) Structural conservation in the major facilitator superfamily as revealed by comparative modeling. Protein Sci 13:1832–1840.

Vergo S, Johansen JL, Leist M, Lotharius J (2007) Vesicular monoamine transporter 2 regulates the sensitivity of rat dopaminergic neurons to disturbed cytosolic dopamine levels. Brain Res 1185:18–32.

Volles MJ, Lansbury PT (2002) Vesicle Permeabilization by Protofibrillar R-Synuclein Is Sensitive to Parkinson ' s Disease-Linked Mutations and Occurs by a Pore-like Mechanism †. Society:4595–4602.

Waites CL, Garner CC (2011) Presynaptic function in health and disease. Trends Neurosci 34:326–337.

Wang YM, Gainetdinov RR, Fumagalli F, Xu F, Jones SR, Bock CB, Miller GW, Wightman RM, Caron MG (1997a) Knockout of the vesicular monoamine transporter 2 gene results in neonatal death and supersensitivity to cocaine and amphetamine. Neuron 19:1285–1296.

Wang YM, Gainetdinov RR, Fumagalli F, Xu F, Jones SR, Bock CB, Miller GW, Wightman RM, Caron MG (1997b) Knockout of the vesicular monoamine transporter 2 gene results in neonatal death and supersensitivity to cocaine and amphetamine. Neuron 19:1285–1296.

Wey MC-Y, Fernandez E, Martinez PA, Sullivan P, Goldstein DS, Strong R (2012) Neurodegeneration and motor dysfunction in mice lacking cytosolic and mitochondrial aldehyde dehydrogenases: implications for Parkinson's disease. PLoS One 7:e31522.

Whitehead RE, Ferrer J V., Javitch JA, Justice JB (2001) Reaction of oxidized dopamine with endogenous cysteine residues in the human dopamine transporter. J Neurochem 76:1242–1251.

Wilson NR, Kang J, Hueske E V, Leung T, Varoqui H, Murnick JG, Erickson JD, Liu G (2005) Presynaptic regulation of quantal size by the vesicular glutamate transporter VGLUT1. J Neurosci 25:6221–6234.

Wilson WW, Shapiro LP, Bradner JM, Caudle WM (2014) Developmental exposure to the organochlorine insecticide endosulfan damages the nigrostriatal dopamine system in male offspring. Neurotoxicology 44:279–287.

Wimalasena K (2011) Vesicular monoamine transporters: structure-function, pharmacology, and medicinal chemistry. Med Res Rev 31:483–519.

Wirdefeldt K, Adami H-O, Cole P, Trichopoulos D, Mandel J (2011a) Epidemiology and etiology of Parkinson's disease: a review of the evidence. Eur J Epidemiol 26 Suppl 1:S1–S58.

Wirdefeldt K, Gatz M, Reynolds CA, Prescott CA, Pedersen NL (2011b) Heritability of Parkinson disease in Swedish twins: a longitudinal study. Neurobiol Aging 32:1923.e1–e8.

Xu J, Kao S-Y, Lee FJS, Song W, Jin L-W, Yankner BA (2002) Dopamine-dependent neurotoxicity of alpha-synuclein: a mechanism for selective neurodegeneration in Parkinson disease. Nat Med 8:600–606.

Yero T, Rey JA (2008) Tetrabenazine (Xenazine), An FDA-Approved Treatment Option For Huntington ’ s Disease – Related Chorea. 33:690–694.

Zarrindast MR, Eliassi A (1991) Differential effects of dopamine agonists on locomotion in intact and reserpine-treated mice. Gen Pharmacol 22:1027–1031.

Zimmermann H, Volknandt W, Wittich B, Hausinger A (1993) Synaptic vesicle life cycle and synaptic turnover. J Physiol Paris 87:159–170.